

C **ε**
22
COMPENG
2022 IEEE

2022 IEEE WORKSHOP ON COMPLEXITY IN ENGINEERING

Florence, July 18-20, 2022



The electronic version of this booklet can be found at:
<https://compeng2022.ino.cnr.it/>

Contents

About	4
COMPENG	4
Timetable	6
Monday, 18 of July	6
Tuesday, 19 of July	9
Wednesday, 20 of July	12
List of Abstracts – Talks	14
Monday 18th	14
Tuesday 19th	68
Wednesday 20th	110
List of Posters	129
Useful Information	143

About

COMPENG

COMPENG is a series of international workshops founded in 2010 aimed at providing a forum for experts and professionals working on the latest developments in complexity science and its application in an engineering perspective.

Previous editions of the workshop were held in Rome, Italy (2010); Aachen, Germany (2012); Barcelona, Spain (2014); Catania, Italy (2016); Florence, Italy (2018).

General Chairs

Riccardo Meucci (CNR-INO)
Francesco Marino (CNR-INO)

Co-chairs Organizers

Marzena Ciszak (CNR-INO)
Francesca Di Patti (University of Perugia)
Duccio Fanelli (University of Florence)
Giacomo Innocenti (University of Florence)
Massimo Materassi (CNR-ISC)

Local Organizing Committee

Elisabetta Baldanzi (CNR-INO)
Lorenzo Chicchi (University of Florence)
Lorenzo Giambagli (University of Florence)
Mauro Morandini (INFN)
Pasquale Poggi (CNR-INO)

Publication Chair

Francesca Di Patti (University of Perugia)

Treasurer

Pisana Placidi (University of Perugia)

Steering Committee

Paolo Pietro Arena (IEEE Italy Section)
Ermanno Cardelli (IEEE Italy Section)
Silvano Donati (IEEE Life Fellow)
Sergio Rapuano (IEEE Italy Section Chair)

Scientific Committee

Stefano Boccaletti (CNR-ISC)
Guanrong Chen (City University of Hong Kong)
Claudio Conti (CNR-ISC)
Mario Di Bernardo (University of Naples Federico II)
Duccio Fanelli (University of Florence)
Luigi Fortuna (University of Catania)
Mattia Frasca (University of Catania)
Jean-Marc Ginoux (Laboratory of Information and System Science)
Stefano Lepri (CNR-ISC)
Roberto Livi (University of Florence)
Elisa Masi (University of Florence)
Antonello Monti (Aachen University)
Alessandro Rizzo (Polytechnic University of Turin)
Marti Rosas-Casals (Technical University of Catalonia)
Alberto Tesi (University of Florence)

Timetable

CT: Contributed Talk, KL: Keynote Lecture.

Monday, 18 of July

8:45–9:15	Registration	
9:15–9:30	Opening	
	Plenary session [Chair: F. Marino] - Room A	
9:30–10:15	KL	C. Laschi Soft robotics: from bioinspired principles to model-informed design
10:15–11:00	KL	A. Torcini Next Generation Neural Mass Models
11:00–11:20	Coffee break	
	Complex networks and applications [Chair: F. Di Patti] - Room A	
11:20–11:40	CT	M. Frasca Network-based control of synchronization and failures in power grids
11:40–12:00	CT	M. Bonnin Logic gates based on nonlinear oscillators
12:00–12:20	CT	S. Olmi Spontaneous symmetry breaking in identically coupled inhibitory neural masses with adaptation
12:20–12:40	CT	I. M. Diop Robustness analysis of the weighted world air transportation network through its component structure
12:40–13:00	CT	M. Dahlmanns Optimal geometry of urban transport networks
	Neurocybernetics (Methods) [Chairs: C. M. Sweeney-Reed, S. J. Nasudo, D. C. Soriano] - Room B	
11:20–11:40	CT	C. M. Sweeney-Reed, S. J. Nasudo, D.C. Soriano Introduction to the Neurocybernetics

11:40–12:00	CT	M. Deliano	Criticality and its relationship to oscillatory brain dynamics
12:00–12:20	CT	D. Gurnari	How to see in high dimensions
12:20–12:40	CT	J. Signerska-Rynkowska	On Takens theorem and embedding methods
12:40–13:00	CT	Michał Lipiński	From a discrete orbit to a dynamical feature
13:00–14:00	Lunch		
Complex networks and applications [Chair: G. Innocenti] - Room A			
14:00–14:20	CT	G. Ruzzene	Emergence of undesired synchronisation of flexible loads in power grids with distributed frequency control
14:20–14:40	CT	D. Segura	NB-IoT latency evaluation with real measurements
14:40–15:00	CT	E. M. H. Shalma	Optimal Practical Design and Reduced Complexity of 6G sub-Terahertz Wireless Backhaul Networks
15:00–15:20	CT	J. A. Trujillo	Autonomous monitoring framework for cellular networks
15:20–15:40	CT	A. Boukhriss	ADRC Control for a Single-Stage Photovoltaic System Connected to the Three-Phase Electrical Grid
Neurocybernetics (Methods) [Chairs: C. M. Sweeney-Reed, S. J. Nasuto, D.C. Soriano] - Room B			
14:00–14:20	CT	P. Carelli	Accessing signatures of criticality in neuronal data using maximum entropy models
14:20–14:40	CT	V. M. B. da Silva	Critical cells in the primary visual cortex
14:40–15:00	CT	D. C. Soriano	Motor-Dependent Synaptic Balance Modulation and Critical Phenomena in the Subthalamic Nucleus: A New Framework for Adaptive Deep Brain Stimulation

15:00–15:20	CT	M. Wairagkar	Ongoing long-range temporal correlations in broadband EEG and intracortical neural activity during voluntary movement
15:40–16:00	Coffee break		
Non linear dynamics and data analysis [Chair: M. Materassi] - Room A			
16:00–16:20	CT	A. Aleksandrov	Agent-based and Logistic population growth models comparison
16:20–16:40	CT	J. Plucar	Blockchain Based Platform for Sensitive Medical Data Management
16:40–17:00	CT	S. Celikovsky	On the equivalence of the three-link to almost linear form
17:00–17:20	CT	G. Chesi	On reducing the topological entropy of linearized nonlinear systems
17:20–17:40	CT	M. Italia	A mathematical analysis of the socio-economic impacts of a patent waiver on COVID-19 vaccines
17:40–18:00	CT	L. Bettini	Optimal initial perturbations in a boundary layer with wall actuation
Neurocybernetics (Applications) [Chairs: C. M. Sweeney-Reed, S. J. Nasuto, D.C. Soriano] - Room B			
16:00–16:20	CT	C. Reichert	Visual spatial attention shifts decoded from the electroencephalogram enable sending of binary messages
16:20–16:40	CT	C. M. Sweeney-Reed	Timing of functional electrical stimulation using a brain-computer interface improves rehabilitation outcome early post-stroke
16:40–17:00	CT	L. C. Mendes	Objective Evaluation of Bradykinesia Using a Serious Game
17:00–17:20	CT	Y. Kordi	Effect of sevoflurane on cardiovascular activity at maintenance and emergence from anesthesia during surgery
18:30	Visit to Villa Galileo and welcome cocktail		

Tuesday, 19 of July

	Plenary session [Chair: R. Meucci] - Room A		
9:15–10:00	KL	S. Donati	Complexity at Increasing Levels of Feedback in Diode Laser
10:00–10:45	KL	J. M. Ginoux	Minimal Universal Model for Chaos and Generalized Multistability in a Laser
10:45–11:10	Coffee break		
	Engineering Algorithms in Complex Systems [Chairs: I. Zelinka, J. Plucar, L. Skanderova, A. Adamatzky, N. V. Kuznetsov] - Room A		
11:10–11:30	CT	Z. K. Oplatková	Mining Top-K High Utility Itemset Using Bio-Inspired Algorithms
11:30–11:50	CT	M. Pluhacek	Inner Dynamic of Particle Swarm Optimization Interpreted by Complex Network Analysis
11:50–12:10	CT	D. Davendra	Chaotic Ant Lion Optimization Algorithm
12:10–12:30	CT	V. Dodonov	Optimal allocation of resources in a three-sector dynamical model of an economy: analytical approach and evolutionary algorithms
	Neuromorphic Photonics [Chairs: B. Romeira, A. Hurtado] - Room B		
11:10–11:30	CT	C. Mesaritakis	Bayesian Training in Photonic Neuromorphic Meshes
11:30–11:50	CT	k. Ludge	Delay-based Reservoir Computing: Role of Timescales and Memory for Optimizing Performance
11:50–12:10	CT	A. Hurtado	Neuromorphic Photonic Computing with Vertical-Cavity Surface-Emitting Lasers
12:10–12:30	CT	S. Barbay	Neuromorphic processing in delay-coupled and spatially coupled micropillar lasers

12:30–13:30	Lunch	
13:30–14:00	Poster Session (Hybrid)	
	Engineering Algorithms in Complex Systems [Chairs: I. Zelinka, J. Plucar, L. Skanderova, A. Adamatzky, N. V. Kuznetsov] - Room A	
14:00–14:20	CT	D. Davendra Crosshair Optimizer
14:20–14:40	CT	R. Matousek Stabilization of Higher Periodic Orbits of Chaotic Maps using Permutation-selective Objective Function
14:40–15:00	CT	T. Kadavy Exploring clustering in SOMA
15:00–15:20	CT	T. Alexeeva Forecasting and stabilizing chaotic regimes in two macroeconomic models: interaction of AI technologies and time-delay control methods
	Neuromorphic Photonics [Chairs: B. Romeira, A. Hurtado] - Room B	
14:00–14:20	CT	S. Yanchuk Deep neural networks using a single neuron: folded-in-time architecture using feedback-modulated delay loops
14:20–14:40	CT	R. Stabile SOA-based Photonic Integrated Deep Neural Networks
14:40–15:00	CT	B. Romeira Neuromorphic NanoLEDs
15:00–15:20	CT	X. Porte Neural network computing with large-area lasers
15:20–15:40	Coffee break	
	Laser dynamics, nonlinear and quantum optics [Chair: F. Marino] - Room A	
15:40–16:00	CT	S. Barbay Extreme events prediction with imperfect data from a spatiotemporally chaotic system
16:00–16:20	CT	A. Lapucci Enhancing the Power in the Bucket (PIB) in Coherent Laser Beam Combining

16:20–16:40	CT	K. Tamersit	High-Performance Detection of Toxic Gases Using a New Microsensor based on Graphene Field-Effect Transistor
Robotics [Chair: C. Laschi] - Room B			
15:40–16:00	CT	M. C. De Simone	Multibody Modeling for the Design of an Autonomous Rover for Precision Agriculture Applications in Developing Countries
16:00–16:20	CT	F. C. Di Martino	Design of a Test-Rig for Space Applications in Microgravity Conditions
16:20–16:40	CT	E. Manzoni	Mimicking the Complex Human Circulatory System via a Custom Hydro-mechanical Pulse Duplicator
16:40–17:00	CT	S. Summa	Bioinspired controller for a robotic knee orthosis
Non linear dynamics and data analysis [Chair: G. Innocenti] - Room A			
16:40–17:00	CT	P. M. Mariano	Nonlinear oscillators with memory: solutions with the same period of perturbations
17:00–17:20	CT	A. Di Garbo	Dynamics of interneurons in the presence of a sodium channel mutation
17:20–17:40	CT	S. Mohammadi	Mining Intraday Electricity Market Trades
20:00	Social Dinner		

Wednesday, 20 of July

Laser dynamics, nonlinear and quantum optics [Chair: F. Marino] - Room A			
9:10–9:30	CT	J. A. Roversi	On the effect of the number of photons on the generation and transfer of entangled states between toroidal cavities via a chain of artificial atoms
9:30–9:50	CT	K. Tamersit	High photosensitivity in band-to-band tunneling regime of carbon nanotube field-effect phototransistor: Numerical investigation
9:50–10:10	CT	M. Castelluzzo	Experimental evidence of a nonlinear dynamics in a two-level non-autonomous laser model
Remote monitoring [Chairs: R. Meucci, E. Pugliese, M. Locatelli] - Room B			
9:10–9:30	CT	M. Spampan	Modern solutions for Remote SHM
9:30–9:50	CT	N. Signorini	Seismic monitoring in the Tuscany region
9:50–10:10	CT	M. Locatelli	Infrastructure remote monitoring in Tuscany
10:10–10:30	Coffee break		
Machine Learning [Chairs: L. Giambagli, L. Chicchi] - Room A			
10:30–10:50	CT	A. Amini	A Machine Learning Based Model for Monitoring of Composite Drilling Tools During Assembly Production Using Laser Profiler Data
10:50–11:10	CT	A. Groza	Detecting fake news using machine learning and reasoning in Description Logics
11:10–11:30	CT	A. Lorusso	Predictive maintenance and Structural Health Monitoring via IoT system

11:30–11:50	CT	S. Mohammadi	A Machine Learning Approach for Prosumer Management in Intraday Electricity Markets
11:50–12:10	CT	D. Sun	Attention-based Dependability Prediction for Industrial Wireless Communication Systems
Remote monitoring [Chair: R. Meucci] - Room B			
10:30–10:50	CT	G. Lacanna	Integrating modal analysis and seismic interferometry for structural dynamic identification and soil-structure interaction
10:50–11:10	CT	Y. Giambastiani	Web scraping technology for a dynamics analysis of tree crown streamlining, in relationship with wind and meteorological data
11:10–11:30	CT	M. C. De Simone	A Methodology for The Design of Dynamic Absorbers for Structural Mitigation of Steel Buildings
11:30–11:50	CT	F. Bocchi	An adaptive modal filter for tracking frequency variation in the operating condition
11:50–12:10	CT	M. Betti	A quality based OMA framework for data-driven SHM of heritage buildings
12:30	Lunch		

List of Abstracts – Talks

Monday 18th

Soft robotics: from bioinspired principles to model-informed design

C. Laschi¹

KL

¹National University of Singapore, Singapore

Soft robotics is a relatively young field of robotics that takes advantage of soft materials and compliant structures to improve robot interactions with their surrounding environment, and ultimately provide them with enhanced abilities. It is largely grounded in bioinspiration and the soft robotics community is traditionally interdisciplinary. When we observe living beings, we see systems that look simple in their behaviour, in natural environments, efficient and adaptable to unexpected situations. Yet, they are in fact way more complex than our robots. What are the principles for making the behaviour of complex systems simple? This is the lesson that we can learn from nature, for robotics. We learn that intelligence is not only in brain and computation, but also in the body. A soft body can help take advantage of such embodied intelligence and reduce computation and energy needs. An effective bioinspired approach passes through modelling the principles observed in nature. Can we fully grasp embodied intelligence by modelling the interactions of our soft robots with their surrounding environment? Answering this question can help soft robotics transition from a prototype-based pioneering field to a model-informed discipline, in an interdisciplinary dialogue.

Next Generation Neural Mass Models

A. Torcini¹



¹Cergy Paris Université, Cergy-Pontoise, France and Institute of Complex Systems, CNR, Italy

I will first give a brief overview of the next generation neural mass models, which represent a complete new perspective for the development of exact mean field models of heterogeneous spiking networks [1]. Then I will report recent results on the application of this formalism to reproduce relevant phenomena observed in neuroscience ranging from cross-frequency coupling [2] to theta-nested gamma oscillations [3], from slow and fast gamma oscillations [4] to synaptic-based working memory tasks [5]. I will finally show how these neural masses can be extended to capture fluctuations driven phenomena induced by dynamical sources of disorder naturally present in brain circuits, such as background noise and current fluctuations due to the sparseness in the connections [6,7].

References

- [1] Montbrió, Ernest, Diego Pazó, and Alex Roxin. "Macroscopic description for networks of spiking neurons." *Physical Review X* 5.2 (2015): 021028.
- [2] A.Ceni, S. Olmi, A. Torcini, D. Angulo Garcia, "Cross frequency coupling in next generation inhibitory neural mass models", *Chaos* ,30, 053121 (2020)
- [3] M. Segneri, H.Bi, S. Olmi, A.Torcini, "Theta-nested gamma oscillations in next generation neural mass models", *Frontiers in Computational Neuroscience* , 14:47 (2020)
- [4] H. Bi, M. Segneri, M. di Volo,A.Torcini, "Coexistence of fast and slow gamma oscillations in one population of inhibitory spiking neurons", *Physical Review Research* ,2, 013042 (2020)
- [5] H. Taher, A. Torcini, S. Olmi, "Exact neural mass model for synaptic-based working memory", *PLOS Computational Biology* , 16(12):e1008533 (2020)
- [6] M. di Volo, A. Torcini, "Transition from asynchronous to oscillatory dynamics in balanced spiking networks with instantaneous synapses", *Phys. Rev. Lett.* 121 , 128301 (2018)
- [7] D. Goldobin, M. di Volo, A. Torcini, "A reduction methodology for fluctuation driven population dynamics", *Physical Review Letters* 127,038301 (2021)

Network-based control of synchronization and failures in power grids

S. Olmi^{1,2}, L. V. Gambuzza³ and M. Frasca^{3,4}

¹ CNR - Consiglio Nazionale delle Ricerche - Istituto dei Sistemi Complessi, Sesto Fiorentino, Italy

² INFN, Italy

³ Department of Electrical Electronic and Computer Science Engineering, University of Catania, Italy

⁴ Istituto di Analisi dei Sistemi ed Informatica "A. Ruberti", Consiglio Nazionale delle Ricerche (IASI-CNR), Roma, Italy

In this work, we study the problem of controlling a power grid subject to large perturbations that cause the failure of a node of the grid. Under such circumstances, the system may lose synchrony and, in addition, a cascade of line failures can be triggered as an effect of the flow redistribution that activates the protection mechanisms equipped on each line of the grid. To devise a control action for addressing this problem, we adopt a network-based description of the power grid that incorporates an overflow condition to model the possibility of cascading failures [1]. In this model, each node is associated with a rotating machine whose dynamics is described by a swing equation. Let \mathcal{N} be the set of nodes with $|\mathcal{N}| = N$, \mathcal{N}_g (with $|\mathcal{N}_g| = N_g$) the subset of generator nodes, and \mathcal{E} (with $|\mathcal{E}| = E$) the set of links describing the power grid topology. To each node i with $i = 1, \dots, N$, a mechanical rotor angle $\theta_i(t)$ that corresponds to the voltage phase angle and its angular velocity $\omega_i = d\theta_i/dt$, relative to a rotating reference frame with velocity $\Omega = 2\pi f$ ($f = 50\text{Hz}$ or $f = 60\text{Hz}$, depending on the geographical area under study) are associated. The dynamics of these variables are described by the swing equation [2]:

$$\frac{d\theta_i}{dt} = \omega_i \quad (0.1)$$

$$I_i \frac{d\omega_i}{dt} = P_i - \gamma_i \omega_i + \sum_{(i,j) \in \mathcal{E}'} K_{ij} \sin(\theta_j - \theta_i) + u_i \quad (0.2)$$

where the parameters I_i , γ_i , and P_i represent the rotating machine inertia, damping coefficient, and power that is positive, $P_i > 0$, for generators, or negative, $P_i < 0$, for loads. Here $\mathcal{E}' \subseteq \mathcal{E}$ represents the set of the operating (i.e., not failed) links of the power grid and K_{ij} are the elements of the weighted adjacency matrix describing its topology. The term $u_i(t)$ represents the control input, and is here obtained as the sum of two contributions: $u_i(t) = u_i^P(t) + u_i^I(t)$. The term $u_i^P(t)$ is a distributed action obtained by setting for each link a control law proportional to the difference of the frequencies at the extremes [3]: $u_i^P(t) = g_P \sum_{j=1}^N a_{ij}^P (\omega_j(t) - \omega_i(t))$. The term u_i^I is also a distributed action, that however implements an integral action, defined by specifying the dynamics

of the term itself [4]: $\dot{u}_i^l = g_l \xi_i^l \sum_{j=1}^N a_{ij}^l (\omega_j - \omega_i)$, where $\xi_i^l = 1$ if node i is a generator, and $\xi_i^l = 0$, otherwise.

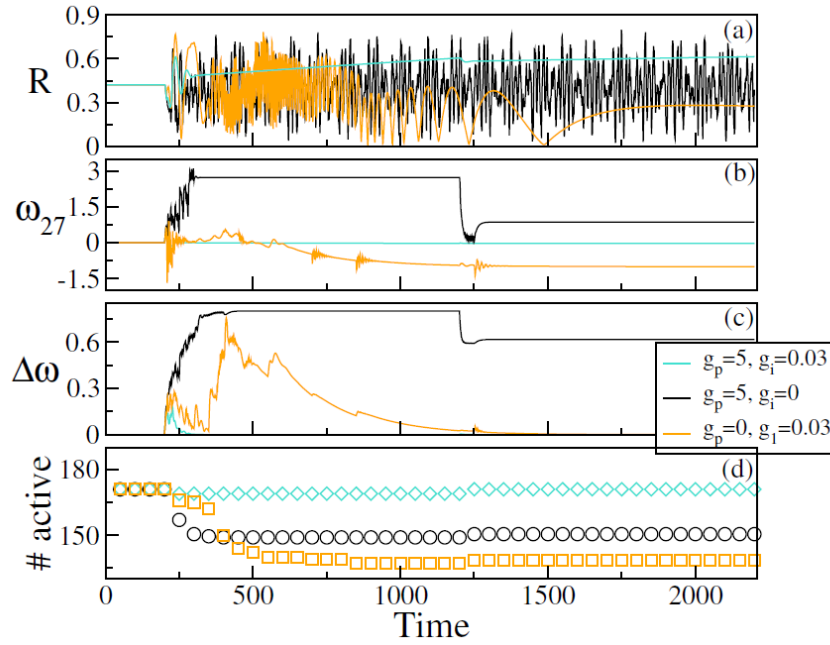


Figure 0.1: Comparison of evolution of the power grid under three different conditions for control: $g_p = 5$ and $g_i = 0$, representing the activation of only the proportional layer; $g_p = 0$ and $g_i = 0.03$ representing the activation of only the integral layer; $g_p = 5$ and $g_i = 0.03$ representing the simultaneous activation of the two layers.

Although the two control laws have been studied when acting separately [3, 4], here we investigate their combined effect to reduce the deviation from synchronization, while simultaneously preventing that cascading failures are triggered. In more detail, in our work we study the effect of the control laws as their associated topologies (modeled by the coefficients a_{ij}^p and a_{ij}^l , respectively) are changed. For sake of page limitation, in this extended abstract we only show a single example of control (Fig. 1) carried out on the mathematical model of the Italian high-voltage power grid, for different values of the two control gains g_p and g_l . We assume that a perturbation occurs at node 27 of the grid causing its failure in the time interval $t \in [250s, 1250s]$. In absence of any control, this initial fault triggers the cascading failure of several lines (Fig. 1(d)). The number of failures is reduced when the proportional control is activated, but it is still large. When both controls are active, there are no other failures than the lines associated to the affected node. The beneficial effect of the control actions when simultaneously activated is also visible inspecting the evolution of the order parameter R (Fig. 1(a)) and the frequency deviation $\Delta\omega$ (Fig. 1(c)). It can be noticed that, while the integral control reduces the frequency deviation also in the absence of the proportional action,

the combined action of the two terms is more effective in that it achieves lower values of $\Delta\omega$ and higher values of R .

Acknowledgments This work was supported by the Italian Ministry for Research and Education (MIUR) through Research Program PRIN 2017 under Grant 2017CWMMF93, project "Advanced Network Control of Future Smart Grids - VECTORS".

References

- [1] B. Schöfer, D. Witthaut, M. Timme, and V. Latora, "Dynamically induced cascading failures in power grids," *Nature communications*, vol. 9, no. 1, pp. 1–13, 2018.
- [2] G. Filatrella, A. H. Nielsen, and N. F. Pedersen, "Analysis of a power grid using a kuramoto-like model," *The European Physical Journal B*, vol. 61, no. 4, pp. 485–491, 2008.
- [3] M. Frasca and L. V. Gambuzza, "Control of cascading failures in dynamical models of power grids," *Chaos, Solitons & Fractals*, vol. 153, p. 111460, 2021.
- [4] C. H. Totz, S. Olmi, and E. Schöll, "Control of synchronization in two-layer power grids," *Physical Review E*, vol. 102, no. 2, p. 022311, 2020.

Logic gates based on nonlinear oscillators

M. Bonnin¹, F. Bonani¹ and Fabio L. Traversa²

¹ Dept. of Electronics and Telecommunications, Politecnico di Torino Turin, Italy

² MemComputing Inc. San Diego, CA, USA

For almost a century, the von Neumann architecture has been the standard reference for the design of electronic computing machines, especially for the general purpose ones. Its most basic description encompasses an input module, a central processing unit, a memory bank and an output module. Sets of instructions (programs) can be written in the memory, and the processing unit accesses the program and processes input data performing a sequence of operations, including reading and writing repeatedly the memory, before ending the program and returning the output [1]. However, the same design naturally reveals its drawbacks, such as the famous von Neumann bottleneck [1], dictating that the system throughput is limited by the data transfer between CPU and memory, as the majority of the computation energy is used for the data movement rather than for the actual computation [1]. Recently, novel or rediscovered alternative architectures for computation have been proposed. Among others, non- conventional computing solutions based on the use of oscillators as building blocks for both von Neumann and non-von Neumann architectures have been revived. They were initially introduced independently by Goto [2], [3] and von Neumann [4] in the 1950s. In this paper we present a theoretical framework for the analysis of networks of coupled nonlinear oscillators, and the design of logic gates based on this type of dynamical systems. Networks of coupled nonlinear oscillators exhibit collective behaviors in the form of stable synchronous oscillations. In our architecture, information is encoded in the phase difference between oscillators, and computation is performed by manipulating these phase differences through ingenious design of the couplings. First we give a rigorous definition for the phase of nonlinear oscillators of arbitrary order. The definition is based on the concept of the asymptotic phase or isochrons [5]. The definition permits to measure the phase of oscillators exploiting a linear decomposition based on Floquet's theory, and is suitable to be applied to practical nonlinear oscillators, such as the van der Pol oscillator or Chua circuit. Second we show how a phase equation, e.g. an equation for the time evolution of the oscillators' phases, can be derived from the state equations. The derivation procedure is based on the application Floquet's theory, and it is valid irrespective of the nature of the oscillators (electrical/electronic circuits, mechanical systems, biological or neural systems, ...). The phase equation greatly simplifies the analysis of the network dynamics. In fact for a network composed by N nonlinear oscillators of order n , the research of stable synchronous oscillations in a system of $n \times N$ ordinary differential equations (ODEs), is reduced to the research of stable equilibrium points in a system of N ODEs. Stability analysis is simplified as well. Finally we show how the phase equation can be used to design logic gates, that implement a complete set of logic operation (NOT, OR, and AND). The

procedure is based on a proper design of the couplings between the oscillators, in such a way that the stable synchronous states correspond to the desired set of phase relationships between the oscillators. We show architectures for the basic logic gates, that can be easily implemented and scaled to realize bio-inspired architectures that implement Boolean logic. The proposed architecture offers several relevant advantages. In particular, the resulting logic gates are reciprocal, in the sense that there is no distinction between input and output terminals. For instance for the proposed NOT gate, any of the two terminals can be used as input, and the other as the output. For a three terminals gate, such as a NOT or an AND gate, any pair of terminals can be used as inputs, and the remaining one as the output. We discuss the advantages of reciprocal logic gates in terms of scalability and self organizing properties of the network. As an example, we apply the theoretical framework to networks of coupled van der Pol oscillators. We show how the couplings can be designed in such a way, that the proposed architectures realize a complete set of logic gates. Networks for NOT, AND and OR logic gates are presented. Results are supported by numerical simulations.

References

- [1] J. L. Hennessy and D. A. Patterson, *Computer Architecture, sixth Edition: A Quantitative Approach*. San Francisco, CA, USA: Morgan Kaufmann Publishers Inc., 2017.
- [2] E. Goto, "New parametron circuit element using nonlinear reactance," *KDD Kenkyu Shiryo*, 1954.
- [3] E. Goto, "The parametron, a digital computing element which utilizes parametric oscillation," *Proceedings of the IRE*, vol. 47, pp. 1304–1316, aug 1959.
- [4] J. von Neumann, "Non-linear capacitance or inductance switching, amplifying, and memory organs," patent # US2815488A, 1954.
- [5] A. T. Winfree, "Biological rhythms and the behavior of populations of coupled oscillators," *Journal of Theoretical Biology*, vol. 16, pp. 15–42, jul 1967.

Spontaneous symmetry breaking in identically coupled inhibitory neural masses with adaptation

A. Ferrara¹, S. Olmi^{2,3}, D. Angulo-Garcia⁴, Alessandro Torcini^{2,5}

¹Institut de la Vision, Sorbonne Universit ´e, Paris, France

²CNR - Consiglio Nazionale delle Ricerche - Istituto dei Sistemi Complessi, 50019, Sesto Fiorentino, Italy

³INFN, Sezione di Firenze, Via Sansone 1, I-50019 Sesto Fiorentino (FI), Italy

⁴Grupo de Modelado Computacional-Din ´amica y Complejidad de Sistemas, Instituto de Matem ´aticas Aplicadas, Universidad de Cartagena, Carrera 6 36-100, Cartagena de Indias 130001, Colombia

⁵Laboratoire de Physique Th ´eorique et Mod ´elisation, UMR 8089, CY Cergy Paris Universit ´e, CNRS, 95302 Cergy-Pontoise, France

Whisking is the rhythmic cyclic vibrissae sweeping action, consisting of repetitive forward (protraction) and backward (retraction) movements at an average frequency of about 8 Hz [3, 15, 16]. Whisking is controlled by a neuronal oscillator located in the vibrissa-related region of intermediate reticular formation of the medulla (vIRt) [5, 10, 11]. This region includes facial premotor neurons and neurons whose spiking activity is either in phase or in anti-phase with whisking protraction. In particular the vIRt nucleus in the medulla is composed of inhibitory neurons which innervate motoneurons of the vibrissa muscles [1]. Starting from the microscopic dynamics of quadratic integrate-and-fire (QIF) neurons, we construct and analyze an exact neural mass model of the vIRt circuit composed of two inhibitory coupled neuronal populations with adaptation and exponentially decaying synapses, with the purpose of finding a model able to explain the generation of a rhythm driving the whisking activity in rodents. An exact derivation is possible for networks of QIF neurons, representing the normal form of Hodgkin's class I excitable membranes [6], thanks to the analytic techniques developed for coupled phase oscillators [9, 12]. This exact neural mass model has been successfully employed to reveal the mechanisms at the basis of theta-nested gamma oscillations, the coexistence of slow and fast gamma oscillations and to model working memory [2, 4, 13, 14]. Each population is composed of N fully connected QIF neurons with exponential inhibitory synapses and adaptation. The dynamics of the membrane potential of each of the neuron V_i is governed by the following set of equations:

$$\tau \dot{V}_i(t) = V_i^2(t) + \eta_i + JS(t) - A_i(t) \quad (0.1)$$

$$\tau_A \dot{A}_i(t) = -A_i(t) + \frac{\alpha}{N} \sum_{k=1} \delta(t - t_k^i) \quad (0.2)$$

$$\tau_S \dot{S}(t) = -s(t) + \frac{1}{N} \sum_{k=1}^N \delta(t - t_k^N) \quad (0.3)$$

$$i = 1, \dots, N. \quad (0.4)$$

Here, τ is the membrane time constant, η_i is the excitability of the i -th neuron and J is the synaptic strength which is assumed to be identical for each synapse. Moreover, $S(t)$ is the global synaptic field accounting for the history of all the spikes emitted by the network at times t_k^N and has an exponential decrease with time constant τ_S . The adaptation variable $A_i(t)$ for each neuron accounts for the decreased excitability each time a neuron i emits a spike at times t_k^i . The level of decreased excitability is quantified by the parameter α and such adaptation decreases exponentially with time constant τ_A . The QIF network emits a spike at time t_k whenever $V_i(t_k^-) \rightarrow \infty$, and it is instantaneously reset to $V_i(t_k^+) \rightarrow -\infty$.

Following [7 – 9], assuming $N \rightarrow \infty$, it is possible to reduce the set of equations (1) via a mean field approach. Thus we can describe the dynamics of the average membrane potential $V(t)$ and instantaneous firing rate of the network $R(t)$ as

$$\tau \dot{R} = \frac{\Delta}{\tau \pi} + 2RV \quad (0.5)$$

$$\tau \dot{V} = V^2 + \bar{\eta} - (\pi \tau R)^2 + JS\tau - A \quad (0.6)$$

$$\tau_S \dot{S} = -S + R \quad (0.7)$$

$$\tau_A \dot{A} = -A + \alpha \tau R \quad (0.8)$$

In this work, various dynamical regimes can be observed thanks to the role played by the adaptation in guiding the emergent dynamics: periodic collective oscillations (in phase and in antiphase), asymmetric collective oscillations, asymmetric fixed points and various bistability regions in the parameter space. In addition to that, it is found that adaptation is a mechanism by which Cross-Frequency Coupling between theta and gamma frequencies can occur. We also introduce the effects of the pre-Bötzinger complex through an external inhibitory oscillating forcing and we study the phase locking between the two populations, in order to evaluate the forcing influence on both populations. It turns out that phase locked states are possible and there are cases in which the forced populations are not fully entrained with the external input.

References

[1] Adibi, M. (2019). Whisker-mediated touch system in rodents: from neuron to

behavior. *Frontiers in systems neuroscience*, page 40.

[2] Bi, H., Segneri, M., Di Volo, M., and Torcini, A. (2020). Coexistence of fast and slow gamma oscillations in one population of inhibitory spiking neurons. *Physical Review Research*, 2(1):013042.

[3] Carvell, G. E., Simons, D. J., Lichtenstein, S. H., and Bryant, P. (1991). Electromyographic activity of mystacial pad musculature during whisking behavior in the rat. *Somatosensory & motor research*, 8(2):159–164.

[4] Ceni, A., Olmi, S., Torcini, A., and Angulo-Garcia, D. (2020). Cross frequency coupling in next generation inhibitory neural mass models. *Chaos: An Interdisciplinary Journal of Nonlinear Science*, 30(5):053121.

[5] Deschênes, M., Takato, J., Kurnikova, A., Moore, J. D., Demers, M., Elbaz, M., Furuta, T., Wang, F., and Kleinfeld, D. (2016). Inhibition, not excitation, drives rhythmic whisking. *Neuron*, 90(2):374–387.

[6] Ermentrout, G. B. and Kopell, N. (1986). Parabolic bursting in an excitable system coupled with a slow oscillation. *SIAM journal on applied mathematics*, 46(2):233–253.

[7] Gast, R., Schmidt, H., and Knosche, T. R. (2020). A mean-field description of bursting dynamics in spiking neural networks with short-term adaptation. *Neural Computation*, 32(9):1615–1634.

[8] Montbrío, E. and Pazó, D. (2020). Exact mean-field theory explains the dual role of electrical synapses in collective synchronization. *Physical Review Letters*, 125(24):248101.

[9] Montbrío, E., Pazo, D., and Roxin, A. (2015). Macroscopic description for networks of spiking neurons. *Physical Review X*, 5(2):021028.

[10] Moore, J. D., Deschênes, M., Furuta, T., Huber, D., Smear, M. C., Demers, M., and Kleinfeld, D. (2013). Hierarchy of orofacial rhythms revealed through whisking and breathing. *Nature*, 497(7448):205–210.

[11] Moore, J. D., Deschênes, M., Kurnikova, A., and Kleinfeld, D. (2014). Activation and measurement of free whisking in the lightly anesthetized rodent. *Nature protocols*, 9(8):1792–1802.

[12] Ott, E. and Antonsen, T. M. (2008). Low dimensional behavior of large systems of globally coupled oscillators. *Chaos: An Interdisciplinary Journal of Nonlinear Science*, 18(3):037113.

[13] Segneri, M., Bi, H., Olmi, S., and Torcini, A. (2020). Theta-nested gamma oscillations in next generation neural mass models. *Frontiers in computational neuroscience*, 14:47.

[14] Taher, H., Torcini, A., and Olmi, S. (2020). Exact neural mass model for synaptic-based working memory. *PLoS Computational Biology*, 16(12):e1008533.

[15] Welker, W. (1964). Analysis of sniffing of the albino rat 1. *Behaviour*, 22(3-4):223–244.

[16] Wineski, L. E. (1983). Movements of the cranial vibrissae in the golden hamster (*Mesocricetus auratus*). *Journal of Zoology*, 200(2):261–280.

Robustness analysis of the weighted world air transportation network through its component structure

I. M. Diop¹, C. Cherifi², C. Diallo¹ and H. Cherifi³

¹ Université Gaston Berger, Saint Louis, Sénégal

² Université de Lyon 2, Lyon, France

³ Université de Bourgogne Franche-Comté, Dijon, France

The robustness of a system indicates its ability to withstand disturbances while maintaining its properties, performance, and efficiency. There are plenty of studies on the robustness of air transport networks in the literature. However, few works consider its mesoscopic organization. Building on the recently introduced component structure [1], we explore the impact of targeted attacks on the weighted world air transportation network on its local components. Indeed, its main features include five local components covering different regions (North America-Caribbean, Europe-Russia, East and Southeast Asia-Oceania, Africa-Middle East-Southern Asia, South America) and one global component scattered all over the world. We investigate attacks based on the Strength and the Weighted Betweenness. We use a weighted and undirected network originating from FlightAware [2]. It represents the flight information collected during six days (between May 17, 2018, and May 22, 2018). Nodes represent airports, and links represent the number of direct flights between airports. We extract the component structure of the world transportation network to evaluate the impact of a targeted attack on its regional and inter-regional constituents. The robustness evaluation process proceeds as follows:

1. Disconnect a node from the world air transportation network according to an attack strategy.
2. Disconnect the same node from its local component.
3. Disconnect the same node from the global component if possible.
4. Extract the giant component from the world air transportation network.
5. Extract the giant component from the concerned local component.
6. Extract the giant component from the global component.

This approach allows us to evaluate the impact of removing a critical airport in the world air transportation network on the robustness of the regional and inter-regional networks. Fig1 gives the LCC as a function of the fraction of top Strength and Weighted Betweenness nodes removed from the world air transportation network. It also reports

the corresponding LCC values of the large components. In addition, as the fraction of removed nodes increases, the components break away from the world air transportation network one after the other. In the two attack strategies, the different areas break away successively when removing a given fraction of critical airports from the world air transportation network. Nevertheless, the order of isolation of the regions differs. After the Strength attack, North America-Caribbean, East- Southeast Asia-Oceania, and South America leave the world air transportation network. South America, the North America-Caribbean, and the East and Southeast Asia-Oceania regions disconnect in this order after removing top Weighted Betweenness airports from the world air network. Finally, in both attack strategies, Africa-Middle East-Southern Asia separates from the Europe-Russia component. In addition, results show that in the Africa-Middle East- Southern Asia and South America regions, the removed critical airports cause severe damage. The weighted world air transportation network is more vulnerable to attack based on Weighted Betweenness than Strength. Indeed, fewer vital airports are required in the Weighted Betweenness to isolate the different regions. Nevertheless, in the case of the Weighted Betweenness attack, the LCC of the isolated components retains a high proportion of the initial component structure, keeping their regional performance. In contrast, in degree-based attacks, the LCC of the components are much smaller, and therefore travel is more challenging in what remains from the initial components. The component structure allows a better understanding of the resilience of the global air transportation network. Weighted Betweenness attack dismantles the world air transportation network rapidly by isolating large geographic areas. However, this vulnerability is relative since travel in these areas remains seamless. Future work will focus on developing attack strategies tailored to the component structure. We also plan to perform a comparative analysis with the unweighted world air transportation network.

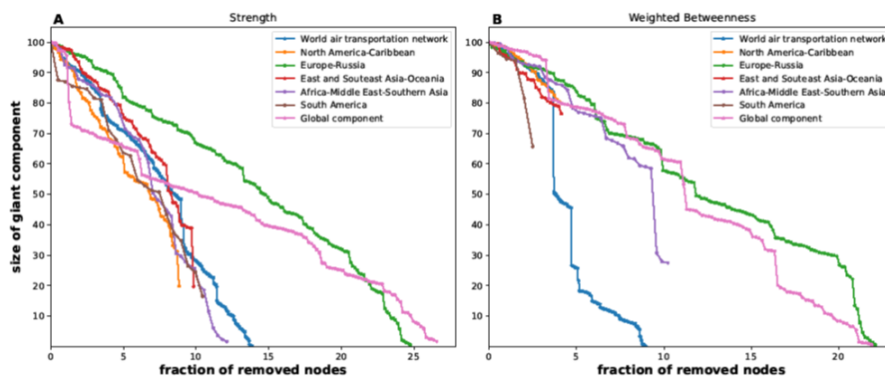


Figure 0.1: The size of the giant component of the world air transportation network, and the large components as a function of removed nodes under targeted attacks on the world air transportation network.

References

[1] I.M. Diop, C. Cherifi, C. Diallo, H. Cherifi: Revealing the component structure of the world air transportation network. *Applied Network Science* 6(1), 1–50 (2021)

[2] FlightAware: <https://flightaware.com/> (2018)

Optimal geometry of urban transport networks

M. Dahmanns¹

¹ Forschungszentrum Jülich, IEK-STE

Urban transport systems are gaining in importance, as an increasing share of the global population lives in cities and mobility-based carbon emissions must be reduced to mitigate climate change. Furthermore, pollution and congestion caused by car traffic generate severe adverse health effects. Thus, the share of public transport systems in urban traffic must be increased. However, building and maintaining public transport systems is expensive and congestion effects lower their quality, raising the question of how to optimise them to cope with these challenges. We analyse the optimal shape of urban transport networks under economical constraints with the objective to minimise the average travel time for commuters in the city. We propose a versatile numerical approach to find the optimal network geometry for different spacial city structures, travel modes and congestion models.

Criticality and its relationship to oscillatory brain dynamics

M. Deliano¹

¹ Behavioral Physiology Group, Combinatorial Neuroimaging Core Facility (CNI), Leibniz Institute for Neurobiology (LIN), Magdeburg

Criticality refers to the dynamics of complex systems at the edge of order and disorder. It has been studied in physical model systems like the avalanche dynamics of sand piles [1], and it has been successfully transferred to neurophysiological model systems describing the propagation of spike avalanches in cultured neural networks in vitro [2]. However, criticality in the intact brains of awake and behaving subjects is still poorly understood [3]. The brain displays an oscillatory dynamics, which is strongly related to cognition, and which still is a major focus of neuroscientific research. Whereas these oscillations have a defined temporal and often spatial scale, critical states are marked, within limits, by a scale-free distribution of activity across space and time [4]. Also, oscillatory brain dynamics is highly intermittent and non-stationary [5,6], whereas most measures of criticality are rather global, and assume a stationary dynamical state [4]. Moreover, on a macroscopic level, e.g. in the EEG and the MEG, the physiological nature of neural avalanches remains unclear, as EEG/MEG signals originate from a mixture of sources superimposed by volume conduction. Our goal is to address these questions by directly investigating the relationship between criticality and macroscopic brain oscillations. Therefore, we have carried out a frequency-specific analysis of criticality in the MEG. During the recording, subjects were brought in defined cognitive states, either through mindfulness breathing meditation or instructed mind-wandering [7]. In our analysis, we employed a two-step approach. We first assessed whether the macroscopic neural avalanche dynamics is scale-free by evaluating the goodness of a power-law fits of cascade size and duration distributions of MEG deflections in different frequency bands. Then, in a second step, we determined how close the power-law exponents were to a critical value of -1.5. We thoroughly evaluated power-law fitting by permutation testing, by fitting of alternative distributions, and by a cascade shape analysis. Finally, criticality was verified through hypothesized relationships of exponents of cascade size and duration distributions. The analysis showed that a scale-free near-critical dynamics was found in broad-band high-frequency (> 100 Hz)

MEG activity, but not in lower bands. Interestingly, high-frequency MEG activity has been associated with action potential firing. Thus, our results provide an interesting link between criticality of cascades of macroscopic spatiotemporal events in the MEG, and critical spike avalanches on a microscopic level in cell cultures. Notably, a change of mental state from mind-wandering to mindfulness meditation shifted the avalanche dynamics closer towards a critical point by a reduction of neural noise. Shifts of the network dynamics towards a critical point might promote the generation of meta-stable

patterns, allow for adaptation to changing environments, and might be associated with cognitive flexibility.

References

- [1] Bak P. *How Nature Works*. 2nd ed. copernicus; 1996
- [2] Beggs JM, Plenz D. Neuronal Avalanches in Neocortical Circuits. *J Neurosci*. 2003; 23(35):11167–77.
- [3] Cocchi L, Gollo LL, Zalesky A, Breakspear M. Criticality in the brain: A synthesis of neurobiology, models and cognition. *Prog Neurobiol*. 2017; 158:132–52.
- [4] Beggs JM, Timme N. Being critical of criticality in the brain. *Front Physiol*. 2012; 3 JUN(June):1–14.
- [5] Kozma R, Freeman WJ. Cinematic Operation of the Cerebral Cortex Interpreted via Critical Transitions in Self-Organized Dynamic Systems. *Front Syst Neurosci*. 2017 Mar 14;11:10.
- [6] Ohl FW, Deliano M, Scheich H, Freeman WJ. Early and late patterns of stimulus-related activity in auditory cortex of trained animals. *Biol Cybern*. 2003 May;88(5):374–9.
- [7] Dürschmid S, Reichert C, Walter N, Hinrichs H, Heinze HJ, Ohl FW, Tononi G, Deliano M. Self-regulated critical brain dynamics originate from high frequency-band activity in the MEG. *PLoS One*. 2020 Jun 11;15(6):e0233589.

How to see in high dimensions

D. Gurnari¹

¹ Dioscuri Centre in TDA, IMPAN

Visualization is a fundamental step of exploratory data analysis. However, it is (currently) impossible for humans to directly visualize high dimensional data. Many methods have been proposed to extract low dimensional representations, such as principal components analysis or multidimensional scaling, but such projections may cause loss of information and can be difficult to interpret. Mapper–type algorithms are tools from Topological Data Analysis that aim to provide qualitative descriptors of the shape of data, in the form of abstract graphs. Moreover, they can be used to visualize functions on top of high dimensional datasets. Such methods have been successfully used in a number of different applications such as medical data analysis, material science and economics. In this talk I will present both the original Mapper (Carlsson et al, 2007) and the Ball Mapper (D-lotko, 2019) algorithms. I will then discuss some recent extensions of the latter that allow to consider the underlying symmetries in the data and to explore the relations between different feature sets. I will provide examples using data from biology, computer vision and knot theory.

On Takens theorem And embedding methods

P. Dłotko¹, M. Lipiński¹, Justyna Signerska-Rynkowska¹

¹ Dioscuri Centre in TDA, IM PAN

The problem of deriving relevant information about, possibly, high dimensional system when only a time series of low dimensional observables is given, is still challenging for both real and theoretical dynamical systems. It often requires finding a good embedding for a time series and is connected with the spectrum of methods referred to as dynamic reconstruction. The celebrated Takens' Embedding Theorem ([3]) with its various generalisations, including [2], provides a mathematical background for reconstructing the dynamics from delay vectors and establishes conjugacy between reconstructed and original system. However, the choice of an appropriate embedding dimension and the time lag is not a trivial task for a finite time series or a finite part of a (discretized) trajectory. We mention most popular existing methods of finding the embedding dimension and the time-lag in order to reconstruct the underlying dynamics. In particular, we recall the False Nearest Neighbours (FNN) algorithm introduced in [1]. Next, we propose our extension of this algorithm that can be also used, among others, for testing systems conjugacy and existing relations or causality between two processes. Moreover, contrary to the classical FNN algorithm, our method provides clearer criterion (measure) for drawing conclusions on systems (semi-)conjugacy and thus enables assessing of the of quality of the obtained dynamics reconstruction.

References

- [1] M.B. Kennel, R. Brown, H.D.I. Abarbanel, Determining embedding dimension for phase-space reconstruction using a geometrical construction, *Phys. Rev. A* 45, 3403–3411 (1992)
- [2] T. Sauer, J.A. Yorke, M. Casdagli, *Embedology*, *J. Stat. Phys.* 65, 579–616 (1991)
- [3] F. Takens, Detecting strange attractors in turbulence. (1981) In: Rand D., Young LS. (eds) *Dynamical Systems and Turbulence*, Warwick 1980. *Lecture Notes in Mathematics*, vol 898. Springer, Berlin, Heidelberg

From a discrete orbit to a Dynamical features

P. Dłotko¹, M. Lipiński¹, Justyna Signerska-Rynkowska¹

¹ Dioscuri Centre in TDA, IM PAN

In this talk, we will briefly present two projects (in progress) aiming at extracting dynamical features from a finite input time series. The goal of the first project is to determine whether two time series come from qualitatively similar dynamical systems. The criterion for the developed similarity measures is based on the notion of topological conjugacy of dynamical systems. The conjugacy of two maps $f : X \rightarrow X$ and $g : Y \rightarrow Y$ requires the existence of a homeomorphism $h : X \rightarrow Y$ such that $hof = goh$. Since we have access only to a finite data set, it is impossible to determine the relation of time series rigorously. The False Nearest Neighbour (FNN) statistic is the leading example of a conjugacy test for a finite time series. The original purpose of it is to study the proper embedding dimension, i.e., the problem related to Taken's embedding theorem, where one usually compare the embedding of an input time series to a d and $d + 1$ dimensional space. Informally, FNN measures how a neighborhood of points in one embedding is disturbed when translated to the second embedding. In our work, we try to generalize the usage of FNN for testing the conjugacy of any two time series. Moreover, we introduce new statistics, inspired by FNN, that overcome some of the limitations of the base method. For instance, our KNN method extends the range of the tested neighborhood to k -nearest neighbors. Another statistic, ConjTest allows to compare two time series with different initial conditions, which is an assumption of the FNN adapted to our problem. However this approach requires the knowledge of the connecting homeomorphism h , which is an implicit part of a time series in case of FNN. The broader goal of this project is to build a benchmark that will allow us to study and compare different methods of measuring the similarity of dynamical systems given by time series. The second project aims in extracting an inner structure of an attractor under the assumption that the input time series behaves flow-like, i.e., $\|x_i - x_{i+1}\|$ is small. Using the theory of multivector fields and ball-mapper, we construct a combinatorial model of the dynamics. From the obtained model we may extract the critical areas of the phase space, like saddles, and construct a compact summary of the system using a newly developed concept of Morse pre-decomposition.

Emergence of undesired synchronisation of flexible loads in power grids with distributed frequency control

G. Ruzzene¹ D. Gomila¹ and P.Colet¹

¹ IFISC, Institute for Physics of Complex Systems (CSIC-UIB), Campus Universitat Illes Balears, 07122 Palma de Mallorca, Spain

The ecological transition towards more sustainable energy production presents various challenges for the operation of power grids, whose stable operations require generation-demand balance. Besides usual demand fluctuations the stability of the grid may be affected by the intermittent nature of renewable energy resources, such as wind and solar power. Despite the control mechanisms present in conventional power plants to adapt generation to demand, the increasing share of renewables within the energy mix calls for new control mechanisms that rely less on conventional control provided by the system operator and more on distributed control mechanisms on the demand side. This is particularly relevant on islands, since the small size of the power grid makes them more vulnerable to fluctuations. In this work we study the interplay between conventional primary and secondary controls in power plants and a distributed control protocol implemented through smart devices with flexible loads. In AC grids, frequency fluctuations are a proxy of the imbalance between demand and generation, thus we focus here on the analysis of such fluctuations on different scenarios. Our model consists of a conventional power plant with primary and secondary control [3, 4] coupled with N houses equipped with electric heat pumps. The temperature dynamics inside the houses follows two differential equations, for indoor and envelope temperatures and includes heat pump heating and thermostat control [2]. These heat pumps can be used as flexible loads for distributed control by combining the temperature thermostat control with a frequency control mechanism based on [1] which modifies the house heating cycle by advancing or postponing the turning on/off of its heat pump according to the measured frequency of the electric current. As a first scenario, we show that for short time scales (minutes), the control algorithm presented here is effective to reduce frequency peaks caused by abrupt changes in the demand. As a second scenario we consider the interaction of the distributed controllers on longer time scales (days). The demand profile is taken as a constant load plus the load coming from the heat pumps. We randomise the buildings thermal parameters and initial internal temperatures. Without distributed frequency control, heat pumps switch on and off at uncorrelated times leading to small frequency fluctuations as shown in Figure 1 (a). Once we activate the frequency control protocol described above we observe some large peaks in the frequency (Figure 1 (b)). This is due to the fact that a fraction of the houses are synchronised and they turn on/off

at the same time. We show that this synchronisation emerges from the interplay of conventional control in power plants and distributed control with flexible demand devices. This synchronised behaviour of the flexible loads is undesirable for the stability of the grid and one has to consider it when implementing distributed control mechanisms to reduce frequency fluctuations. The analysis of the mechanism behind synchronisation allows us to propose some possible solutions: the first one is to introduce a deadband in the frequency and the second one is to have a centralised controller that decides a maximum number of devices that can switch on/off at the same time.

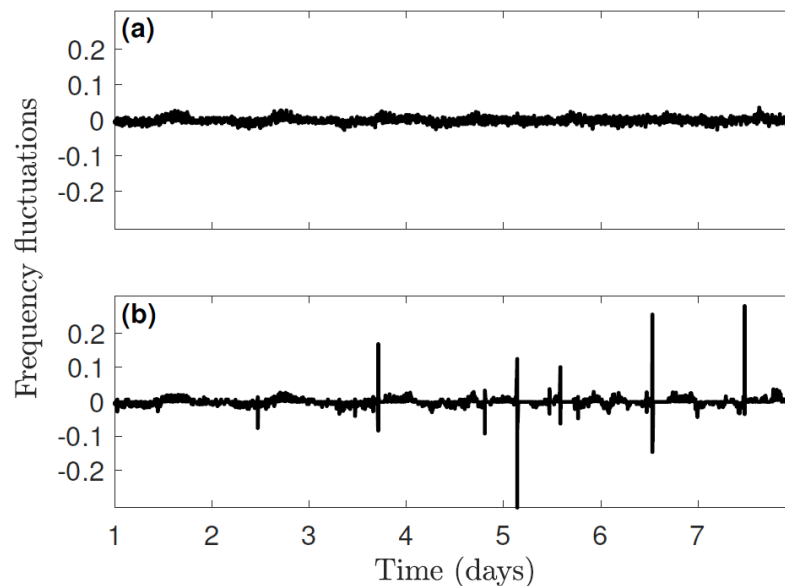


Figure 0.1: Frequency fluctuations caused by $N = 200$ houses equipped with electric heat pumps (consumption of 2.5 kW each) without frequency control (panel (a)) and with frequency control (panel (b)).

We acknowledge funding from the European Commission, Horizon 2020 program, grant agreement number 957852, Virtual Power Plants for Interoperable and Smart Islands.

References

- [1] M. Cheng, S.S. Sami, J. Wu, Benefits of using virtual energy storage system for powers system frequency response, *Applied Energy*, 194, 376-385 (2017).
- [2] A. P. Ramallo-Gonzalez, M. E. Eames, D. A. Coley, Lumped parameter models for building thermal modelling: An analytic approach to simplifying complex multi-layered constructions, *Energy and Buildings*, 60, 174-184, (2013).
- [3] H. Saadat, *Power system analysis*, McGraw Hill, (1999).
- [4] E. B. Tchawou Tchuisseu, D. Gomila, D. Brunner, P. Colet, Effects of dynamic-demand-control appliances on the power grid frequency, *Physical Review E*, 96, 2, 022302 (2017).

Robustness analysis of the weighted world air transportation network through its component structure

D. Segura¹, E. J. Khatib¹, J. Munilla² and R. Barco¹

¹ Telecommunication Research Institute (TELMA) University of Malaga Malaga, Spain

² Department of Communication Engineering University of Malaga, Malaga, Spain

In the 3GPP LTE Release 13, NB-IoT was standardized to provide wide-area connectivity for IoT. To optimize network signalling and power consumption, control plane (CP) optimization was introduced. In Release 15, to support infrequent small data transmissions, Early Data Transmission was also included, in which the data are sent during the random access procedure. Thus, this paper analyses the latency performance of the different NB-IoT optimizations for the CP. The study, carried out in a real device, has been performed for different packet sizes and coverage levels. Evaluation results show lower latencies for EDT, particularly with small packets, where a reduced transport block is used, being more efficient from a network point of view. Additionally, we verify that EDT, unlike Release 13 optimization, fulfills 3GPP latency requirement for extreme coverage.

Optimal Practical Design and Reduced Complexity of 6G sub-Terahertz Wireless Backhaul Networks

E. M. H. Shalma¹, M. M. H. Shalma²

¹ Faculty of Computer science Tanta university, Tanta, Egypt

² Faculty of Information Engineering Technology, The German university in Cairo, Cairo, Egypt

With the 6G being required to deliver data rates exceeding 100 Gbps for a single user, suitable wireless backhaul networks should be properly designed to carry these data to the backhaul network. In this paper, the complexity and practical aspects of designing these links in the sub-terahertz band with hardware power limitations, frequency selectivity, severe path loss, beam misalignment, coupling and noise figure losses is addressed with optimal power allocation where a new reduced complexity power allocation algorithm is proposed to realize faster data processing and lower computational delay and provide the effect of these factors on system performance. The bit rate achieved is expected to exceed 1 Tbps for 1 km using practical antennas and practically realized power sources from the literature.

Autonomous monitoring framework for cellular networks

J.A. Trujillo¹, I. de-la-Bandera¹, J.Burgueño¹, D. Palacios² and R. Barco²

¹ Telecommunication Research Institute (TELMA) University of Malaga Malaga, Spain

² Tupl Spain Tupl Inc., Malaga, Spain

The arrival of a new generation of mobile networks as 5G (5th Generation), brings with it greater complexity in the management of the network due to new services and scenarios. In this context, SON (Self-Organizing Networks) becomes a key factor, given its ability for automate tasks and reduce human workload. Monitoring the network turns out be a crucial task, as it acts as the basis for the other SON functions. This paper proposes a methodology for automate monitoring of mobile networks based on their KPI (Key Performance Indicator).

ADRC Control for a Single-Stage Photovoltaic System Connected to the Three-Phase Electrical Grid

A. Boukhriss¹

¹ SAEDD, Higher School of Technology of Essaouira Caddy Ayad University, Morocco

The aim of this work is to study the active disturbance rejection control ADRC associated with incremental conductance IC (ADRC-IC) applied to the single-stage grid-connected PV system under atmospheric variation conditions to control the maximum power point MPP. The control technique is compared with the conventional P&O control. ADRC is also used to control the inverter, connected to the grid through a RL filter, to keep the DC bus voltage constant with respect to the reference provided by the MPP control block and to ensure a unity power factor for the power injected into the grid.

I. SYSTEM STRUCTURE

The model studied consists of a single-stage PV system connected to the grid. The MMP block provides the DC bus voltage reference corresponding to the maximum power point. The grid is connected to the inverter via a filter and a DY transformer whose secondary winding (high voltage) is connected to the grid. A filter consisting of a resistor R_g in series with an inductance L_g is used to reduce the harmonics generated by the use of power electronics semiconductors (IGBTs-Diodes). The photovoltaic field formed by modules in series and strings in parallel produces 300 kW under standard test conditions (1000 w/m² and 25°C). A 300 kW load, inserted between buses 1 and 2, consumes the power produced by the PV, and in case the PV power is insufficient, it takes the deficit from the grid. Figure 1 shows the schematic diagram of the studied model.

RESULTS AND SIMULATIONS

To evaluate the effectiveness of the control, the system is subjected to a step change in irradiance from 1000 w/m² to 800 w/m² at time $t = 0.6$ s and a second step change from 800 w/m² to 1000 w/m² at time $t = 1.3$ s. The temperature is also varied from 25 °C at time $t = 1$ s to 45 °C, followed by a variation from 45 °C to 25 °C at time $t = 1.6$ s (Fig. 2).

References

[1] [1] A. Boukhriss, A. Essadki, A. Bouallouch, T. Nasser, "Maximization of generated power from wind energy conversion systems using a doubly fed induction generator with active disturbance rejection control," Second World Conference on Complex Systems (WCCS), pp. 330-335, 2014. doi:10.1109/ICoCS.2014.7060907

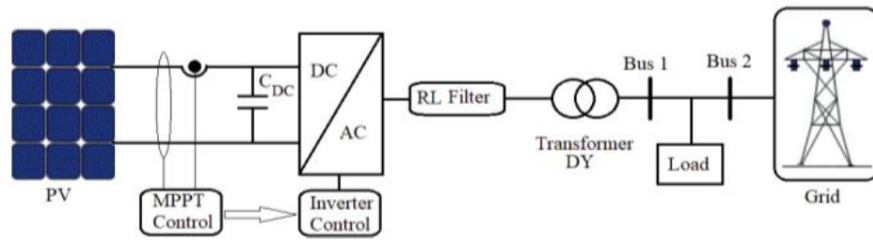


Figure 0.1: Schematic diagram.

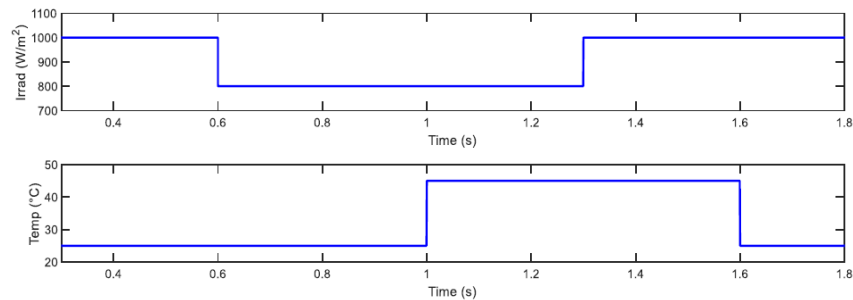


Figure 0.2: Irradiation and temperature variations.

Accessing signatures of criticality in neuronal data using maximum entropy models

P. V. Carelli¹

¹ Federal University of Pernambuco, Brazil

Introduction: Since the pioneer work from Beggs and Plenz [1] reporting neuronal avalanches in cultured cortical slices, the idea that the brain operates in a critical state has gained traction. Since then, most studies obtain signatures of criticality from exponents of size and duration power law distributions of neuronal avalanches[2]. Here we use a completely different and independent approach [3], employing a maximum entropy model to test whether signatures of criticality appear in urethane-anesthetized rats[4]. *Materials and Methods:* We implanted 64-channel silicon probes (BuzsakiA64sp, Neuronexus). All data were sampled at 30 kHz, amplified and digitized in a single head-stage Intan RHD2164. All recordings were analyzed up to a duration of 3 h. After recordings, spike sorting was performed using the Klusta-Team software on raw electrophysiological data. Following Mora et al. [3], a Boltzmann-like distribution is defined. We consider as observable the firing rates K_t , and constrain the probability distribution in two different times, t_1 and t_2 , obtaining the energy function. We then solve an inverse problem to fit the model parameters to the data statistics. Once the model is adjusted to describe the data, we can

perform statistical physics analysis, and the signatures of criticality are obtained from the divergence of the model's generalized specific heat. Results: Using a maximum entropy approach, we found a divergence of the model's generalized specific heat, as the number of experimentally sampled neurons increases (Fig. 1). Since under urethane anesthesia the cortex also slowly drifts along cortical states, we plot the normalized critical temperature obtained as a function of the cortical state inferred by the coefficient of variation of the cortical firing rate. We find an universal curve that collapses the results from all subjects. Finally, we also present preliminary results from spiking neurons model data, where this model successfully differentiate critical from noncritical cases when avalanche analysis is inconclusive.

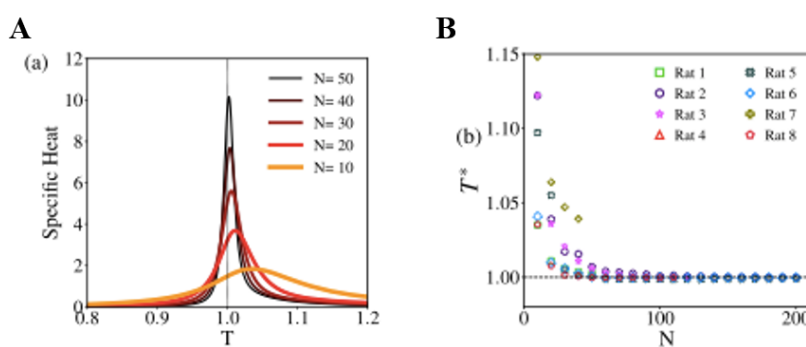


Figure 0.1: Specific heat as a function of the number of neurons sampled. A) Example of the specific heat curves for one subject. B) Peak statistical temperature of the specific heat as a function of the number of neurons sampled for different subjects.

Discussion/Conclusion: We identify signatures of criticality in cortical data using a maximum entropy approach based on the neuronal population firing rates. This method is independent from traditional approaches that rely on the estimation of critical exponents from neuronal avalanches size and duration power law distributions. This approach is particularly valuable when markers of criticality from neuronal avalanches are methodologically flawed or inconclusive.

References

- [1] J. M. Beggs and D. Plenz, Neuronal avalanches in neocortical circuits, *J. Neurosci.* 23, 11167 (2003).
- [2] A. J. Fontenele, N. A. P. de Vasconcelos, T. Feliciano, L. A. A. Aguiar, C. Soares-Cunha, B. Coimbra, L. Dalla Porta, S. Ribeiro, A. J. Rodrigues, N. Sousa et al., Criticality between Cortical States, *Phys. Rev. Lett.* 122, 208101 (2019).
- [3] T. Mora, S. Deny, and O. Marre, Dynamical Criticality in the Collective Activity of a Population of Retinal Neurons, *Phys. Rev. Lett.* 114, 078105 (2015).
- [4] Lotfi, N., Feliciano, T., Aguiar, L.A.A., Lima Silva, T.P., Carvalho, T.T.A., Rosso,

O.A., Copelli, M., Matias, F.S., Carelli, P.V.: Statistical complexity is maximized close to criticality in cortical dynamics. *Phys. Rev. E* 103, 012415 (2021).

Critical cells in the primary visual cortex

V. M. B. Da Silva¹, A. J. Fontenele², C. Soares-Cunha^{3,4}, A. J. Rodrigues^{3,4}, N. Sousa^{3,4}, P. Carelli⁵, N. A. P. de Vasconcelos^{1,3,5}

¹ Biomedical Engineering Department, Federal University of Pernambuco (UFPE), Recife, PE 50670-901, Brazil,

² Department of Physics, University of Arkansas Integrative Systems Neuroscience Group, University of Arkansas, Fayetteville, AR 72701, USA,

³ Life and Health Sciences Research Institute (ICVS), School of Medicine, University of Minho, Braga 4710-057, Portugal,

⁴ ICVS/3Bs-PT Government Associate Laboratory, 4806-909, Braga/Guimarães, Portugal,

⁵ Physics Department, Federal University of Pernambuco (UFPE), Recife, PE 50670-901, Brazil.

Introduction: Since Adrian's studies [1] in the 1920s, we know that nerve cells can fire at a given rate distribution as a way to code information in the nervous system, mainly in sensory processing and navigation [2], [3]. The recent technological developments in simultaneous dense recordings of neuronal activity enabled us to understand the information processing in nervous systems way beyond the single neuron activity [4]. For instance, those advances enabled us to do simultaneous recordings from the spiking activity of large neuronal populations in brain areas, including the primary visual cortex (V1) [5], [6]. Such detailed data paved the way for the sophisticated study of spiking activity from those large neuronal populations. The first experimental support for the critical brain hypothesis took place with Beggs and Plenz in 2003. Recently, using V1's spiking data from both anesthetized and freely moving animals, we have shown that a phase transition occurs in an intermediate level of population spiking activity variability [7]. Herein, we evaluated the firing rate distributions of individual well-isolated cells from those neuronal populations, along with a sample of the diversity of states assumed by those neuronal populations. Do the individual firing rate distributions of V1's neurons depend on the dynamics properties observed in the nearby neuronal population? *Materials and Methods:* These preliminary experimental data are based on the simultaneous recording of extracellular activity in deep layers of the primary visual cortex of urethane-anesthetized rats (n=3, male rats, 350-500g, 3-6 months of age). The recordings last approximately 2 hours, based on a 64-channels recording system, distributed among 6 shanks separated by 200um. All analyzed data herein are initial 2h-long after the first 30min (tissue accommodation period). We used the coefficient of variation (CV) of that neuronal population spiking data (bin size=50ms, window=10s) as a proxy for the cortical state. For each individual neuron (n=285, single-unit activity), we compared (Mann-Whitney U) the firing rate distributions among three different levels of variability (low, intermediate and high) assumed by the neuronal population. *Results:* Figures 1(a-b) show samples of

boxplots of firing rate distributions of 2 neurons ($n = 285$), in three different levels of variability (low, intermediate and high). Taking into consideration comparisons in which we found a strong statistical differences among firing distributions during different cortical states: 191/138 neurons displayed a difference between low/high and intermediate levels of variability, respectively; while 94 neurons displayed a difference between low/high and intermediate levels of variability when compared with both extreme levels (L, H).

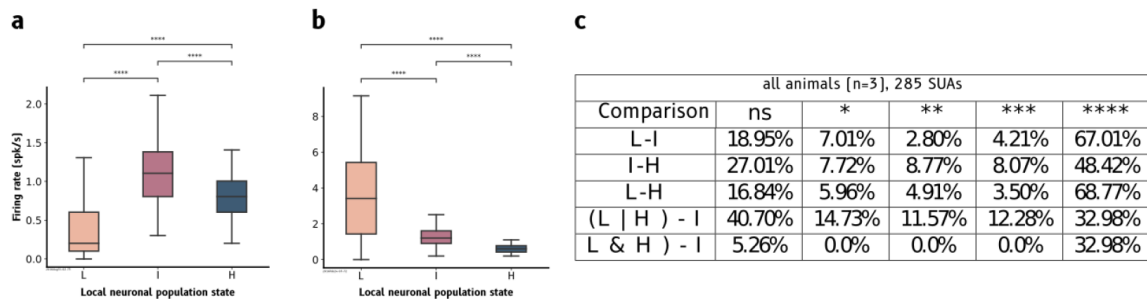


Figure 0.1: (a-b): samples of boxplots of firing rate distributions of V1's neurons, from different animals, along different levels of variability on the neuronal population activity: intermediate (I) level of CV, when compared with other levels (L: low, I:H:high, (L: low, I:H:high, *** : $p \leq 0.0001$, *** : $0.0001 < p \leq 0.001$, ** : $0.001 < p \leq 0.01$, * : $0.01 < p \leq 0.05$, ns: $0.05 < p \leq 1$, Mann-Whitney-U); (c): table with group data ($n = 3$ animals).

Discussion/Conclusion: Our work suggests that a significant fraction of neurons in the primary visual cortex is able to display a peculiar firing rate distribution along with different cortical states. Further, we found a significant fraction of neurons in V1 which display a peculiar firing rate distribution when its population activity shows strong signatures of criticality. Together, the results suggest a noteworthy fraction of neurons in V1 have significant rate code specificity for some cortical state. More specifically, the last result suggests significant rate code specificity for criticality in a remarkable fraction of neurons in V1.

References

- [1] E. D. Adrian and Y. Zotterman, "The impulses produced by sensory nerve-endings: Part II. The response of a Single End-Organ.," J Physiol (Lond), vol. 61, no. 2, pp. 151–171, Apr. 1926, doi: 10.1113/jphysiol.1926.sp002281.
- [2] D. H. Hubel and T. N. Wiesel, "Receptive fields of single neurones in the cat's striate cortex.," J Physiol (Lond), vol. 148, pp. 574–591, Oct. 1959, doi:10.1113/jphysiol.1959.sp006308.
- [3] T. Solstad, C. N. Boccara, E. Kropff, M.-B. Moser, and E. I. Moser, "Representation of geometric borders in the entorhinal cortex.," Science, vol. 322, no. 5909, pp. 1865–1868, Dec. 2008, doi: 10.1126/science.1166466.
- [4] I. H. Stevenson and K. P. Kording, "How advances in neural recording affect data analysis.," Nat. Neurosci., vol. 14, no. 2, pp. 139–142, Feb. 2011, doi: 10.1038/nn.2731.

- [5] N. A. P. de Vasconcelos, C. Soares-Cunha, A. J. Rodrigues, S. Ribeiro, and N. Sousa, "Coupled variability in primary sensory areas and the hippocampus during spontaneous activity.," *Sci. Rep.*, vol. 7, p. 46077, Apr. 2017, doi: 10.1038/srep46077.
- [6] A. Bragin, J. Hetke, C. L. Wilson, D. J. Anderson, J. Engel, and G. Buzsáki, "Multiple site silicon-based probes for chronic recordings in freely moving rats: implantation, recording and histological verification.," *J. Neurosci. Methods*, vol. 98, no. 1, pp. 77–82, May 2000, doi: 10.1016/s0165-0270(00)00193-x.
- [7] A. J. Fontenele et al., "Criticality between Cortical States.," *Phys. Rev. Lett.*, vol. 122, no. 20, p. 208101, May 2019, doi: 10.1103/PhysRevLett.122.208101

Motor-Dependent Synaptic Balance Modulation and Critical Phenomena in the Subthalamic Nucleus: A New Framework for Adaptive Deep Brain Stimulation

D. C. Soriano¹, B. L. Bianqueti¹, L. R. Trajano¹, A. Fim Neto¹, J. B. de Luccas¹, T. P. Almeida², A. K. Takahata¹, M. S. Rocha³, N. A. P. de Vasconcelos⁴, S. J. Nasuto⁵, F. Godinho^{1,3,6}

¹Federal University of ABC, Brazil

²University of Leicester, Leicester, UK

³Santa Marcelina Hospital, Brazil

⁴Federal University of Pernambuco, Brazil

⁵University of Reading, UK

⁶University of São Paulo, Brazil

Introduction: The power spectrum density (PSD) of local field potential (LFP) provides valuable electrophysiological information at the micro and meso neuronal scales. Recent works have shown that the LFP PSD decay is a result of intricate interactions between fast synaptic (e.g., glutamatergic) excitatory currents and slow inhibitory synaptic (e.g., GABAergic) activity [1]. Moreover, $1/f^\alpha$ PSD decay has also been extensively investigated in the context of scale-free statistics and neuronal avalanches defining crucial signatures for critical phenomena [2]. The present study aims to show that the decay (α -parameter) of the subthalamic nucleus (STN) LFP PSD exhibits a power-law at the beta frequency range, which can be selectively modulated by movement activity in Parkinson's disease (PD) patients. These findings contribute with evidence to motor-induced synaptic balance changes at the STN level and for the possible underlying role of critical phenomena at beta range, which opens the perspective for a whole set of new markers aiming for adaptive deep brain stimulation (aDBS).

Materials and Methods: STN-LFPs were recorded (24 kHz) during surgery for DBS electrodes implanted in 24 patients for 60s (totaling 35 LFP recordings, 13 bilateral and 9 unilateral) in rest and active arm flexion movement. Recordings were notch filtered and z-score normalized before PSD evaluation through the Welch method. Spectral decay (α) was estimated in the log (PSD) vs. log (f) using spectral windows of 8 Hz width in steps of 1 Hz through the spectrum (13-45 Hz). The p-values for decay (α -parameter) comparison between rest and movement conditions across the spectrum were obtained by permutation tests and corrected by multiple comparisons.

Results: STN-LFPs PSD for the PD population show a linear decay in beta band in the log x log plot suggesting a power-law behavior (Figure 1A). The differences between rest and movement decays are selectively observed for central frequencies (CF) within 24 to 28 Hz (Figure 1B) interval. The CF at 26 Hz (i.e., 22 – 30 Hz band) best discriminates

motor activity ($p < 0.0001$, $N=35$, Figure 1C).

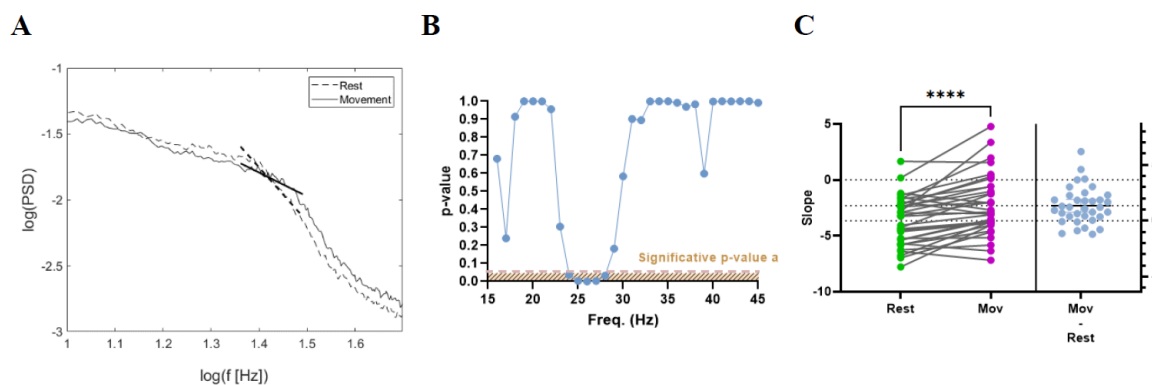


Figure 0.1: A – log (PDSm) vs. log (f) plots of STN-LFP under rest (dashed line) and movement for the PD population. PSDm denotes the mean of PSD. B – Corrected p-values for α -parameter across CF concerning rest vs. movement comparison. C – α -parameter values for rest and movement conditions (left) and the difference between them (right).

Discussion/Conclusion: Our work suggests a movement-dependent decay modulation within the beta band for PD patients on STN-LFP, the main target for treating PD motor symptoms. This synaptic-based (or, possibly, other criticality-based) feature can outline a new investigating paradigm for PD pathophysiology and define new markers to aDBS strategies.

References:

- [1] Gao R et al. doi: 10.1016/j.neuroimage.2017.06.078.
- [2] Lombardi et al. doi: 10.1063/1.4979043

Ongoing long-range temporal correlations in broadband EEG and intracortical neural activity during voluntary movement

M. Wairagkar^{1,2}, Y. Hayashi² and S. J. Nasuto¹

¹University of California, Davis

² University of Reading

Long-range temporal correlations (LRTCs) are ubiquitously present in several neuronal processes at different scales from mesoscopic Electroencephalography (EEG) to microscopic multi-unit neural activity. EEG is composed of both oscillatory and arrhythmic broadband components, however, there is more focus on studying oscillatory processes. Temporal dynamics of arrhythmic broadband EEG have not been investigated before and were considered as background noise. Here, we explore temporal dynamics of arrhythmic components by investigating long-range temporal correlations in broadband EEG during voluntary movement paradigm.

LRTCs are typically characterised in the amplitude envelope dynamics of the narrow alpha band EEG oscillations over long timescales. This LRTC is considered as an invariant property of EEG over such long timescales spanning several seconds to hours. However, in this study we demonstrate that broadband EEG also contains long-range temporal correlations, and in fact these LRTCs show ongoing changes over short timescales during voluntary movement. Additionally, we also studied simultaneous changes in short-term dependencies in broadband EEG. We developed the process to characterise these instantaneous dynamics of both short- and long-range temporal correlations in broadband EEG. We first estimated the scaling coefficient for LRTC using detrended fluctuation analysis (DFA) [1] and then modelled these temporal dynamics using autoregressive fractionally integrated moving average (ARFIMA) model [2] on very short 2 s broadband EEG segments. A significant increase was observed in the broadband LRTC ($p < 0.05$) in EEG over motor cortex during voluntary movement intention, execution, and imagination. This indicates that broadband LRTC is not time-invariant and changes instantaneously accompanied by complementary changes in short- range correlations.

We have applied broadband LRTC to detect finger tapping movement intention in EEG with high accuracy which has applications in brain-computer interfaces. We were able to detect movement intention approximately 1 s prior to its onset with the accuracy of $88.3 \pm 4.2\%$ in single EEG trials using short- and long-range temporal correlations determined by DFA and ARFIMA. We were also able to detect different types of movement imagery and execution of fist and feet accurately. These changes in the broadband LRTC are complementary to the changes in the oscillatory band power (event-related desynchronisation) and movement-related cortical potentials that are traditionally used to detect movement. Broadband LRTCs are also complementary to the conventional

LRTCs obtained from narrowband oscillations.

Finally, applying broadband analysis using DFA to publicly available intracortical neural data [3,4] also revealed long-range temporal correlations in the multi-unit neural activity and local-field potentials (LFPs) recorded using micro-electrode array implanted over hand area of motor cortex. Similar increase in LRTC was observed in the intracortical neural dynamics including LFPs and spiking activity over 0.2-0.5 s timescales during voluntary movement in monkey and human participants. We were able to detect movement intention 1 s prior to its onset with accuracies of 95.121.06% on single trial basis in intracortical neural activity.

Broadband LRTC is hence a novel complementary neural correlate of movement which evolves instantaneously enabling detection of movement intention and imagery over short timescales. Thus, broadband LRTC is a fundamental property of neuronal dynamics that is present in processes at different scales from EEG, LFP to neural spiking activity.

References:

- [1] M Wairagkar, Y Hayashi, SJ Nasuto, "Dynamics of long-range temporal correlations in broadband EEG during different motor execution and imagery tasks", *Frontiers in Neuroscience*, 15, 660032, 2021.
- [2] M Wairagkar, Y Hayashi, SJ Nasuto, "Modeling the ongoing dynamics of short and long-range temporal correlations in broadband EEG during movement", *Frontiers in Systems Neuroscience*, 13, p.66, 2019.
- [3] T Brochier, L Zehl, Y Hao, et al., "Massively parallel recordings in macaque motor cortex during an instructed delayed reach-to-grasp task", *Scientific data*, 5 (1), 2018.
- [4] FR Willett, DT Avansino, LR Hochberg, et al., "High-performance brain-to-text communication via handwriting", *Nature*, 593(7858), p.249-254, 2021.

Agent-based and Logistic population growth models comparison

Andrei Aleksandrov¹

¹ LUT University, Lappeenranta, Finland

Simulation and analyses of the systems with interacting agents is a wide field of research. The agent-based models allow to simulate a very complex phenomena using a simple rule set for individual agents. Large number of studies were performed in the area of population growth, covering different phenomena using variety of approaches from non-formal agents' interaction description to mathematical models. The aim of the current study was to create an agent-based population growth model with multiple adjustable parameters and compare it with an equation-based Logistic population growth model. Both models of population growth were built using NetLogo software for the convenience of comparison. Large variety of settings was attempted for the comparison, such as population size, available space for agents, etc. Agent-based model population dynamics turned out to be comparable on the qualitative level to the Logistic model for a limited number of the initial parameters. However, for some initial values Logistic model population dynamic converges towards a certain population level, which was not obtained for the Agent-based model. The agent-based models allow us to simulate population growth with much more wide set of settings, than that of an equation-based logistic model. This research focuses on analyzing the differences and similarities observed in the behavior of these two models in order to get better understanding of population growth phenomenon and how to simulate it.

References

[1] Garland, J., Bradley, E. (2013). On the Importance of Nonlinear Modeling in Computer Performance Prediction. In: Tucker, A., Höppner, F., Siebes, A., Swift, S. (eds) Advances in Intelligent Data Analysis XII. IDA 2013. Lecture Notes in Computer Science, vol 8207. Springer, Berlin, Heidelberg

Blockchain Based Platform for Sensitive Medical Data Management

J. Plucar¹, M. Szczypka¹

¹ Department of Computer Science, FEI VSB-Technical University of Ostrava, Ostrava, Czech Republic

There are many ways to manage and store a patient's electronic medical record (EMR). Unfortunately, recently there has been a significant increase in the number of cyberattacks on hospitals [1] [2], that lack the resources and expertise to prevent attacks. From an EMR management perspective, this can be a significant problem, as there may be situations where a system based on one centralized server becomes unavailable and patient information doesn't reach the doctor in time. Additionally, the data could be modified or deleted altogether. Therefore, the use of Blockchain technology is proposed in this article. Blockchain can be used as a decentralized storage, meaning that the data will not be stored only in one place and therefore the system will be more resistant to failures. At the same time, Blockchain ensures the immutability and transparency of all stored information. All of these features present a unique opportunity to develop a secure and trustworthy EMR data management solution. Another problem that the use of Blockchain can solve is the controlled sharing of EMR [3]. Each hospital or specialist often has its own database, which creates time and logistics problems when transferring records. Several authors have worked on a similar idea, and this article builds and expands on some of the previously published results. One of the papers mentioning the applicability of Blockchain technology in conjunction with healthcare data was the work of Yue et al [4]. In their work, the authors presented the possible positive impacts of using Blockchain technology and proposed an application based on its principles called the Healthcare Data Gateway (HDG). HDG allows patients to easily and securely own, control, and share their own data without compromising their privacy, representing a potentially new way to improve the intelligence of healthcare systems while preserving patient privacy. The requirement for trustworthiness, data integrity, and access control has been and is still a major concern. The authors of [5] have addressed this problem and in their paper they emphasize on designing a secure and efficient mechanism for concurrent data sharing. The proposed system, whose implementation is based on the Ethereum platform [6], offers the addition or retrieval of patients' health data by an authorized physician, but only with the consent of the individual patient. Data integrity is discussed in detail by the authors in [7]. The papers present a medical data preservation system (DPS). This DPS provides a reliability data storage solution that ensures the primitiveness and verifiability of the stored data while protecting the user. The paper focuses on the situation where data may be damaged and its recovery process. Some eHealth projects are already using Blockchain and achieving great success. However, they still face some challenges and obstacles, which the authors of SPChain [8] are trying to solve. In the paper, the authors mention that a system based on public Blockchain is not entirely appropriate. Therefore, they have

chosen their own implementation of Blockchain which contains special key blocks and micro blocks to store their EMR in. SPChain is also implementing a reputation system to incentivize healthcare facilities to use it. The above articles are not isolated, other papers [9], [10], [11], deal with the same topic in a similar approach. Since the data in Blockchain is transparent and available to everyone, there is a possibility to create various analyses over this data. Transactions can be transmitted, aggregated, and anonymized; this would create an anonymized data layer that would allow real-time analysis of transactions on the Blockchain by the scientific community. Experts and doctors around the world could use this data to build various prediction models. The models could identify or look for health problems in patients, even at an early stage of disease development. In this article we are proposing an architecture of complex EMR management system. Key features of the proposed solution are:

- Decentralization and transparency: there is no central node in Blockchain, all nodes are equal. All transactions and data are recorded in multiple locations.
- Tamper-proof: The use of blockchain provides tamperproofing by creating a record that cannot be altered. Thus, Blockchain helps prevent fraud and unauthorized activities.
- Traceability: Blockchain creates an audit trail that documents the origin of the EMR at every step of its journey. This allows the data to be used to track disease progression and potentially create predictive models.
- Privacy: Using a combination of generic identifiers and well- encrypted storage outside the blockchain, a solution can be created that offers full privacy.
- Legislative standards compliance: the solution attempts to design an architecture that would offer the ability to meet the legislative requirements for data storage in the organization.
- Randomized data publication: the solution contains a mechanism for automatic publication of anonymized EMR key features.

Literature has shown that a blockchain-based solution is a suitable option for EMR management. The use of Blockchain can make the entire process of working with EMRs more efficient both for medical personnel and patients, and allow for better predictive models to be created.

References

[1]H. S. Lallie, L. A. Shepherd, J. R. C. Nurse, A. Erola, G. Epiphaniou, C. Maple, X. Bellekens. Cyber security in the age of COVID-19: A timeline and analysis of cyber-crime

- and cyber-attacks during the pandemic. *Computers & Security*, 2021, 105: 102248.
- [2] M. Muthuppalaniappan, K. Stevenson. Healthcare cyber-attacks and the COVID-19 pandemic: an urgent threat to global health. *International Journal for Quality in Health Care*, 2021, 33.1: mzaa117.
- [3] S.M. Pournaghi, M. Bayat, Y. Farjami. MedSBA: a novel and secure scheme to share medical data based on blockchain technology and attribute-based encryption. *Journal of Ambient Intelligence and Human- ized Computing*, 2020, 11.11: 4613-4641.
- [4] X. Yue, H. Wang, D. Jin, M. Li, W. Jiang. Healthcare data gateways: found healthcare intelligence on blockchain with novel privacy risk control. *Journal of medical systems*, 2016, 40.10: 1-8.
- [5] R. Zou, X. Lv, J. Zhao. SPChain: blockchain-based medical data sharing and privacy-preserving eHealth system. *Information Processing & Management*, 2021, 58.4: 102604.
- [6] A. Azaria; A. Ekblaw; T. Vieira; A. Lippman. Medrec: Using blockchain for medical data access and permission management. In: 2016 2nd international conference on open and big data (OBD). IEEE, 2016. p. 25-30.
- [7] X. Liu, Z. Wang, C. Jin, F. Li, G. Li . A blockchain-based medical data sharing and protection scheme. *IEEE Access*, 2019, 7: 118943-118953.
- [8] N. Rifi, N. Agoulmine ,N. C. Taher, E. Rachkidi. Blockchain technology: is it a good candidate for securing iot sensitive medical data?. *Wireless Communications and Mobile Computing*, 2018, 2018
- [9] A. Farouk, A. Alahmadi, S. Ghose, A. Mashatan. Blockchain platform for industrial healthcare: Vision and future opportunities. *Computer Communications*, 2020, 154: 223-235.
- [10] P. Bhattacharya; S. Tanwar; U. Bodkhe; S. Tyagi; N. Kumar. Bindaas: Blockchain-based deep-learning as-a-service in healthcare 4.0 applica- tions. *IEEE transactions on network science and engineering*, 2019, 8.2: 1242-1255.
- [11] T. Veeramakali, R. Siva, B. Sivakumar, P. C. Senthil Mahesh, N. Krishnaraj. An intelligent internet of things-based secure healthcare framework using blockchain technology with an optimal deep learning model. *The Journal of Supercomputing*, 2021, 77.9: 9576-9596.

num

On the equivalence of the three-link to almost linear form*

Sergej Čelikovský¹, Milan Anderle¹

¹ M. Anderle and S. Čelikovský are with The Czech Academy of Sciences, Institute of Information Theory and Automation (ÚTIA AV ČR), 182 08 Prague 8, Czech Republic, [anderle, celikovs]@utia.cas.cz

Planar “three-link” depicted in Fig. 0.1 is the underactuated mechanical system having 3 degrees of freedom and 2 actuators, thereby mimicking the pair of legs without knees and torso mounted at their hips. The i -th link ($i = 1, 2, 3$) is actually a thin homogeneous rod of mass μ_i with attached point mass M_i . It is equivalently modelled by a virtual one-dimensional mass-less rigid segment carrying the overall mass $m_i = \mu_i + M_i$ at its center of mass (COM) located at the black bold point. The virtual mass-less link moment of inertia I_i with respect to COM can be computed from I_i, μ_i, M_i .

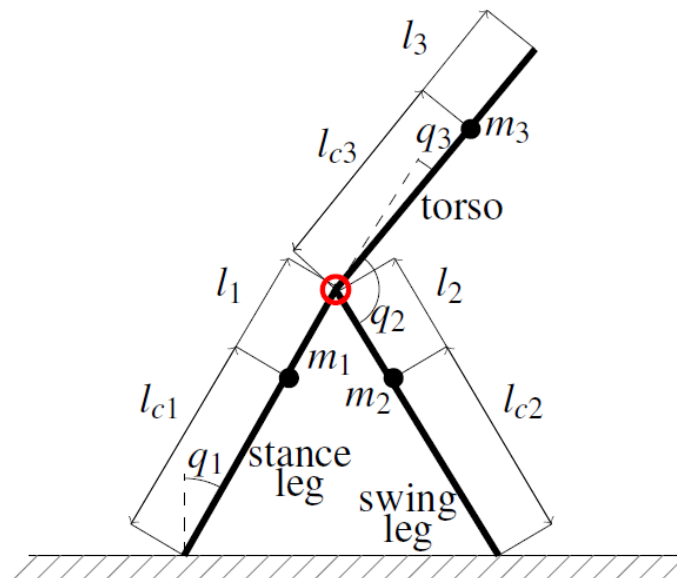


Figure 0.1: The “three-link” with upward torso position.

The standard mechanical model of the planar three-link in Fig. 0.1 can be obtained by Euler-Lagrange formalism as

$$D(q)\ddot{q} + C(q, \dot{q})\dot{q} + G(q) = \begin{bmatrix} 0 \\ u_2 \\ u_3 \end{bmatrix}, \quad q := \begin{bmatrix} q_1 \\ q_2 \\ q_3 \end{bmatrix}, \quad (0.1)$$

*Supported by the Czech Science Foundation grant No. 21-03689S

$$\begin{aligned}
D &= [d_{ij}], \quad i, j = 1, 2, 3, \quad D^\top = D > 0, \quad G = [G_1, G_2, G_3]^\top, \\
d_{11} &= l_1 + l_2 + l_3 + l_1^2 m_2 + l_1^2 m_3 + l_{c1}^2 m_1 + \\
&\quad l_{c2}^2 m_2 + l_{c3}^2 m_3 + 2l_1 l_{c2} m_2 \cos q_2 + 2l_1 l_{c3} m_3 \cos q_3, \\
d_{12} &= m_2 l_{c2}^2 + l_1 m_2 \cos q_2 l_{c2} + l_2 \\
d_{13} &= m_3 l_{c3}^2 + l_1 m_3 \cos q_3 l_{c3} + l_3, \quad d_{23} = 0, \\
d_{22} &= m_2 l_{c2}^2 + l_2, \quad d_{33}(q_2, q_3) = m_3 l_{c3}^2 + l_3, \\
G_1 &= -g [l_1 m_2 \sin q_1 + l_1 m_3 \sin q_1 + l_{c1} m_1 \sin q_1 + \\
&\quad l_{c2} m_2 \sin(q_1 + q_2) + l_{c3} m_3 \sin(q_1 + q_3)], \quad G_2 = \\
&\quad -g l_{c2} m_2 \sin(q_1 + q_2), \quad G_3 = -g l_{c3} m_3 \sin(q_1 + q_3).
\end{aligned} \tag{0.2}$$

Fig. 0.1 defines generalized coordinates q_1, q_2, q_3 and red circle indicates there two independent actuators providing torques u_2, u_3 acting on **directly actuated** angles q_2, q_3 , respectively. Angle q_1 at the pivot point is the **unactuated** one. Recall, that the Coriolis terms $C(q, \dot{q})\dot{q}$ are straightforwardly determined from the inertia (aka mass) matrix $D(q)$. Introduce the so-called **balancing factor** β

$$\beta := l_{c2} m_2 / (l_{c3} m_3) \tag{0.3}$$

expressing a kind of balance between the swing leg and the torso. The main theoretical novelty of the current paper is:

Theorem 1: (0.1)-(0.2) is state and feedback equivalent to

$$\begin{aligned}
\dot{\xi}_1 &= \xi_2 - 2l_1 l_{c3} m_3 \dot{q}_1 \xi_5, \quad \dot{\xi}_2 = \xi_3, \quad \dot{\xi}_3 = \xi_4, \quad \dot{\xi}_4 = w_2, \\
\dot{\xi}_5 &= \xi_6, \quad \dot{\xi}_6 = w_3,
\end{aligned} \tag{0.4}$$

where new states $\xi_i, i = 1, \dots, 6$, and the inputs w_2, w_3 are

$$\begin{aligned}
\xi_1 &:= d_{11}(q_2^0, q_3^0) q_1 + (m_2 l_{c2}^2 + l_2) q_2 + l_1 l_{c2} m_2 \sin q_2 \\
&\quad + (m_3 l_{c3}^2 + l_3) q_3 + l_1 l_{c3} m_3 \sin q_3, \\
\xi_2 &:= d_{11}(q_2, q_3) \dot{q}_1 + d_{12}(q_2, q_3) \dot{q}_2 + d_{13}(q_2, q_3) \dot{q}_3, \\
\xi_3 &= -G_1(q), \quad \xi_4 := -\nabla G_1(q) \dot{q}, \\
w_2 &:= -\nabla G_1(q) \ddot{q} - \dot{q}^\top \nabla^\top \nabla G_1(q) \dot{q}, \\
\xi_5 &:= \cos q_3 + \beta \cos q_2 - \cos q_3^0 - \beta \cos q_2^0, \\
\xi_6 &:= -\dot{q}_3 \sin q_3 - \beta \dot{q}_2 \sin q_2, \\
w_3 &:= -\ddot{q}_3 \sin q_3 - \beta \ddot{q}_2 \sin q_2 - \dot{q}_3^2 \cos q_3 - \beta \dot{q}_2^2 \cos q_2
\end{aligned} \tag{0.5}$$

and $\ddot{q}_1, \ddot{q}_2, \ddot{q}_3$, are to be substituted from (0.1)-(0.2).

Proof: Detailed proof will be provided in the full version of this contribution. It can be obtained by straightforward time differentiation of ξ_1, \dots, ξ_6 along trajectories of (0.1) and some manipulations except $\dot{\xi}_2 = \xi_3$ which goes back to Olfati-Saber [1] and it is due to the independence of $D(q)$ on the unactuated angle q_1 . Yet, problem with the three-link is that there is no integrating factor for ξ_2 like in case of the so-called Acrobot (aka

compas gait walker), cf. [1]. In such a way, our novelty here is the idea of introducing the variable ξ_5 in such a way that $\xi_2 - 2l_1l_{c3}m_3\dot{q}_1\xi_5$ becomes integrable to ξ_1 thereby giving (0.4)-(0.5).

Remark: Note that (0.4) becomes completely linear for $\xi_5 = 0$ and ξ_5 has a simple linear dynamics with respect to virtual input w_3 and this input can be straightforwardly used to enforce exponentially (or even in finite-time using [2]) the equality $\xi_5 = 0$. The first quadruple of equations in (0.4) then becomes the chain of 4 integrators controlled by the virtual input w_2 . The relations $\xi_5 = \xi_6 = 0$ can be also viewed as the so-called **virtual holonomic constraint (VHC)**. VHCs are widely used in the robotic walking design, see [3], [4] for further references. Note, that the relations $\xi_5 = \xi_6 = 0$ are actually the **collocated VHC** [5], *i.e.* those involving only directly actuated angles and thereby easier to be imposed.

The idea to find the collocated VHC for the three-link (*i.e.* the VHC involving only q_2, q_3) such that the respective constrained dynamics is state and feedback equivalent to linear system was first introduced in [6] and used for the multi-step walking design in [4]. These works did not use the form (0.4)-(0.5) which is, as already noted, the main theoretical novelty of the current paper. Further novelty here is looking for a convenient collocated VHC around the **downward** position of the torso. As a matter of fact, [4],[6] considered torso movement around the **upward** position as indicated in Fig. 0.1. The downward torso position may have rather interesting theoretical interpretation to mimic the balancing role of the hands during the walking. On a practical level, it provides more rich and easier to design collection of the desired collocated VHCs.

Indeed, denote by q_1^0, q_2^0, q_3^0 and q_1^f, q_2^f, q_3^f the double support stance configuration at the beginning and the end of the step, respectively. By a simple triangularization it holds $q_3^0 = q_2^0/2 - \pi/2, q_2^0 \in (\pi, 2\pi), q_3^f = q_2^f/2 - \pi/2, q_2^f \in (0, \pi)$ for the upward torso, while $q_3^0 = q_2^0/2 + \pi/2, q_2^0 \in (\pi, 2\pi), q_3^f = q_2^f/2 + \pi/2, q_2^f \in (0, \pi)$ for the downward torso. Furthermore, $q_2 = \pi$ when the legs are passing by each other.

In such way, the above desired collocated VHC is given by some level curve shown in Fig. 0.2 having intersection with blue (red) line for upward (downward) torso at some $q_2^0 \in (\pi, 2\pi)$ and some $q_2^f \in (0, \pi)$.

For the upward torso position $q_3 \in (-\pi/2, \pi/2)$, after fixing the balancing factor β , there is an unique level curve satisfying the above requirements, as illustrated by Fig. 0.2. Reason is that the blue line passes through the configuration $q_2 = \pi, q_3 = 0$ which is the **saddle** stationary point of the function $\cos q_3 + \beta \cos q_2$ and therefore there is a unique connected curve going from some $q_2^0 \in (\pi, 2\pi)$ to some $q_2^f \in (0, \pi)$. Changing the balancing factor β modifies the shapes of the level curves and their intersections with blue line change, yet there is unique one-to-one correspondence between β and

$q_2^0 \in (\pi, 2\pi)$, $q_2^f \in (0, \pi)$, *i.e.* for a fixed chosen β there is only one possible angle between legs at the initial double support stance position, and vice-versa (provided β is from some reasonable range). Due to that limited choice, only specific mechanical and geometric parameters, laboriously computed in [4] via numerical optimization procedure, were capable to provide a rather special multi-step, hybrid-cyclic walking-like trajectory, namely:

l_1, l_2	length of both legs	0.68	[m]
l_3	length of the torso	1.02	[m]
l_{c1}, l_{c2}	COM location of both legs	0.23	[m]
l_{c3}	COM location of the torso	1.02	[m]
m_1, m_2	mass of both legs	0.97	[Kg]
m_3	mass of the torso	1.71	[Kg]
I_1, I_2	moment of inertia of both legs	0.01	[m ² Kg]
I_3	moment of inertia of the torso	0.60	[m ² Kg]

For the downward torso position $q_3 \in (\pi/2, 3\pi/2)$ the configurations $q_2^0 \in (\pi, 2\pi)$, $q_2^f \in (0, \pi)$, should be intersections of the red line and a level curve in Fig. 0.2. Red line passes through $q_3 = \pi, q_2 = \pi$ which is the local **minimum** stationary point of $\cos q_3 + \beta \cos q_2$, so there is continuum family of level curves circling that minimum. So, there is **always** a level curve passing through **any** $q_2^0 \in (\pi, 2\pi)$, $q_2^f \in (0, \pi)$ and the VHC design is much more flexible.

Summarizing: the full paper version will provide particular design of the walking-like trajectory and its tracking for the three-link with a downward torso movement imitating balancing role of the hands. The equivalent form (0.4)-(0.5) will be derived and used, as well as the collocated VHC $\xi_5 = \xi_6 = 0$ synchronizing mutually the torso and the swing leg movement. Restricted dynamics is described by the first quadruple of equations in (0.4) with $\xi_5 = 0$ - *i.e.* **the chain of four integrators**. The balancing role of “hand” thereby means its synchronization with the swing leg via the VHC having the exact feedback linearizable restricted dynamics. Future outlooks indicate that fairly general underactuation degree 1 walking design may be transformed into the design task for the chain of four integrators (system with 4 states and 1 input). Besides their theoretical analysis our results will be illustrated by the three-link “walking” simulations.

References

- [1] R. Olfati-Saber, “Normal forms for underactuated mechanical systems with symmetry,” IEEE Transactions on Automatic Control, vol. 47, no. 2, pp. 305–308, Feb. 2002.
- [2] S. Bhat and D. S. Bernstein, “Geometric homogeneity with applications to finite-time stability,” Math. Control Signals Systems, vol. 17, pp. 101–127, 2005.
- [3] E. Westervelt, J. Grizzle, C. Chevallereau, J. Choi, and B. Morris, Feedback control of dynamic bipedal robot locomotion. CRC Press, 2007.

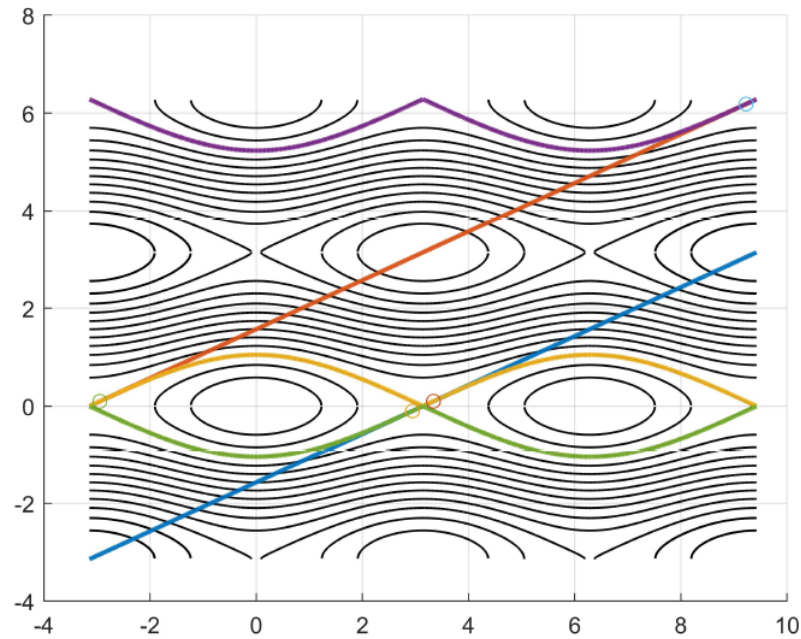


Figure 0.2: Level curves (black, yellow, green) of the function $\cos q_3 + \beta \cos q_2$ plotted in (q_2, q_3) plane for $\beta = 0.2506$ used in [4]. Furthermore, the blue line is the plot of $(q_2, q_2/2 - \pi/2)$ while the red one of $(q_2, q_2/2 + \pi/2)$.

- [4] S. Čelikovsky´ and M. Anderle, “Chain of four integrators as a possible essence of the under-actuated planar walking,” *IFAC-PapersOnLine*, vol. 54, no. 14, pp. 60–65, 2021.
- [5] S. Čelikovsky´, “Flatness and realization of virtual holonomic constraints,” in *Proceedings of the 5th IFAC Workshop on Lagrangian and Hamiltonian Methods for Non Linear Control (2015)*, Lyon, France, 2015, pp. 25–30.
- [6] S. Čelikovsky´ and M. Anderle, “Exact feedback linearization of the collocated constrained dynamics of the three-link with adjustable torso and its application in the underactuated planar walking,” in *2019 IEEE 15th International Conference on Control and Automation (ICCA)*, Edinburg, Scotland, 2019, pp. 1289–1295.

On reducing the topological entropy of linearized nonlinear systems

G. Chesi¹

¹ Department of Electrical and Electronic Engineering The University of Hong Kong, Hong Kong, China

The topological entropy is a measure that quantifies the unstable of a dynamical systems. Specifically, in the case of linear systems, the topological entropy is defined as the sum of the real parts of the unstable eigenvalues (continuous-time systems) or the logarithm of the product of the magnitudes of the unstable eigenvalues (discrete-time systems), see e.g. [10], [1], [12], [3]. It is well-known that the topological entropy plays a key role in control engineering. Indeed, as it has been shown in the literature, the knowledge of the topological entropy is required to establish the existence of stabilizing feedback controllers for linear systems in the presence of communications constraints. For instance, [7] shows that a single-input discrete-time system is stabilizable in the presence of a quantizer if and only if the topological entropy is smaller than a function of the quantization density. Also, [2] shows that a single-input continuous-time system is stabilizable in the presence of noise if and only if the topological entropy is smaller than a function of the signal-to-noise ratio (SNR). Other results similarly related to the topological entropy are proposed in [13], [8], [11], [9], [14]. Recent works have also addressed the determination of the worst-case topological entropy in uncertain systems, see e.g. [5]. Hence, reducing the topological entropy is a problem of fundamental importance in order to achieve stabilizability. This problem has been addressed for linear systems in [6]. In the case of nonlinear systems, the topological entropy is associated with the linearization around an equilibrium point of interest. This means that, contrary to the case of linear systems, the topological entropy in nonlinear systems is also a function of the system input, see e.g. [4]. This paper addresses a class of synthesis problems for nonlinear systems where the target is to determine an operating scenario for reducing the topological entropy associated with the linearization around some equilibrium points of interest over a set of admissible system inputs. Specifically, the operating scenario may be represented by a set of system parameters to be selected or by a controller to be implemented. Each of these, together with the admissible system inputs, affect the possible equilibrium points and the corresponding possible linearizations of the nonlinear system around them. The synthesis problem consists of determining an operating scenario such that the maximum value of the topological entropy associated with all the possible linearizations is not larger than a prescribed threshold.

References

- [1] R. Bowen. Entropy for group endomorphisms and homogeneous space. *Transactions of the American Mathematical Society*, 153:401–414, 1971.
- [2] J. H. Braslavsky, R. H. Middleton, and J. S. Freudenberg. Feedback stabilization

- over signal-to-noise ratio constrained channels. *IEEE Transactions on Automatic Control*, 52(8):1391–1403, 2007.
- [3] W. Chen and L. Qiu. Stabilization of networked control systems with multirate sampling. *Automatica*, 49(6):1528–1537, 2013.
- [4] G. Chesi. Quantifying the unstable in linearized nonlinear systems. *Automatica*, 60:210–218, 2015.
- [5] G. Chesi. Control with communications constraints: measuring the instability in parametric linear systems. *IEEE Transactions on Control of Network Systems*, 4(2):312–322, 2017.
- [6] G. Chesi. Stabilization and entropy reduction via SDP-based design of fixed-order output feedback controllers and tuning parameters. *IEEE Transactions on Automatic Control*, 62(3):1094–1108, 2017.
- [7] N. Elia and S. K. Mitter. Stabilization of linear systems with limited information. *IEEE Transactions on Automatic Control*, 46(9):1384–1400, 2001.
- [8] M. Fu and L. Xie. The sector bound approach to quantized feedback control. *IEEE Transactions on Automatic Control*, 50(11):1698–1711, 2005.
- [9] K. Li and J. Baillieul. Robust and efficient quantization and coding for control of multidimensional linear systems under data rate constraints. *International Journal of Robust and Nonlinear Control*, 17(10-11):898–920, 2007.
- [10] K. Mahler. An application of Jensen’s formula to polynomials. *Mathematika*, 7:98–100, 1960.
- [11] A. Matveev and A. Savkin. Multirate stabilization of multiple sensor systems via limited capacity communication channels. *SIAM Journal on Control and Optimization*, 44(2):584–617, 2005.
- [12] L. Qiu. Quantify the unstable (seminary lecture). In *International Symposium on Mathematical Theory of Networks and Systems*, Budapest, Hungary, 2010.
- [13] S. Tatikonda and S. K. Mitter. Control under communication constraints. *IEEE Transactions on Automatic Control*, 49(7):1056–1068, 2004.
- [14] S. Wan and L. Qiu. Stabilization of networked control systems with finite data rate. In *Asian Control Conference*, pages 1067–1073, Hong Kong, China, 2009.

A mathematical analysis of the socio-economic impacts of a patent waiver on COVID-19 vaccines

M. Italia¹, F. Della Rossa¹ and F. Dercole ¹

¹ DEIB, Politecnico di Milano, Italy

We perform a calibrated mathematical analysis of the potential impacts of a patent waiver on COVID-19 vaccines. In the model, we schematically divide nations into high- and low-income, the latter accounting for 80% of the world population but currently using only 60% of the vaccine production. We show that a significant increase in vaccine production combined with a more equitable distribution – made possible by an intellectual property (IP) waiver – would have stopped the pandemic in 18 months of vaccination and saved tens of millions people in poor countries, compared with the current scenario in which the virus becomes endemic. We hypothesize the peak rollout capacity shown by high-income countries at the beginning of the vaccination campaign and half of that capacity for low-income ones. We even show that the money saved on vaccines globally in the hypothetical IP-waiver scenario overcomes the actual value of the 5-yr profits of the big pharma in the current situation. This profit loss could be immediately covered (mostly by the expected saving of high-income countries) in exchange for the waiver.

Optimal initial perturbations in a boundary layer with wall actuation

L. Bettini¹, F. Auteri¹

¹ Dipartimento di Scienze e Tecnologie Aerospaziali, Politecnico di Milano, via La Masa 34, 20156, Milano (Italy)

Waves of span-wise velocity at the wall are known to be very effective in reducing the friction drag in turbulent channels and boundary layers. They can also delay transition in boundary layers [1]. To investigate this interesting property, in this work we compute linear and nonlinear optimal perturbations [2,3] in a Blasius boundary layer actuated by standing waves of span-wise velocity at the wall. Namely, we look for the initial velocity perturbation able to produce the maximum energy gain in a given target time. The Navier-Stokes equations and their linearized counterparts act as a constraint in the optimisation problem and they are integrated by an incremental pressure- correction scheme based on the direction-splitting technique [4]. The optimization process involves the computation of adjoint equations: results from continuous and discrete approaches are compared. The analysis is carried out for different streamwise wavelengths of the wall actuation in order to uncover the influence of this parameter on transition. In agreement with Cherubini et al.[2], the optimal linear initial perturbation is found to be characterized by pairs of streamwise-modulated counter-rotating vortices, as in Figure 1(a,b), tilted downstream. Nonlinear optimal perturbations exhibit more localized structures which undergo further mutual interactions as a function of time. In both cases, the Orr mechanism is clearly visible, which is responsible for a transient energy growth as the mean flow tilts downstream the structures initially opposing the base flow. Moreover, the lift-up effect triggered by the counter-rotating vortices develops streak-like structures alternated in the streamwise direction. As previously reported [3], the nonlinear temporal evolution of perturbations provides physical insight in the transition scenario: nonlinear couplings result in the generation of Λ -shaped structures, which, amplified and stretched, generate finite-amplitude Λ - vortices. Eventually, nonlinear mixing redistributes vorticity and hairpin structures are formed. It is found that the energy gain of nonlinear optimization is higher than the one of the linear optimization, as several further interactions are triggered. As expected from previous studies [1,5], the presence of the actuation at the wall strongly affects the shape of initial optimal perturbations and, most importantly, the energy gain. Figure 1(c) shows the initial optimal perturbations for an actuation of high wavelength, which increases the energy gain of nearly six times in the linear case. It is remarkable that this purely spatial actuation does not require moving parts and can represent an effective and realizable strategy for transition control. Furthermore, nonlinear analysis shed light on important analogies existing between the evolution of optimal perturbations and the turbulent regeneration cycle.

References

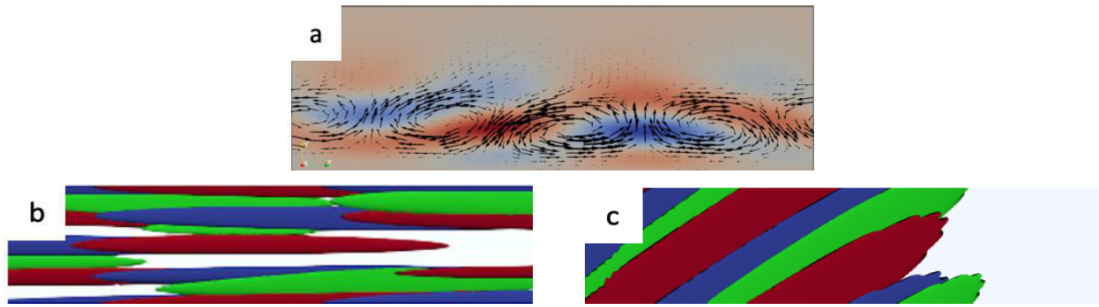


Figure 0.1: (a) Contours (streamwise velocity) with superimposed vectors of the linear initial optimal perturbation plotted in a plane normal to the free-stream flow. (b) and (c) negative streamwise velocity perturbation (green) and streamwise vorticity perturbation (positive in red, negative in blue) for the non-actuated (left) and actuated (right) optimal perturbations, linear case.

- [1] Negi et al., Phys. Rev. Fluids. 4, 063094 (2019).
- [2] Cherubini et al., J. Fluid Mech. 656, 231 (2010).
- [3] Cherubini et al., J. Fluid Mech. 689, 221 (2011).
- [4] Chiarini et al., J. Comput. Phys. 429, 110023 (2021)
- [5] Quadrio et al., J. Fluid Mech. 627, 161 (2009).

Visual spatial attention shifts decoded from the electroencephalogram enable sending of binary messages

Christoph Reichert¹, Stefan Dürschmid¹, Catherine M. Sweeney-Reed², Hermann Hinrichs^{1,2}

¹ Leibniz Institute for Neurobiology, Magdeburg, Germany

² Dept. of Neurology, Otto-von-Guericke University, Magdeburg, Germany

Brain-computer Interfaces (BCIs) permit the control of devices through voluntary modulation of brain activity, commonly recorded using the electroencephalogram (EEG). However, most BCIs do not rely on brain activity alone but also depend on muscle activity, e.g. to direct the gaze to a visual target stimulus. Patients suffering from neurodegenerative motor disorders such as amyotrophic lateral sclerosis (ALS) can use their residual eye movements to respond to questions with 'yes' or 'no' without even using a BCI. However, when the disorder deteriorates such that the patient suffers from complete locked-in syndrome (CLIS), brain activity is the last remaining option for communication [1]. Gaze-independence is therefore a crucial requirement for BCIs intended to help those patients. Several existing approaches meet this requirement, with some of them relying on intact M1 motor neurons [2], while others rely on good vision to discriminate target from non-target stimuli [3]. However, these conditions are frequently absent in ALS patients. Here we introduce an approach that permits communication of 'yes' and 'no' only by shifting attention to a target color illuminated in the left or right visual hemi-field. Thirteen healthy participants were asked to use the BCI to respond with 'yes', if a number read aloud was even and with 'no' otherwise. A sequence of ten visual stimuli was presented to evoke event-related potentials reflecting shifts of attention. At each stimulus event, two custom-made LED panels were illuminated, one with red and the other with green light. The panels were located at a 9.1° visual angle to the left and right of a fixation cross and the panel size was 3.1° by 4.4°, according to visual angle. The side of the green and red illumination changed pseudo-randomly with a stimulus onset asynchrony of 850-1100 ms. The participants communicated 'yes' and 'no' by shifting their attention to the green and red stimulus, respectively, while maintaining their gaze focused on the fixation cross. After the stimulus sequence ended, auditory feedback was presented according to the decoded attention shifts, and the participants indicated whether the feedback was correct or not by button press. We recorded EEG data from 13 occipital electrode sites at a 250 Hz sampling rate and controlled for eye movements by recording the electrooculogram (EOG) in parallel. Consequently, one trial, recorded while the visual stimulus sequence was presented, consisted of 13 time series of electrical brain activity with a low signal-to-noise ratio. To decode these complex data, we bandpass-filtered the signals between 1.0 Hz and 12.5 Hz and resampled them to 50 Hz. Using canonical correlation analysis, we constructed a spatial filter, estimated from a set of training data. This process yields surrogate channels, which emphasize

the hemispheric differences corresponding to attention shifts across the visual fields. The correlation between these surrogate channels and the reference signal, provided by the sequence of left/right presentation of either color, indicated to which color the participant shifted his/her attention. On average, we correctly decoded the participants' answers in 90.1% ($\sigma=6.0\%$) of trials ($N=120$) presented to a participant. To estimate the potential performance of the algorithm when a larger amount of training data is available, we performed cross-validation, which revealed an average decoding accuracy of 93.3% ($\sigma=4.6\%$). In contrast, using the EOG channels with the same decoding approach, only 59.1% ($\sigma=5.9\%$) accuracy was achieved, supporting the assumption that eye movement is a negligible source for the performance of the system. The results indicate that attention to a colored light stimulus can be decoded from noninvasive brain recordings without the need to move the eyes. The finding is of particular interest for people who suffer from CLIS, because this approach could restore their ability to communicate messages to others, albeit only on a binary basis, which is currently assumed to be achievable only invasively [1].

References

- [1] U. Chaudhary et al., "Spelling interface using intracortical signals in a completely locked-in patient enabled via auditory neurofeedback training," *Nat. Commun.*, vol. 13, no. 1, pp. 1–9, 2022, doi: 10.1038/s41467-022-28859-8.
- [2] N. J. Hill et al., "Classifying EEG and ECoG signals without subject training for fast BCI implementation: Comparison of nonparalyzed and completely paralyzed subjects," *IEEE Trans. Neural Syst. Rehabil. Eng.*, vol. 14, no. 2, pp. 183–186, Jun. 2006, doi: 10.1109/TNSRE.2006.875548.
- [3] L. Acqualagna and B. Blankertz, "Gaze-independent BCI-spelling using rapid serial visual presentation (RSVP)," *Clin. Neurophysiol.*, vol. 124, no. 5, pp. 901–908, 2013, doi: 10.1016/j.clinph.2012.12.050.

Timing of functional electrical stimulation using a brain–computer interface improves rehabilitation outcome early post-stroke

Johanna Krueger¹, Richard Krauth¹, Christoph Reichert^{2,3}, Serefeim Perdikis⁴, Serefeim Perdikis⁴, Susanne Vogt⁵, Tessa Huchtemann⁶, Stefan Dürschmid^{2,3}, Almut Sickert⁷, Juliane Lamprecht⁷, Almir Huremovic^{7,8}, Michael Görtler⁵, Robert T. Knight^{9,10}, Hermann Hinrichs^{2,11}, Hans-Jochen Heinze^{2,12}, Sabine Lindquist¹³, Michael Sailer⁷, Jose del R. Millán¹⁴, Catherine M. Sweeney-Reed^{1,3}

¹Neurocybernetics and Rehabilitation, Dept. of Neurology, Otto von Guericke University, Magdeburg, Germany

²Leibniz Institute for Neurobiology, Magdeburg, Germany

³Center for Behavioral Brain Sciences (CBBS), Otto von Guericke University Magdeburg, Germany

⁴School of Computer Science and Electronic Engineering, University of Essex, Colchester, United Kingdom

⁵Dept. of Neurology, Otto von Guericke University Magdeburg, Germany

⁶Dept. of Neurology, University Hospital Münster, Münster, Germany

⁷Neurorehabilitation Centre, Median Hospital, Magdeburg, Germany

⁸Dept. of Neurology, Ingolstadt Hospital, Ingolstadt, Germany

⁹Helen Wills Neuroscience Institute, University of California – Berkeley, Berkeley, USA

¹⁰Dept. of Psychology, University of California, Berkeley, Berkeley, USA

¹¹Dept. of Neurology, Otto von Guericke University Magdeburg, Germany

¹²University Hospital Magdeburg, Otto von Guericke University Magdeburg, Magdeburg, Germany

¹³Dept. of Neurology, Pfeiffersche Stiftung, Magdeburg, Germany

¹⁴Cockrell School of Engineering, University of Texas at Austin, Austin, Texas, USA

Stroke is among the leading causes of motor disability [1]. Recent studies show better motor recovery in chronic stroke patients when functional electrical stimulation (FES) to the paretic limb, providing visuo-proprioceptive feedback on attempted movement, is delivered tightly temporally bound to movement attempts using a brain–computer interface (BCI) [2,3]. The precise timing is determined from motor cortex electroencephalographic (EEG) signals. Here we compared clinical outcome and changes in electrophysiological correlates of motor recovery following BCI-FES with FES delivery timed independently (Sham group) in patients early post-stroke from the Magdeburg cohort of an ongoing multi-center study. We evaluated transcranial magnetic stimulation (TMS)-induced motor evoked potential (MEP) amplitudes and sensorimotor rhythm spectral power. Patients with a first stroke, lasting >24 hours, either < 1 month (acute) or 1-6 months (subacute) after stroke onset, with reduced/absent wrist extension, were recruited on the University Hospital Magdeburg stroke ward, or at the Neurorehabilitation Centre, Median

Hospital Magdeburg, Germany. Patients and clinicians were blinded to the pseudorandom, counterbalanced BCI/Sham group allocation. The primary outcome measure was the Fugl-Meyer Assessment upper extremity (FMA-UE) score (max. 66)[4]. Both groups received 16 EEG electrodes over motor cortex bilaterally at each treatment session (mean number of sessions 18.8 [SD 5.7]). The patients were instructed to attempt to extend their wrist on presentation of a green up-arrow on a screen or to remain at rest in response to a red down-arrow. Feedback was provided by a bar moving up or down the screen respectively. EEG power spectra over 8-30 Hz in 2 Hz bands, at each electrode, were calculated in 1 s windows and classified as a movement attempt or rest. Data from a 5-minute training session were used to identify up to 10 features for initial training of the classifier, based on canonical variates analysis [5]. During the therapy, continuous EEG recordings were classified online 16 times per second to detect movement attempts. On movement attempt identification, FES was delivered to two electrodes placed 5 cm apart over the extensor digitorum communis of the affected upper limb to induce wrist extension. A single therapy session comprised 3-7 blocks, according to patient fatigue, each containing 15 movement attempts. Including breaks, therapy sessions were 10-25 minutes. The classifier was retrained weekly using the most recent therapy EEG data. Routine clinical TMS was applied over primary motor cortex, at EEG locations C3 and C4, before and after therapy. Stimulation began at 70% of capacity and was increased at 10% intervals to attain maximum amplitude MEP recorded using electromyography over extensor digitorum communis. High-density EEG was recorded before and after the therapy program from 60 channels (Fs: 500 Hz), during twelve runs, comprising 10 movement and 5 rest trials in a pseudorandom order. Custom Matlab scripts and the FieldTrip toolbox [6] were used. The data were divided into 1.7 s epochs, from the movement cue, and time-frequency decomposed (4 to 31 Hz) through convolution with 5-cycle Morlet wavelets.

Of the Magdeburg cohort (N = 38), 53% (n = 20) completed the program (BCI: n = 10; Sham: n = 10). We analyzed the largest patient group with similar lesion location: non-dominant hemisphere (as aphasia was an exclusion criterion), subcortical stroke (BCI: n = 6; Sham: n = 6). A repeated measures ANOVA of the FMA-UE scores, with the between-subject factor Group (BCI, Sham), the within-subject factor Time (Pre, Post), and the covariates Age, Sex, Days Post-Stroke, and Days of Therapy showed an interaction only between Time and Group ($F(1) = 8.03$, $p = 0.030$) and a main effect of Time ($F(1,6) = 8.93$, $p = 0.024$). Post hoc tests showed a significant score increase pre to post-treatment in the BCI ($p = 0.004$) but not the Sham group. Including Therapy Start (Acute, Subacute) as a between-subject factor, the interaction Time x Group ($F(1) = 6.66$, $p = 0.049$) remained. Post hoc tests showed a significant FMA-UE score increase only in the BCI group when therapy was started in the acute phase. TMS amplitudes were available from both groups (BCI: n = 3; Sham: n = 3). A repeated measures ANOVA with the between-subject factor Group (BCI, Sham) was applied, correcting for the covariates Age at the time of the stroke and Sex. An interaction occurred between Group and Time ($F(1) = 27.69$, $p = 0.034$). Post hoc T-tests showed a significant increase in

amplitude post- compared with pre-treatment in the BCI group ($p = 0.012$) but not in the Sham group. EEG data from the right-handed patients with a non-dominant hemisphere, subcortical stroke ($N = 8$; BCI: $n = 4$, Sham: $n=4$) were analyzed, to enable electrode level comparison. Spectral power was compared between groups pre- and post-treatment using cluster-based permutation tests with 500 randomizations (paired t-tests threshold: $p = 0.05$). Upper beta (15-25 Hz) spectral power reduction pre- to post-treatment 0.5 to 1.5 s after the movement cue was greater in the BCI than the Sham group over the primary motor cortex at electrode C2 ($p = 0.044$).

Greater motor recovery followed BCI-FES than Sham-FES, with a trend towards better recovery if BCI-FES therapy started in the acute phase. Greater increases in TMS-induced MEP amplitudes pre- to post-treatment in the BCI than the Sham group suggests improved cortico-spinal functional connectivity. Beta spectral power synchrony following the cue to move decreased more in the BCI than the Sham group post-therapy, consistent with reduced compensatory activity. Our findings support the notion that FES delivery in a tight temporal window with movement attempts using a BCI could improve motor recovery, particularly if started early post-stroke.

References

- [1] Kyu, H., Abate, D., Abate, K. & Al., E. (2018) Global, regional, and national disability-adjusted life-years (DALYs) for 359 diseases and injuries and healthy life expectancy (HALE) for 195 countries and territories, 1990 – 2017: a systematic analysis for the Global Burden of Disease Study 2017. *Lancet* 392: 1859–1922.
- [2] Biasiucci, A. et al. (2018) Brain-actuated functional electrical stimulation elicits lasting arm motor recovery after stroke. *Nature Communications* 9(2421): 1-13.
- [3] Remsik, A. B. et al. (2018) Behavioral outcomes following brain computer interface intervention for upper extremity rehabilitation in stroke: A randomized controlled trial. *Frontiers in Neuroscience* 12: 752.
- [4] Fugl-Meyer, A., Jääskö, L., Leyman, I., Olsson, S. & Steglind, S. (1975) The post-stroke hemiplegic patient. 1. A method for evaluation of physical performance. *Scand J Rehabil Med* 7: 13–31.
- [5] Galán, F., Ferrez, P. W., Oliva, F., Guàrdia, J. & Millán, J. D. R. (2007) Feature extraction for multi-class BCI using canonical variates analysis. in 2007 IEEE International Symposium on Intelligent Signal Processing, WISP.
- [6] Oostenveld, R., Fries, P., Maris, E. & Schoffelen, J. M. (2011) FieldTrip: Open source software for advanced analysis of MEG, EEG, and invasive electrophysiological data. *Computational Intelligence and Neuroscience*, 156869.

Objective Evaluation of Bradykinesia Using a Serious Game

L. C. Mendes, C. M. Alves, I. A. Marques, A. M. Cabral, Y. Morère and A. d. O. Andrade

Introduction: Interventions based on serious games have been receiving substantial attention in health care and are increasingly used for monitoring and assessing symptoms of several diseases, such as Parkinson's disease (PD). PD is a common neurological disorder that affects body movements, and the main motor symptom perceived in individuals with this disease is bradykinesia, essential for the diagnosis of PD. Bradykinesia is manifested by the following characteristics: slowness in the execution of voluntary movements; prolongation of the reaction time; prolongation of the movement time; and, consequently, prolongation of the response time, defined as the sum of the reaction time and the movement time. Currently, the clinical assessment of bradykinesia is mainly based on scales, and the most used is the Movement Disorder Society - Unified Parkinson's Disease Rating Scale (MDS - UPDRS). The clinical evaluation of bradykinesia is based on the analysis of the patient's ability to perform rapid, repetitive, and alternating hand movements. However, the degree of experience of the evaluator, the cooperation of the patient and individual bias are factors that contribute to the subjectivity and inaccuracy of this type of assessment. Thus, aiming to evaluate bradykinesia in an objective, collaborative and impartial way, a serious game – called RehaBEElitation – for upper limbs was developed, tested and applied. To interact with the game, a human-machine interface composed of inertial and resistive sensors was developed specifically for this application.

Objective: The aim of this study was to evaluate bradykinesia objectively using the serious game developed.

Methodology: Fifteen individuals with PD and fifteen healthy individuals participated in this study, constituting the Experimental Group (EG) and Control Group (CG), respectively, matched in age and sex. Data collection was performed in ON and OFF states of medication for the EG. In this study, bradykinesia was assessed using the gold standard tool (MDS-UPDRS), and calculating the response time and estimating the participants' angular velocity of movement when playing RehaBEElitation. The response time was measured through the definition of an event, responsible for characterizing "the instant when visual and sound stimuli are presented to the player, indicating that he/she can start the movement required to score points" and "the instant when the player executes the movement and consequently scores in the game". Related to angular velocity of movement, the gyroscope signal was used, which indicates how fast the movement was performed. The t-test and the Wilcoxon-Mann-Whitney test were applied to confirm the differences in response times and angular velocities between: CG and EG, EG in the two

medication states, CG and EG in ON state, and CG and EG in OFF state. To compare the results of the three forms of bradykinesia assessment, the data were normalized and then descriptive statistics were used.

Results: The results showed that, for all comparisons, significant differences were found between the groups ($p < 0.001$). Furthermore, the response times of the participants in the CG were the shortest, followed by the EG in ON state, and the EG in OFF state; and the angular velocities were higher for CG, followed by the EG in ON state and the EG in OFF state. Descriptive statistics also showed that in ON state participants obtained better results for UPDRS, response time and angular velocity compared to OFF state.

Conclusion: It can be concluded that it is possible to objectively assess bradykinesia of individuals with PD using a serious game, and that patients in ON medication state have more reduced bradykinesia compared to patients in OFF medication state.

Effect of sevoflurane on cardiovascular activity at maintenance and emergence from anesthesia during surgery

Y. Kordi¹, N. Nicolaou¹

¹Department of Basic and Clinical Sciences, University of Nicosia Medical School, Nicosia, Cyprus

Aims: The purpose of this preliminary study is to investigate the effect of sevoflurane, an inhalational anesthetic agent routinely used during surgery, on the patients' cardiovascular activity (Heart Rate – HR and Perfusion Index – PI) during the maintenance and emergence phases of surgery, as well as identify if there is any significant correlation between HR and PI at either of the two phases of surgery.

Background: General anesthesia is a reversible state of unconsciousness, caused by administration of a “cocktail” of agents to achieve the targets of unconsciousness, amnesia, analgesia and immobility [1]. Even today, the patient status under anesthesia is monitored manually by the anesthesiologist. Some monitors of brain activity (representing the anesthetic action on the central nervous system) are also commercially available for this purpose, but they are not used routinely due to cost and robustness issues [2]. During anesthesia, the sympathetic nervous system (SNS) activity is increased due to surgical stress, but is also decreased by the effects of anesthetic agents [3]. As anesthetics affect the body holistically, effective monitoring should combine indices from central and autonomic nervous systems. In this study, we investigate the effect of sevoflurane on the level of the SNS, as reflected through cardiovascular parameters, during anesthetic maintenance and emergence.

Methods: The data was obtained from a publicly available dataset by the University of Queensland [4], which contains patient monitoring data and vital signs recorded during surgery under general anesthesia. Based on specific inclusion/exclusion criteria, including the type of anesthetic agent, data from 11 patients were selected from the dataset. The maintenance (surgical anesthesia) and emergence (waking up at the end of surgery) phases of surgery were identified based on the Minimum Alveolar Concentration (MAC) values (estimation of the concentration of the inhaled anesthetic in the body, within the alveoli). For each phase of interest, descriptive statistics (mean, median, standard deviation) of HR and PI, and the HR-PI correlation, were estimated along consecutive 5-min intervals (statistical significance: Mann-Whitney U test, $\alpha=0.05$).

Results: There was a statistically non-significant reduction in HR, but a statistically significant decrease in the PI during the emergence phase compared to the maintenance phase. The two cardiovascular parameters were not significantly correlated during either of the surgical phases studied. Sevoflurane is a mild cardiovascular depressor, that has

minimal or no effect on the parasympathetic tone of the heart, but reduces cardiac output. Healthy individuals compensate to reduced cardiac output by increasing their HR. In addition, peripheral vasomotor tone is physiologically controlled by the SNS. The decrease in adrenergic outflow during the maintenance phase (low SNS activity) causes the peripheral vessels to dilate in response, causing a decrease in blood pressure, and a corresponding increase the blood flow perfusion (PI) to the periphery.

Conclusions: This preliminary investigation supports further investigation into the use of continuous monitoring of PI values during surgery to reflect the level of the SNS activity and potentially assess the adequacy of anesthesia, which can help in detecting any awakening episodes and adjusting the doses of anesthetic agents accordingly to prevent anesthesia awareness. Further research is required to investigate the mechanisms of how the autonomic nervous system affects different cardiovascular parameters during surgery with different anesthetic agents and to extract measures of both SNS and parasympathetic nervous system activity. Also, to assess and compare the reliability of PI values monitoring compared to brain monitoring tools in detecting any brain awakening episodes.

References:

- [1] E.N. Brown, et al., *Anesth. Analg.*, 127(5):1246-58, 2018;
- [2] A.A. Dahaba, *Anesth. Analg.*, 128(5):1042- 44, 2019;
- [3] S. Eis & J. Kramer, *Anesthesia Inhalation Agents Cardiovascular Effects*, In: *StatPearls* [Internet], StatPearls Publishing, 2021; [4] D. Liu, et al., *Anesth. Analg.*,114(3):584-9, 2012.

Tuesday 19th

Complexity at Increasing Levels of Feedback in Diode Laser

S.Donati¹



¹University of Pavia, Italy

Using Lang and Kobayashi equations for diode lasers, we study the delayed optical feedback (DOF) in the intermediate region between short and long cavity. We find that regimes of unperturbed oscillations, period one, multi-periodic and chaos are dictated by interplay of coupling factor K , distance L , phase F of the external reflector, and linewidth enhancement factor a . We plot the boundaries of different regimes in the K - F plane for several values of L and a , and characterize the transition from very short cavity ($L < 0.01L_{fr}$) with negligible high-level effects, to long cavity ($L = 0.5 L_{fr}$) where the K - F plane is almost completely filled with chaos. We show that chaos and periodicity regimes are only found at $C > 1$, while self-mixing induced FM and AM of the optical signal are found in all regions of stable oscillations, and for $C > 1$ frequency switching occurs at a certain F for any K and L . Chaos develops at increased K and L in correspondence to loci of frequency switching. We complete our analysis with a revisited version of the Tkack and Chaprivly diagram of feedback effects

Minimal Universal Model for Chaos and Generalized Multistability in a Laser

J. Ginoux¹, Riccardo Meucci², Stefano Euzzor²

KL

¹ Aix Marseille Univ, Université de Toulon, CNRS, CPT, Marseille, France

² National Institute of Optics – CNR, Florence, Italy

This talk is given in memory of our distinguished colleague and friend Prof. F. Tito Arecchi University of Florence, Florence, Italy.

The aim of this talk is to present a model of laser with feedback and the minimal nonlinearity leading to chaos. First, we recall the way to build a minimal universal model for chaos in LASER starting from the well-known two levels model. Then, a mathematical and numerical stability analysis and bifurcation diagrams highlight the “route to chaos” for such model. Secondly, we analysed the generalized multistability of such minimal universal model and we demonstrate its dependence with regards to the dissipation of this system. The model is then tested under the action of a secondary sinusoidal perturbation which is able to remove bistability when a suitable relative phase is chosen. The surviving attractor is the one with less dissipation. This control strategy is particularly useful when one of the competing attractors is a chaotic attractor.

References

- [1] F. T. Arecchi, R. Meucci, G. Puccioni, and J. Tredicce “Experimental Evidence of Subharmonic Bifurcations, Multistability, and Turbulence in a Q-Switched Gas Laser” *Phys. Rev. Lett.* 49, 1217 (1982)).
- [2] U. Feudel, “ Complex dynamics in multistable systems” *Int. J. Bifurcation and Chaos* 18, 1607 -1626 (2008).
- [3] U. Feudel, A. N. Pisarchik and K. Showalter , “ Multistability and tipping : from Mathematics and physics to climate and brain- Minireview and preface to the focus issue”, *Chaos* 28 , 033501 (2018).
- [4] R. Meucci, S. Euzzor, F. T. Arecchi and J-M. Ginoux, “ Minimal Universal Model for Chaos in a Laser with Feedback “ *International Journal of Bifurcation and Chaos* 31, 2130013 (2021).
- [5] L. Ricci a. Perinelli, M. Castelluzzo, S. Euzzor and R. Meucci , “ Experimental Evidence of Chaos generated by a Minimal Universal Oscillator Model” *International Journal of Bifurcation and Chaos* 31, 2150205 (2021)
- [6] R. Meucci, S. Euzzor, F. T. Arecchi, M. Mehrabbeik, S. Jafari and J-M. Ginoux, “Generalized Multistability and its control in a laser” accepted for publication on *Chaos* (2022).

Mining Top-K High Utility Itemset Using Bio-Inspired Algorithms

Nam Ngoc Pham^{1*}, Zuzana Komínková Oplatková^{1†}, Huy Minh Huynh^{1‡}, Bay Vo^{2§}

¹ Faculty of Applied Informatics Tomas Bata University, Zlín City, Czech Republic

² Faculty of Information Technology, Ho Chi Minh City University of Technology Ho Chi Minh City, Vietnam

H

High utility patterns (itemsets) (HUIs) mining is a necessary research problem in the field of knowledge discovery and data mining. Many algorithms for Top-K HUIs mining have been proposed. However, the principal issue with these algorithms is that they need to store potential top-k patterns in the memory anytime, and they request the minimum utility threshold to automatically rise when finding HUIs. Consequently, the performance of existing exact algorithms for Top-K HUIs mining tends to decrease when the database size and the number of distinct items in the databases rise. To address this issue, we suggest a Binary Particle Swarm Optimization (BPSO) based algorithm for Top-K HUIs mining effectively, namely TKO- BPSO (Top-K high utility itemsets mining in One phase based on Binary Particle Swarm Optimization). The main idea of TKO- BPSO is not only to use a one-phase model and different strategies (RUC, RUZ, and EPB) to effectively increase the border thresholds for pruning the search space but also to adopt the sigmoid function in the updating process of the particles, which might significantly reduce the combinational problem in traditional HUIM when the database size and the number of distinct items in the databases rise. Consequently, its performance outperforms existing exact algorithms for Top-K HUIs mining because it efficiently overcomes the problem of the vast amount candidates. Substantial experiments conducted on publicly available several real and synthetic datasets show that the proposed algorithm has better results than existing state-of-the-art algorithms in terms of runtime, which can significantly reduce the combinational problem and memory usage.

*npham@utb.cz

†oplatkova@utb.cz

‡huynh@utb.cz

§vd.bay@hutech.edu.vn

Inner Dynamic of Particle Swarm Optimization Interpreted by Complex Network Analysis

Michal Pluhacek, Tomas Kadavy, Anezka Kazikova, Adam Viktorin, Roman Senkerik

Faculty of Applied Informatics, Tomas Bata University in Zlin, T.G. Masaryka 5555, 760 01 Zlin, Czech Republic
pluhacek, kadavy, kazikova, aviktorin, senkerik@utb.cz

The Particle Swarm Optimization algorithm (PSO) is one of the most popular metaheuristic optimizers to date. Since its inception in 1995 [1], it has maintained the interest of both researchers and practitioners. PSO is extensively studied and modified [2-5]. One of the latest trends that aim to tackle the ever-increasing complexity of real-world optimization challenges is self-adaptivity [6, 7], a process in which the algorithm tries to alternate its behavior to improve its performance. For successful adaptation, it is essential to provide the adaptive mechanism with enough data describing the inner state of the metaheuristic algorithm. One of the commonly used metrics is population diversity [8], in theory, a perfect tool to uncover premature convergence or stagnation of the algorithm. However, as the inner dynamic of a metaheuristic is immensely complex, quantifying the population diversity into a single number comes with many drawbacks [9]. One of the main issues is that the computational cost of measuring the population diversity scales up dramatically with the problem's dimensionality. As a result, for practical use, another way to describe the inner state of the population and help shape the adaptive mechanics is demanded. One of the promising directions is the study of complex networks created by metaheuristics [10 - 12] that has been shown to produce encouraging results [13, 14]. An initial study on capturing the inner dynamic of PSO into a complex network-like structure was published in 2015 [15]. In this work, we choose to re-explore the possible ways of capturing the PSO population dynamic into a complex network. We aim to propose a set of quantifiable indicators, based on the tools for complex network analysis that would allow us to accurately describe the current state of the population (and in extension the algorithm), enabling new and more effective adaptive mechanics to be designed. One of the main advantages and appeals for practitioners of the proposed concept is that the computational demands of complex network analysis do not scale up with the problem's dimensionality, promising a significant time saving for adaptive mechanics using the complex network features.

References

- [1] J. Kennedy and R. Eberhart, "Particle swarm optimization", in Proceedings of the IEEE International Conference on Neural Networks, 1995, pp. 1942–1948.
- [2] Y. Shi and R. Eberhart, "A modified particle swarm optimizer," in Proceedings of the

IEEE International Conference on Evolutionary Computation (IEEE World Congress on Computational Intelligence), 1998, pp. 69–73. I. S.

[3] J. Kennedy, "The particle swarm: social adaptation of knowledge," in Proceedings of the IEEE International Conference on Evolutionary Computation, 1997, pp. 303–308.

[4] F. van den Bergh, A.P. Engelbrecht, A study of particle swarm optimization particle trajectories, *Information Sciences*, Volume 176, Issue 8, 22 April 2006, pages 937-971, ISSN 0020-0255.

[5] M. Montes de Oca, J. Pena, T. Stutzle, C. Pinciroli, and M. Dorigo. "Heterogeneous particle swarm optimizers," in Proceedings of the IEEE Congress on Evolutionary Computation, 2009, pp. 698–705.

[6] A. Ratnaweera, S. Halgamuge, and H. Watson, "Self-organizing hierarchical particle swarm optimizer with time-varying acceleration coefficients," *IEEE Transactions on Evolutionary Computation*, vol. 8, no. 3, pp. 240–255, 2004.

[7] Deng, W., Zhao, H., Yang, X., Xiong, J., Sun, M., & Li, B. (2017). Study on an improved adaptive PSO algorithm for solving multi-objective gate assignment. *Applied Soft Computing*, 59, 288-302.

[8] Morrison, R. W., & Jong, K. A. D. (2001, October). Measurement of population diversity. In *International conference on artificial evolution (evolution artificielle)* (pp. 31-41). Springer, Berlin, Heidelberg.

[9] Pluhacek, M., Viktorin, A., Kadavy, T., & Kazikova, A. (2021, December). On the common population diversity measures in metaheuristics and their limitations. In *2021 IEEE Symposium Series on Computational Intelligence (SSCI)* (pp. 1-7). IEEE.

[10] I. Zelinka, D. Davendra, R. Senkerik, R. Jasek, Do Evolutionary Algorithm Dynamics Create Complex Network Structures? *Complex Systems* 2, 0891–2513, 20, 127–140, 2011

[11] I. Zelinka, D. Davendra, M. Chadli, R. Senkerik, T.T. Dao, L. Skanderova, Evolutionary Dynamics as The Structure of Complex Networks. In: Zelinka, I., Snasel, V., Abraham, A. (eds.) *Handbook of Optimization*. ISRL, vol. 38, pp. 215–243. Springer, Heidelberg (2013)

[12] I. Zelinka, Investigation on relationship between complex network and evolutionary algorithms dynamics, *AIP Conference Proceedings* 1389 (1) 1011–1014, 2011.

[13] D. Davendra, I. Zelinka, R. Senkerik. and M. Pluhacek, Complex Network Analysis of Discrete Self-organising Migrating Algorithm, in: Zelinka, I. and Suganthan, P. and Chen, G. and Snasel, V. and Abraham, A. and Rossler, O. (Eds.) *Nostradamus 2014: Prediction, Modeling and Analysis of Complex Systems*, *Advances in Intelligent Systems and Computing*, Springer Berlin Heidelberg, pp. 161–174, 2014.

[14] D. Davendra, I. Zelinka, M. Metlicka, R. Senkerik, M. Pluhacek, "Complex network analysis of differential evolution algorithm applied to flowshop with no-wait problem," *Differential Evolution (SDE)*, 2014 IEEE Symposium on , vol., no., pp.1,8, 9-12 Dec, 2014

[15] Pluhacek, M., Janostik, J., Senkerik, R., Zelinka, I., & Davendra, D. (2016). PSO as complex network—capturing the inner dynamics—initial study. In *Proceedings of the Second International Afro-European Conference for Industrial Advancement AECIA 2015*

(pp. 551-559). Springer, Cham.

Chaotic Ant Lion Optimization Algorithm

Donald Davendra¹, Magdalena Metlicka and Magdalena Bialic-Davendra

¹ Central Washington University, 400 E. University Way, Ellensburg, WA 98926, Email: donald.davendra@cwu.edu

The Ant Lion Optimization (ALO) algorithm is a relative recent metaheuristic, designed on the concept of predator ant lions. The basic concepts revolve around hunting prey such as the random walk of ants, building traps, entrapment of ants in traps, catching preys, and re-building traps. The proposed algorithm focus on the stochasticity of the algorithm, with the embedding of chaos maps as pseudo-random number generation. The uniqueness of this approach is to evaluate the behavior of ALO, which employs minimal tuning parameters, and to observe the effectiveness of chaotic systems in mostly self-tuning algorithms. The experimentations was conducted on standard benchmark unimodal and multimodal problems and the results compared with the canonical version of ALO and other published algorithms. Based on the results comparisons, the Chaotic Ant Lion Optimization (CALO) performed significantly better than ALO and most compared algorithms.

Optimal allocation of resources in a three-sector dynamical model of an economy analytical approach and evolutionary algorithms

T. Alexeeva^a, L. Chechurin^a, V. Dodonov^a, N. Kuznetsov^b

^aLUT University, Finland

^bUniversity of Jyväskylä, Finland

In the theory of economic growth, of particular interest is the problem of the optimal allocation of resources on sectors of the economy, which social planner pays close attention to. Economic growth takes place at uneven rates across different sectors of the economy. One of the reasons for this is structural changes under the implications of different sectoral total factor productivity growth rates, which can occur both over long periods of time and abruptly. During structural changes the aggregate capital-output ratio can remain constant and the aggregate economy is on a balanced growth path. This problem can be solved as a problem of social planning, in which the utility function is maximized, represented as the final consumption sector. we consider a three- sector closed economy with sectors producing materials, investment good, and consumption good. Capital in each sector is immobile while labor and investment could be freely moved between the sectors. Mathematically, this problem can be present as the following optimal control problem in continuous time

$$\max_{S_j, \theta_j} = \delta \int_0^T e^{-\delta t} C(t), \quad (0.6)$$

where objective function is given as (1), $U(t) = X_2 = e^{-\delta t} C(t)$ is utility function, $C(t)$ is consumption (output of second sector X_2), $\delta > 0$ is discount rate, X_2 is a control variable, $X_0, X_1, K_j, L, L_j, j = 1, 2, 3$ are state variables. Sectoral allocations are controls that satisfy to balanced conditions for shares of labor and investment

$$\begin{aligned} \theta_j &= \frac{L_j}{L}, \theta_0 + \theta_1 + \theta_2 = 1, \\ S_j &= \frac{I_j}{X_1}, S_0 + S_1 + S_2 = 1, \end{aligned} \quad (0.7)$$

We solve this optimization problem analytically for the case of balanced economy and obtain optimal solution when shares of labor and investment could be redistributed in order to change (increase) output of the final consumption sector.

Despite the classical problem statement, this problem is technically complex. Note that,

on the one hand, analytical solution of the problem is extremely difficult because production function has fractional powers, need to take into account large number of constraints for the balanced economy, utility function includes discounting $\delta > 0$ which leads to inhomogeneous effect of current decisions on the future allocations. On the other hand, numerical algorithms may apply to find local solutions only. And, as rule, this task is considered at the steady state and in per capita variables that it is more simply. Thus, numerical solution, as well as solution in case of balanced economy and the "golden rule" solution, do not guarantee absence of corner solutions that satisfy given constraints for arbitrary values of initial values.

We overcome the above limitations and show how evolutionary algorithms (EAs) can be effectively applied to solve the high-dimensional and non-linear global dynamical optimization problem. Thus, by combining the analytical and empirical approach based on EAs, we successfully solve the problem of optimal resource allocation for the presented model.

Bayesian Training in Photonic Neuromorphic Meshes

Charis Mesaritakis¹, George Sarantoglou¹, Adonis Bogris², Sergios Theodoridis³

¹Dept. Information & Communication Systems Engineering. University of the Aegean Samos, Greece

²Dept. Informatics and Computer Engineering. University of West Attica, Egaleo-Greece

³Dept. of Electronic Systems, Aalborg University, Denmark

Neuromorphic computers based on reconfigurable photonic integrated chips (RPICs) can offer zero-latency processing, marginal power consumption and operational flexibility. On the other hand, they are subject to, performance affecting, operational/fabrication deviations in their building blocks. Here, we present a Bayesian learning framework that when combined with device characterization, can dramatically decrease power consumption beyond 74% and significantly simplify the driving circuitry.

Delay-based Reservoir Computing: Role of Timescales and Memory for Optimizing Performance

Lina Jaurigue¹, Tobias Hülser², Felix Köster², Kathy Lüdge^{1,*}

¹Institut of Physics, Technische Univ. Ilmenau, Weimarer Str. 25, 98684 Ilmenau, Germany

²Institut für Theoretische Physik, Technische Univ. Berlin, Hardenbergstr. 36, 10623 Berlin, Germany

*kathy.luedge@tu-ilmenau.de

Delay-based reservoir computing (RC) is a machine learning technique that is especially suited to learn time series prediction problems [1,2]. During the last years it has become more and more apparent that the computing performance in these time-multiplexed systems is strongly correlated to the timescales of the RC system [1]. This includes the timescales of the internal system dynamics as well as the time of one data input cycle (clock cycle T) and the time which the signal spends in the external delay loop (time delay τ). While it is possible to link the linear memory capacity of the network to the small signal response of the reservoir [3], it is still difficult to predict the performance of a delay-based setup for a specific task. We investigate this problem and clarify the role of multiple delay times in delay-based reservoir computing realizations. Our system under study is a small delay-coupled laser network that is driven by time-multiplexed input data and trained for an efficient one-step ahead prediction (Fig1a). While we find that delay-time tuning is very efficient in order to improve the performance for a specific task, we also find that optimal parameters vary and crucially depend on the task. The dependence of the memory capacities as a function of the coupling delays (shown left in Fig1b) is modulated by the resonance structure of τ_1 , τ_2 , and T , but it does not allow to predict a task specific performance (three specific performances of well-known tasks are shown in Fig1b).

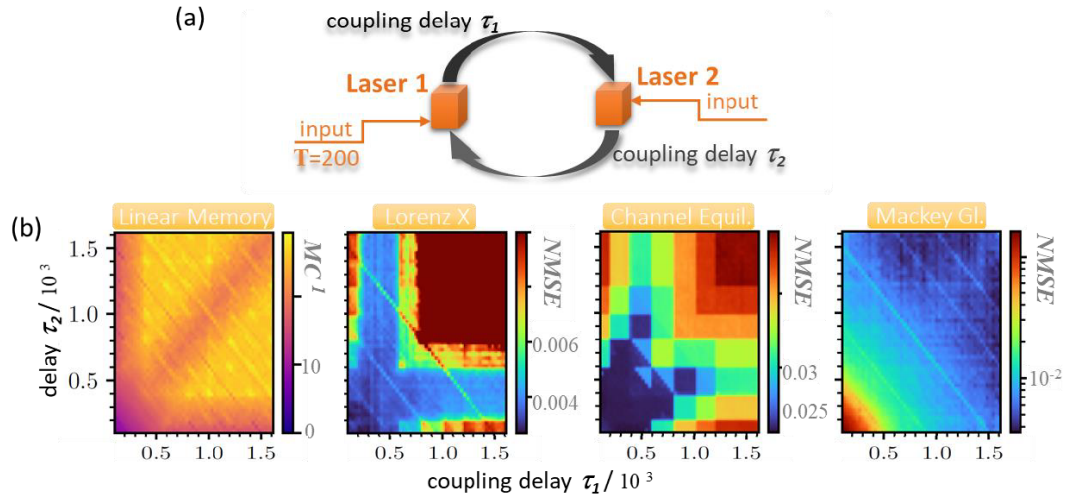


Figure 0.1: (a) Setup of a delay-coupled laser network with two nodes, (b) Linear Memory capacity of the network as well as the normalized mean square error (NMSE) of 3 different time series prediction tasks (Lorenz X, Channel equalization, Mackey Glass) plotted color coded as a function of the two coupling delays τ_1 and τ_2 . Input cycle $T = 200$.

By analyzing the correlation properties of the time-series used as input for the different tasks as well as their expansion into a series of Legendre polynomials, we are able to predict parameters for optimal performance. For time dependent problems with long correlations times (as e.g. the Mackey Glass time series) it is crucial to provide the relevant timescales via the coupling delay or additionally by an easily tunable delayed input.

Acknowledgements

The authors acknowledge the financial support of the DFG within the framework of SFB910.

References

- [1] T. Hülser, F. Köster, L. C. Jaurigue, and K. Lüdge, Role of delay-times in delay-based Photonic Reservoir Computing, *Opt. Mater. Express* 12, 1214 (2022).
- [2] A. Röhm, L. C. Jaurigue, and K. Lüdge, Reservoir Computing Using Laser Networks, *IEEE J. Sel. Top. Quantum Electron.* 26, 7700108 (2019).
- [3] F. Köster, S. Yanchuk, and K. Lüdge, Insight into delay based reservoir computing via eigenvalue analysis, *J. Phys. Photonics* 3, 024011 (2021).

Neuromorphic Photonic Computing with Vertical- Cavity Surface-Emitting Lasers

Dafydd Owen-Newns, Weikang Zhang, Juan Alanis, Julian Bueno, Joshua Robertson, Matej Hejda and Antonio Hurtado*

Institute of Photonics, Dept. of Physics, University of Strathclyde, Technology and Innovation Centre, 99 George Street, G1 1RD, Glasgow (Scotland, United Kingdom)

*antonio.hurtado@strath.ac.uk

Photonic techniques emulating the brain's powerful computational capabilities are receiving increasing research effort for novel paradigms in ultrafast information processing and Artificial Intelligence (AI). In this talk, I will introduce our research work on light-enabled neuromorphic systems built with artificial photonic neurons based upon Vertical-Cavity Surface Emitting Lasers (VCSELs). The latter are key- enabling, ubiquitous optical devices that can found in mobile phones for auto-focus functionalities, supermarket barcode scanners, head-light automotive sensors and optical transceivers in data centres, to transmit internet data traffic over optical communication networks. There is therefore great potential in adding intelligence and processing functionalities in VCSEL systems for a wide range of novel technological developments across strategic industrial sectors (e.g. communications, computing, security, etc.). Our research work has demonstrated that a wide range of neuronal computational features (e.g. spiking) can be optically emulated in VCSELs at ultrafast speeds (up to 9 orders of magnitude faster than the millisecond timescales in biological neurons) [1-3]. In this talk I will report how we utilise the ultrafast neural-like responses observed in VCSELs in order to develop new neuromorphic (spike-based) photonic processing systems for use in key applications (e.g. pattern recognition, image processing) and neuronal circuit emulation [1-3]. This talk will also review our recent work on laser (VCSEL-) -based, Recurrent and Spiking Neural Networks (RNNs and SNNs) for new photonic Reservoir Computing architectures, delivering excellent performance in a diversity of complex computing tasks at high-speeds [4]. Finally, in this talk I will review our recent work on neuromorphic photonic systems combining lasers and Resonant Tunnelling Diode (RTD) elements for new ultrafast, low-energy, chip-scale spike-processing systems and SNNs, for new light-enabled hardware towards neuro-inspired computing and AI [5].

Acknowledgements

UKRI Turing AI Acceleration Fellowships Programme (EP/V025198/1); US Office of Naval Research Global (Grant ONRG-NICOP-N62909-18-1-2027); European Commission (Grant 828841-ChipAI-H2020-FETOPEN-2018-2020); Engineering and Physical Sciences Research Council ((EP/N509760/1, EP/P006973/1)).

References

- [1] J. Robertson et al., IEEE J. Sel. Top. Quantum Electron., 26, 7700715 (2020).
- [2] J. Robertson et al., Sci. Repts., 10, 6098 (2020).
- [3] J. Robertson et al., Sci. Repts., 12, 4874 (2022).
- [4] J. Bueno et al., IEEE Phot. Tech. Letts., 33, 920 (2021).
- [5] M. Hejda et al., Phys. Rev. Appl., 17, 024072 (2022).

Neuromorphic processing in delay-coupled and spatially coupled micropillar lasers

V. A. Pammi¹, L. Soun¹, A. Masominia¹, R. Braive^{1,2}, K. Pantzas¹, G. Beaudoin¹, I. Sagnes¹, S. Terrien³, N. Broederick³, B. Krauskopf³, M. G. Clerc⁴, K. A. Bittner⁵, S. Barbay^{1,*}

¹ Centre de Nanosciences et de Nanotechnologies, CNRS, Université Paris-Saclay, Palaiseau, France

² Université Paris-Cité, Paris, France

³ The Dodd-Walls Centre for Photonic and Quantum Technologies, The University of Auckland, Auckland, New Zealand

⁴ Departamento de Física and Millennium Institute for Research in Optics, FCFM, Universidad de Chile, Santiago, Chile

⁵ Departamento de Matemática Aplicada, Ciencia e Ingeniería de los Materiales y Tecnología Electrónica, Universidad Rey Juan Carlos, Madrid, Spain

*sylvain.barbay@c2n.upsaclay.fr

Photonic neuromorphic systems constitute a novel and promising substrate for brain-inspired processing. We present recent results obtained in neuromimetic micropillar lasers which were shown to behave as photonic neurons with fast excitable responses (hundreds of picoseconds). In addition to behaving as leaky integrate-and-fire neurons, these photonic neurons have refractory periods, can integrate delayed stimuli and can act as coincidence detectors. We investigate two different configurations: delayed self-connection and spatial coupling. In the first one, the micropillar is connected to itself similarly to an autapse. We reveal the long term behaviour of the system and evidence peculiar dynamical features such as symmetry-broken timing responses. We discuss how this dynamics can be used to form a delay-based associative memory. In the second configuration, the micropillars are spatially coupled through evanescent coupling. This gives rise to the possibility of integrated, on-chip circuits. We show how the saltatory propagation properties of excitations in this system naturally leads to excitable logic-gates. Importantly, these can form the basis of more advanced circuits able to recognize spike timing sequences on-chip.

Crosshair Optimizer

Donald Davendra¹ and Jason Torrence

¹ Central Washington University, 400 E. University Way, Ellensburg, WA 98926, Email: donald.davendra@cwu.edu

A novel local search based optimization algorithm named Crosshair Optimizer (CHO) is introduced in this paper. In most algorithms, much of the computational resources are used to explore around a solution space, but in reality, much of the time there are only parts of an optimal solution that can be improved. Using this information, if an algorithm explores the space around an optimal solution using a random number of its dimensions to dictate their placements, rather than all of them, the solution space is explored in a less random fashion. CHO employs a rapid neighborhood generation on each iteration and selects a sub-sequences of best performing solutions. These selected solutions then randomly generate neighboring solutions only in certain search space dimensions. Exploration is done by randomly generating solutions in only two dimensional axis to the neighborhood cluster. This speeds up the search process with fine grain sampling, and is quickly able to migrate the search space to another location without using drift migration. Experimentation was conducted on the standard unimodal and multimodal problems, with CHO performing extremely well against standard evolutionary algorithms.

Stabilization of Higher Periodic Orbits of Chaotic Maps using Permutation-selective Objective Function

Radomil Matousek^{1,†}, Tomas Hulka^{1,*}, René Pierre Lozi²

¹Dept. of Applied Computer Science Brno University of Technology Brno, Czech Republic

² Laboratoire J. A. Dieudonné (UMR 7351) University Côte d'Azur, Nice, France

rene.lozi@univ-cotedazur.fr

*tomas.hulka@vutbr.cz

† ORCID 0000-0002-3142-0900

This paper deals with the design of an advanced objective function capable of proper evaluation of the individuals during the process of chaotic system stabilization through the means of evolutionary metaheuristic optimization. The challenging problem of stabilisation of chaotic systems generates many unexpected difficulties. One of them is the evaluation of a sample stabilized run during optimization. Even more so, when the target state of the chaotic system is a stable cycle oscillating periodically between several target positions. In this study, a two-dimensional dynamical system, known as the Hénon map, is stabilized by the ETDAS method. The success of this method depends entirely on two control parameters which determine the quality of the stabilized solution. These solutions are then evaluated through conventional methods (SSE, ITAE, ...) with their respective shortcomings and the advanced permutation-selective objective function, which achieves significantly better results.

Exploring clustering in SOMA

Tomas Kadavy, Michal Pluhacek, Adam Viktorin, Anezka Kazikova, Roman Senkerik

Faculty of Applied Informatics, Tomas Bata University in Zlin, T.G. Masaryka 5555, 760 01 Zlin, Czech Republic
kadavy, pluhacek, aviktorin, kazikova, senkerik@utb.cz

In recent decades, evolutionary algorithms (EA) gained popularity and reputation as robust and effective tools for solving various optimization tasks. This reputation is probably the main drive behind the yearly increasing number of research papers discussing applications, modifications, performance improvements, adaptation schemes, hybridization of many techniques from soft computing universe, and novel algorithms. The importance of finding a well-performing algorithm grows with the increase in dimension and complexity in current optimization tasks. When developing EA, it is very important to find out what benefit a particular modification of the mechanism has in the population or in the adaptation of parameters, and therefore how effectively the enhanced algorithm works on the selected benchmark sets or in practical application. Using the information from cluster analysis with other information from the algorithm, it is possible to control the organizational process, the communication of individuals, or e.g. to detect different stages of optimization - i.e. whether exploration, stopping or convergence is occurring. Or to obtain other information leading to a more accurate adjustment of the hyper-parameters of the algorithm. The aim of this paper is to follow the current challenges of "good practices in benchmarking" [1] and to present a detailed review of different approaches to the use of clustering in a selected EA. However, the goal of this research is not only to show what results have been achieved compared to other versions of the algorithm or state-of-the-art techniques, but also in what ways clustering can be applied in the population and how to identify, using appropriately chosen tools or metrics, what is happening in the population and what is causing the observed convergence and overall result. The chosen algorithm is Self-Organizing Migrating Algorithm (SOMA) [2], where it was shown that changing the organizational process in the population has a significant effect on the performance of the algorithm [3], [4]. Also, the number of different strategies affecting the selection of interacting individuals is suitable for the implementation of clustering. The research reported here is tracking the development of different versions of Self-Organizing Migrating Algorithm with Clustering-aided migration (SOMA-CL) [5], [6]. The workflow of the clustering enhanced SOMA can be divided into three phases: search space mapping, clustering of the mapped space, and the exploitation by performing a more detailed screening of areas of interest discovered during the first phase. The CEC 2021 single objective bound-constrained optimization benchmark testbed [7] is used for the performance evaluation. This paper introduces several modifications of

population organization process with application of clustering. The comprehensive review of algorithm modifications and analysis of the results presented here can be inspiring for other researchers working on the development and modifications of various EA.

References

- [1] T. Bartz-Beielstein, C. Doerr, D. v. d. Berg, J. Bossek, S. Chandrasekaran, T. Eftimov, A. Fischbach, P. Kerschke, W. La Cava, M. Lopez-Ibanez et al., “Benchmarking in optimization: Best practice and open issues,” arXiv preprint arXiv:2007.03488, 2020.
- [2] I. Zelinka, “Soma—self-organizing migrating algorithm,” in *Self- Organizing Migrating Algorithm*. Springer, 2016, pp. 3–49.
- [3] K. Price, N. Awad, M. Ali, and P. Suganthan, “Problem definitions and evaluation criteria for the 100-digit challenge special session and competition on single objective numerical optimization,” in *Technical Report*. Nanyang Technological University, 2018.
- [4] Q. B. Diep, I. Zelinka, S. Das, and R. Senkerik, “Soma t3a for solving the 100-digit challenge,” in *Swarm, Evolutionary, and Memetic Computing and Fuzzy and Neural Computing*, A. Zamuda, S. Das, P. N. Suganthan, and B. K. Panigrahi, Eds. Cham: Springer International Publishing, 2020, pp. 155–165.
- [5] T. Kadavy, M. Pluhacek, A. Viktorin, and R. Senkerik, “Self-organizing migrating algorithm with clustering-aided migration,” in *Proceedings of the 2020 Genetic and Evolutionary Computation Conference Companion*, ser. GECCO '20. New York, NY, USA: Association for Computing Machinery, 2020, p. 1441–1447. [Online]. Available: <https://doi.org/10.1145/3377929.3398129>
- [6] ———, “Self-organizing migrating algorithm with clustering-aided migration and adaptive perturbation vector control,” in *Proceedings of the Genetic and Evolutionary Computation Conference Companion*, ser. GECCO '21. New York, NY, USA: Association for Computing Machinery, 2021, p. 1916–1922. [Online]. Available: <https://doi.org/10.1145/3449726.3463212>
- [7] A. Wagdy, A. A. Hadi, A. K. Mohamed, P. Agrawal, A. Kumar, and P. N. Suganthan, “Problem definitions and evaluation criteria for the cec 2021 special session and competition on single objective bound constrained numerical optimization.” *Technical Report*, Nanyang Technological University, Singapore, 2020

Forecasting and stabilizing chaotic regimes in two macroeconomic models: interaction of AI technologies and time-delay control methods

T.A. Alexeeva^a, A.Y. Belyaev^{b,c}, Q.B. Diep^d, N.V. Kuznetsov^{b,e}✉, T.N. Mokaev^b, I. Zelinka^d

^aSt. Petersburg School of Physics, Mathematics and Computer Science, HSE University, Russia

^bFaculty of Mathematics and Mechanics, St. Petersburg State University, Russia

^cArloyd Automation, Ltd, UK

^dFaculty of Electrical Engineering and Computer Science, VSB-TUO, Czech Republic

^eInstitute for Problems in Mechanical Engineering RAS, Russia

Modern challenges in the economy associated with a change in its structure, technology transformation, climatic, energy, and epidemiological cataclysms stimulated posing of new problems both in the real economy and in an economic science. At the macro level, these tasks are strongly focused on modelling the behavior of economic agents, forecasting the dynamics of economic processes and controlling various regimes that arise in the economic mechanism, including under conditions of complex irregular dynamics leading to crisis states. In nonlinear mathematical models, early signals of crisis conditions can manifest themselves in the form of complex dynamics, including periodic and even chaotic ones. Irregular dynamics reduces the reliability of forecasts and thus undermines the predictive power of the model. In this case, decision-makers do not have the ability to predict and regulate the expectations of agents as well as estimate their economic implications. Additional complexity of the dynamics can be also associated with various unstable orbits embedded into the chaotic attractor of the dynamical system. The usage of artificial intelligence technologies such as evolutionary algorithms (EAs) and reinforcement learning in combination with the time-delay feedback control method (TDFC) proposed by K.Pyragas allows making significant progress in forecasting the qualitative properties of the model dynamics, including revealing of regular and irregular (periodic and chaotic) regimes, overcoming the problems associated with fractional-power nonlinearities in economic variables, optimization of the model parameters, and stabilization of unstable orbits by applying control procedures We demonstrate the effectiveness of this approach for two discrete-time macroeconomic models as an example. The first one is based on pioneering OLG model by Nobel laureates P. Samuelson (1970) and P. Diamond (2010). OLG models as a theoretical framework explain various effects of economic policies in an intergenerational context and helps understanding how the economic system functions given the finite life cycle of economic agents, including forecasting the allocation of consumption, labor, savings, the implication of tax, pension reforming and education transfers. We derive our OLG model with government spending that serves as a control

✉Corr. author email nkuznetsov239@gmail.com

function

$$\begin{cases} c_{t+1} = (r_t^\gamma - c_t^\theta)^{1/\alpha}, \\ l_{t+1} = b(\beta l_t - c_t - g_t), \end{cases} \quad t \in \mathbb{Z}_+. \quad (0.8)$$

We use computational abilities of a supercomputer to show how the combination of the most powerful EAs, i.e. differential evolution (DE) and the self-organized migration algorithm (SOMA), with the Pyragas method can significantly increase the efficiency of chaotic behavior control and allows us much faster and more accurate fine-tuning control parameters to achieve the desired state of the model and improve its forecasting behavior.

$$p_{j+1} = \frac{1}{\gamma_2} (-\beta - \gamma_1 p_{j-1} + (2 + \beta(1 + \lambda))p_j - \beta \lambda p_j^2) \quad (0.9)$$

and can be represented by the well-known Hénon map

$$\begin{cases} x_{j+1} = a + by_j - x_j^2 \\ y_{j+1} = x_j \end{cases} \quad (0.10)$$

Using this model as an example, we show how successful could be a combination of reinforcement learning (actor-critic method) and the Pyragas method to identify unstable periodic solutions and further suppress chaotic behavior, which makes it possible to improve forecasting pricing in the markets of goods and give recommendations for optimizing the formation of economic agents' expectations with respect to future prices.

Deep neural networks using a single neuron: folded-in-time architecture using feedback-modulated delay loops

Serhiy Yanchuk^{1,2}, Florian Stelzer³, André Röhm⁴, Raul Vicente³, Ingo Fischer⁵

¹Potsdam Institute for Climate Impact Research, 14473 Potsdam, Germany

²Institut für Mathematik, Humboldt Universität zu Berlin, 10117 Berlin, Germany

³Institute of Computer Science, University of Tartu, Tartu, Estonia

⁴Department of Information Physics and Computing, Graduate School of Information Science and Technology, The University of Tokyo, Tokyo, Japan

⁵Instituto de Física Interdisciplinar y Sistemas Complejos, IFISC (UIB-CSIC), Campus Universitat de les Illes Balears, Palma de Mallorca, Spain

This talk is based on our results from the recently published work [1], where we present a method for folding a deep neural network of arbitrary size into a single neuron with multiple time-delayed feedback loops. This single-neuron deep neural network comprises only a single nonlinearity and appropriately adjusted modulations of the feedback signals. The network states emerge in time as a temporal unfolding of the neuron's dynamics. By adjusting the feedback-modulation within the loops, we adapt the network's connection weights. These connection weights are determined via a back-propagation algorithm, where both the delay-induced and local network connections must be taken into account. Our approach can fully represent standard Deep Neural Networks (DNN), encompasses sparse DNNs, and extends the DNN concept toward dynamical systems implementations. The new method, which we call Folded-in-time DNN (Fit-DNN), exhibits promising performance in a set of benchmark tasks.

References

[1] Stelzer, F., Röhm, A., Vicente, R., Fischer, I., Yanchuk, S. (2021). Deep neural networks using a single neuron: folded-in-time architecture using feedback-modulated delay loops. *Nature Communications*, 12(1), 5164. <https://doi.org/10.1038/s41467-021-25427-4>

SOA-based Photonic Integrated Deep Neural Networks

Ripalta (Patty) Stabile¹

¹Technische Universiteit Eindhoven, the Netherlands

Neuromorphic photonics is an emerging research field that develops an alternative approach to electronic computation with the attempt to set a milestone in increasing computing speed and decreasing energy efficiency using photons, instead of electrons. Recent works on neuromorphic photonics has been proposed via diverse integration schemes, but most of the time prevented by further scalability of photonic neural networks. In our work we demonstrate the implementation and investigation of scalable photonic integrated deep neural networks which utilizes semiconductor optical amplifier (SOA) technology. Indium Phosphide (InP) integration technology has enabled sophisticated photonics circuit design, co-integrating both passive and active elements. We adopted the SOA technology for neuromorphic photonics to enable high weighting dynamic range and optical signal gain on chip. To this end, a photonic feed-forward neural network is demonstrated via an 8×8 InP cross-connect chip, where up to 8 linear neurons (weighted addition circuits) are integrated on-chip, based on SOA and array waveguide grating (AWG) technologies. The exploitation of these technologies as neural network is evaluated by implementing a trained 3-layer photonic deep neural network to solve the Iris flower classification problem. Prediction accuracy of 85.8% is achieved, with respect to the 95% accuracy obtained via a computer. A comprehensive analysis of the error evolution in our system reveals that the electrical/optical and digital-to- analog conversions dominate the error contribution, bringing down the overall accuracy, and suggests that an all-optical approach is preferable for future neuromorphic computing hardware design. To enhance scalability and computing speed of photonic integrated ANN, a wavelength converter is exploited as nonlinear function, based on cross-gain modulation in SOA, and co- integrated with the previously verified SOA- and AWG-based linear unit on a single chip. The monolithically integrated neuron shows better accuracy than the corresponding hybrid device at the same data rate. This all-optical neuron scheme is then used to simulate a 2-layer photonic deep neural network with 64 inputs, 64 neurons at the hidden layer and 10 neurons at the output layer for MNIST classification, showing an 89.5% best-case accuracy at 10 GS/s. Furthermore the energy consumption for the synaptic operation, considering the full end-to- end system, which includes the transceivers, the optical neural network and the electrical control part, is estimated. For the scalability investigation, a model of the noise evolution is proposed for cascaded SOA- based AONNs, including an extended analysis of the noise figure on the SOAs and wavelength converter. The model is derived from the noise figure estimation and the use of the small-signal method. We demonstrate and simulate the scalability of SOA-based AONN by tuning the optical signal to noise ratio (OSNR) at the neuron input. Experimental results have been used to calibrate the noise

evolution model and thereafter to investigate the depth of the AONN, demonstrating that noise compression happens after a certain number of layers, making possible to scale up to arbitrarily deep networks. Finally, a perspective neuromorphic computing structure is proposed, employing a 3D integration scheme and exploiting best-in-class available technologies. Here, InP technology, and specifically InP nano-photonics, still play a key role, together with ultra-low loss propagation platforms and novel phase changing materials. With its estimated compactness, ultra-high efficiency and lossless interconnectivity, a 3D neuromorphic photonic engine is foreseen to allow peta-scale computation and ultra-low latency and is expected to shape the future of neuromorphic computing.

Neuromorphic NanoLEDs

Bejoys Jacob¹, João Lourenço², Filipe Camarneiro¹, José M. L. Figueiredo², Jana B. Nieder¹, Bruno Romeira^{1,*}

¹INL – International Iberian Nanotechnology Laboratory, Ultrafast Bio- and Nanophotonics group, Av. Mestre José Veiga s/n, 4715-330 Braga, Portugal

²Centra-Ciências and Departamento de Física, Faculdade de Ciências, Universidade de Lisboa, Campo Grande, 1749-016 Lisboa, Portugal

*bruno.romeira@inl.int

Biological-inspired spike-emitting light sources biomimicking excitable neurons are of key importance for energy-efficient spiking neural networks and artificial intelligence [1]. Despite the significant advances in developing optical artificial neurons and synapses using phase-change materials, lasers, photodetectors, and modulators [2], compact light sources and detectors suited for spike-based signal processing and sensing, as needed for neuromorphic (brain-inspired) computing nanotechnologies, are still lacking. In this talk we cover our recent results towards near-infrared (NIR) light-sensitive micro- and nanopillar-LEDs as key-enabling artificial spiking neurons [3]. Our approach uses III-V semiconductor double barrier quantum well nanostructures integrated with light-emitting and receiving materials. This strategy provides to the current-voltage of nanoLEDs a unique light-sensitive nonlinear negative differential resistance characteristic [4]. As a result, this enables extremely low-energy activation (using either electrical or optical signals) of all-or-nothing spiking (pulsed) dynamic responses analogous to excitable neurons. We discuss the strategies to improve the quantum efficiency [5] of these NIR light-sensitive spiking LEDs to achieve low energy consumption (<100 fJ/spike), and efficient electro-optical and opto-electrical spiking signal conversion. Lastly, we discuss the spiking dynamical responses and the most suited learning protocols for functional spatio-temporal information spike-based processing applications. The nanophotonic light-emitting and receiving artificial neurons presented here pave the way for exciting novel neuromorphic optoelectronic chips and photonic circuits by utilizing the exceptional nanoscale properties of these light-spiking sources and detectors. **References**

[1] M. Hejda, et al. Resonant Tunneling Diode Nano-Optoelectronic Excitable Nodes for Neuromorphic Spike- Based Information Processing. *Phys. Rev. Applied* 17, 024072 (2022)

[2] B. J. Shastri, et al. Photonics for artificial intelligence and neuromorphic computing. *Nat. Photonics* 15, 102– 114 (2021).

[3] B. Romeira, J. M. L. Figueiredo, and J. Javaloyes. NanoLEDs for energy-efficient and gigahertz-speed spike- based sub- λ neuromorphic nanophotonic computing. *Nanophotonics* 9, 20200177 (2020).

- [4] I. Ortega-Piwonka, O. Piro, J. M. L. Figueiredo, B. Romeira, and J. Javaloyes. Bursting and Excitability in Neuromorphic Resonant Tunneling Diodes. *Phys. Rev. Appl.* 15, 34017 (2021).
- [5] B. Romeira, J. Borme, H. Fonseca, J. Gaspar, and J. B. Nieder. Efficient light extraction in subwavelength GaAs/AlGaAs nanopillars for nanoscale light-emitting devices. *Optics Express* 28, 32302-32315 (2020).

Neural network computing with large-area lasers

Xavier Porte^{1,*}, Anas Skalli¹, Nasibeh Haghighi², Stephan Reitzenstein², James A. Lott², and Daniel Brunner¹

¹Institut FEMTO-ST, Université Bourgogne Franche-Comté CNRS UMR 6174, Besançon, France

²Institut für Festkörperphysik, Technische Universität Berlin, Hardenbergstraße 36, 10623 Berlin, Germany

*javier.porte@femto-st.fr

High-performance computing hardware is crucial for advanced neural network (NN) computing schemes [1,2]. Photonics promises strong advantages in terms of parallelism, yet until now scalable and integrable concepts are scarce and partially rely on exotic substrates [3]. Here, we discuss the advantages of using large-area semiconductor lasers as photonic neuromorphic substrates. As practical case, we implement a fully parallel photonic reservoir computer based on the spatially distributed modes of an efficient and fast large-area vertical-cavity surface-emitting laser (LA-VCSEL) [4]. Such electro-optic devices are especially appealing for neuromorphic applications due to their high energy efficiency and modulation bandwidths [5]. As photonic neuron substrate we use the complex multimode field of an injection locked LA-VCSEL of 50 μm diameter emitting around 920 nm. Our LA-VCSEL was fabricated via standard commercial technology and follows a minimalistic design principle boosting its small-signal modulation bandwidths beyond 20 GHz. Noteworthy, all the photonic NN connections to- and from- the LA-VCSEL are implemented in hardware: the injected information is Boolean encoded on a digital micro-mirror device (DMD). Intra-cavity fields and carrier diffusion intrinsic to LA-VCSELs recurrently couple the >300 photonic neurons, and trainable readout weights are encoded on a second DMD and photo-detected to directly provide the computational result. We online train the readout weights to perform n-bit header recognition, XOR and digital-to-analog conversion tasks. We operate our recurrent photonic NN in its steady state with bandwidths of several 100s inferences per second, only limited by the communications with external hardware. Further, we analyze the optimal system parameters and relevant computational metrics for neural network computing [6]. Finally, we discuss the application of our approach to a task relevant for optical communications, i.e. nonlinear channel equalization. For this, we review the steps to adapt our system to c-band optical communications wavelength and to process optical information at multi-GHz rates.

References

[1] N. P. Jouppi, C. Young, N. Patil, and D. Patterson, "A domain-specific architec-

- ture for deep neural networks," *Commun. ACM* 61(9), 50–59 (2018).
- [2] W. J. Dally, Y. Turakhia, and S. Han, "Domain-specific hardware accelerators," *Commun. ACM* 63(7), 48–57 (2020).
- [3] G. Van der Sande, D. Brunner, and M. C. Soriano, "Advances in photonic reservoir computing," *Nanophotonics* 6(3), 561– 576 (2017).
- [4] X. Porte, A. Skalli, N. Haghighi, S. Reitzenstein, J. A. Lott, and D. Brunner, "A complete, parallel and autonomous photonic neural network in a semiconductor multimode laser," *J. Phys. Photonics* 3(2), 024017 (2021).
- [5] A. Skalli, J. Robertson, D. Owen-Newns, M. Hejda, X. Porte, S. Reitzenstein, A. Hurtado, and D. Brunner, "Photonic neuromorphic computing using vertical cavity semiconductor lasers," *Optical Materials Express* 12(6), 2395 (2022).
- [6] A. Skalli, X. Porte, N. Haghighi, S. Reitzenstein, J. A. Lott, and D. Brunner, "Computational metrics and parameters of an injection-locked large area semiconductor laser for neural network computing," *arXiv: 2112.08947* (2021).

Extreme events prediction with imperfect data from a spatiotemporally chaotic system

V. A. Pammi¹, M. G. Clerc², S. Coulibaly³, S. Barbay^{1,*}

¹ Centre de Nanosciences et de Nanotechnologies, CNRS, Université Paris-Saclay, Palaiseau, France

² Departamento de Física and Millennium Institute for Research in Optics, FCFM, Universidad de Chile, Santiago, Chile

³ Laboratoire de Physique des Lasers, Atomes et Molécules, Université de Lille, Lille, France

* sylvain.barbay@c2n.upsaclay.fr

The prediction of the evolution of chaotic systems with a model-free approach is a standard benchmark task for many machine learning algorithms. The task is much harder when considering spatiotemporally chaotic systems, where rare and intense events (extreme events) can form. There has been significant progress in the field recently in this direction. However, these recent results rely on an accurate knowledge of the spatiotemporal field. This is obviously not always possible in natural or physical systems, where only an imperfect knowledge of one observable is possible, with a finite spatial and temporal resolution. We present results on the prediction of extreme events from experimental data from a spatiotemporally chaotic broad area laser. Because of the timescales at stake, the dynamics are only known simultaneously in two different locations of the laser emission profile, and we can record a finite number of locations. Using this information in a machine learning algorithm and by identifying precursors of extreme events, we can achieve cross-prediction of their occurrence in space-time with more than 70% accuracy with a prediction horizon larger than the nonlinear Lyapunov time and at a location disconnected from the correlation area of the extreme event.

Enhancing the Power in the Bucket (PIB) in Coherent Laser Beam Combining

A.Lapucci*, M.Ciofini

Istituto Nazionale di Ottica (INO-CNR), Largo Enrico Fermi 6, 50125 Arcetri (Florence), Italy

* antonio.lapucci@ino.cnr.it

Recently Coherent Beam Combining techniques have been adopted with the aim of attaining high-power laser beams maintaining a good collimation, thus enabling several specific applications such as long-range communications, remote power delivering, or extreme intensity laser/matter interaction. They have received a renewed interest given the very good performances obtainable with high power fiber lasers adopting MOPA architectures and phase locking feedback loops. Combination techniques are commonly divided into two main categories: tiled aperture techniques and filled aperture techniques. In fact there are some schemes that fall in between these two cases, they rely on an aperture filling process.

Aperture Filling was demonstrated several years ago both for semiconductor laser arrays and for wave-guided CO₂ laser arrays. In the case of diode lasers, the process was based on de-phasing the different spatial frequency orders, operating on a Fourier plane. This is substantially the focal plane of a lens that is obviously inaccessible in the case of high power lasers. We showed, more than 20 years ago, that propagation itself performs an advantageous phase retardation between spatial frequency orders, thus beam quality improvements can be obtained without focal plane operations. Here we analyze the suitability of this technique in the case of high-power fiber laser arrays.

We present the numerical analysis performed for two case studies based on 20/400 double-clad fibers: a square array consisting of 16 fibers and an hexagonal array consisting of 19 fibers. We show the effect of phase filtering at distances of the order of few centimeters. Beam quality assessment is given in terms power in the Far Field main lobe. Improvements of PIB from levels in the range 40-60% to values of the order of 85% are demonstrated. We also report on some preliminary experimental activities aimed at validating the method.

High-Performance Detection of Toxic Gases Using a New Microsensor based on Graphene Field-Effect Transistor

Khalil Tamersit^{1,2,3,*}

¹Department of Electronics and Telecommunications, Université 8 Mai 1945 Guelma, Guelma 24000, Algeria.

² Department of Electrical and Automatic Engineering, Université 8 Mai 1945 Guelma, Guelma 24000, Algeria.

³ Laboratory of Inverse Problems, Modeling, Information, and Systems (PIMIS), Guelma University, Guelma 24000, Algeria

*tamersit_khalil@hotmail.fr, khalil.tamersit@univ-guelma.dz

In this paper, a new gas microsensor based on graphene field-effect transistor (GFET) is proposed, modeled, and investigated through a compact drain current model. This latter is based on drift-diffusion carrier transport, which takes into account the sensing and transduction mechanisms and includes the dimensional and physical sensor parameters [1]. The used sensing principle is based on the work function modulation technique [2], [3]. The shift in Dirac point voltage is considered as a sensing metric [4]. The proposed GFET-based gas microsensor, that employs a top sensitive gate as reference and a back gate for control, has exhibited an ultra-sensitive performance toward the toxic gases. Note that the obtained sensing performance can be further improved by tuning the micro sensor electrostatics via the modulation of the top and bottom oxide capacitances. The proposed approach can serve as physical basis while paving the way to optimized fabrication. The obtained results make the proposed GFET-based gas microsensor as a promising candidate for high-performance and low-cost monitoring and defense applications.

References

- [1] K. Tamersit et al., "A new pressure microsensor based on dual-gate graphene field-effect transistor with a vertically movable top-gate: Proposal, analysis, and optimization," *AEU - International Journal of Electronics and Communications*, vol. 124, p. 153346, Sep. 2020.
- [2] J. Janata and M. Josowicz, "Conducting polymers in electronic chemical sensors," *Nature Mater.*, vol. 2, no. 1, pp. 19–24, Jan. 2003.
- [3] K. Tamersit et al., "Double-gate graphene nanoribbon field-effect transistor for DNA and gas sensing applications: Simulation study and sensitivity analysis," *IEEE Sensors Journal*, vol. 16, no. 11., pp. 4180–4191, Jun. 2016.
- [4] F. Schwierz, "Graphene transistors," *Nature Nanotech*, vol. 5, pp. 487–496, 2010.

Multibody Modeling for the Design of an Autonomous Rover for Precision Agriculture Applications in Developing Countries

Marco Claudio De Simone^{1,*}, **Zandra Betzabe Rivera Chavez**^{2,†}, **Angelo Lorusso**^{1,*}
and **Domenico Guida**^{1,*}

¹ Department of Industrial Engineering, University of Salerno Via Giovanni Paolo II, 132 - Fisciano, 84084, Italy

² Engineering Research Institute Universidad Privada San Juan Bautista Av. José Antonio Lavalle N° 302-304 Lima, 15067, Peru'

* fmdesimone,alorusso,guida@unisa.it

† zandra.rivera@upsjb.edu.pe

Precision agriculture can be seen as a vital component of the modern legacy of the third wave of the new agricultural revolutions, also called the Green Revolution, representing the set of research technology transfer initiatives that increased agricultural production in several parts of the world. More specifically, precision agriculture is a farming management concept based on observing, measuring, and responding to the variability in crops. In particular, the main goal of this approach is to define a decision support system for the entire farm management aimed at optimizing returns on inputs, minimizing waste in general, and preserving precious resources like water. The agricultural sector is going through a cultural transition that is rather chaotic due to a market that offers multiple technological solutions, often not yet appropriate to be profitably introduced. Instead, the "industry 4.0" approach to agricultural activities requires effective identification of the technical architecture, the training of operators, and the optimal, reliable creation of products and services. This transformation process can be appreciated, particularly for productive activities in "protected" environments, such as greenhouses and agro-industry (stables, wineries, oil mills, processing industries) where it is possible to create fully controllable conditions. It is instead challenging to implement agricultural activities carried out in open fields subject to climatic variability and the related responses of the territorial elements: slopes, exposures, soil with its structural characteristics and management, the orographic structure, which require continuous management adjustments for the changing conditions and the consequent operational timeliness. The real purpose of innovation is the possibility of implementing effectively and profitably a Sustainable Precision Agriculture (SPA). Low-cost measurement technologies and automated management procedures allow re-gaining possession of abandoned rural territories, using them again for open-field crops or tree crops. Knowledge of the soil conditions of the crop, the environment, and other factors such as pest dynamics population, represents the first primary augmented reality tool that will increase management capabilities both in detail and the extension of corrective actions. This paper presents a design activity carried out to develop a new multipurpose Rover that could be a valuable and ideal companion for small vine-growers

and traditional winemakers in their daily activities while gathering relevant information for decision making. The idea is to design a vehicle that could be assembled with technology readily available in less developed countries, with the use of easily accessible open-source components for sensors, actuators, microcontrollers, and communication equipment, with the least

amount of maintenance. Furthermore, In addition, the vehicle is also designed to perform missions in total autonomy or through collaborative swarms (Swarm Robotics), using techniques of Artificial Intelligence and Sensor Fusion, in order to provide a scientific tool to manage in a rational and targeted phytosanitary intervention in the vineyard, to combat the danger of downy mildew that creates severe damage to wine production and to analyze the characteristics of soil fertility, especially for soils that have high variability, to vary the doses of fertilizer and water according to needs through the use of geographical instructions (prescription map), using satellite images, appropriate sensors and calculation codes, according to which to vary the doses to be distributed thanks to dispensers specifically designed to distribute quantities at a variable rate (Vrt).

Design of a Test-Rig for Space Applications in Microgravity Conditions

Marco Claudio De Simone^{1,*}, Francesca Chiara Di Martino^{2,†} and Domenico Guida^{1,*}

¹ Department of Industrial Engineering, University of Salerno Via Giovanni Paolo II, 132 - Fisciano, 84084, Italy

² Engineering Research Institute Universidad Privada San Juan Bautista Av. Jose ´ Antonio Lavalle N° 302-304 Lima, 15067, Peru´

* fmdesimone, guida@unisa.it

† f.dimartino19@studenti.unisa.it

Lo spazio e' sempre piu' caratterizzato dalla presenza di detriti, che potrebbero essere causa di malfunzionamento o rottura dei velivoli durante la loro missione. Inoltre, la difficolta' di fornire carburante ed effettuare interventi di manutenzione per i sistemi gia' in orbita sottolineano la necessita' di sviluppare nuove tipologie di dispositivi capaci di effettuare operazioni di manutenzione in maniera autonoma. Al campo della robotica orbitale sono affidati tali operazioni che rientrano nel settore dell'On-Orbit Servicing (OOS). Nel futuro e', infatti, previsto l'utilizzo di bracci robotici che presentino configurazioni tali da garantire adeguati interventi di ispezione, rilocazione, ag- giornamento di hardware obsoleto, assemblaggio di moduli ed operazioni di manutenzione ordinarie. L'invio di un mezzo di manutenzione potrebbe rappresentare una soluzione per trarre ulteriore utilita' da quella che sarebbe stata una perdita; a questo scopo, il settore dell'On-Orbit Servicing (OOS) prevede Interventi di ispezione, Rilocazione, Aggiornamento di hardware obsoleto, Assemblaggio di moduli e Operazioni di manutenzione ordinarie. I manipolatori presenti sulle stazioni spaziali sono generalmente impiegati per l'attracco di moduli o navicelle e sono generalmente costituiti da bracci robotici ridondanti dotati di telecamere integrate, di un sistema di illuminazione, end- effector sostituibili, di un meccanismo di attacco, di un sistema GNC (Guida, Navigazione e Controllo) e di un pianificatore. il sistema GNC comprende sensori per la posizione e per la misura di assetto ed e' utilizzato per il controllo dell'avvicinamento al fine di agganciare piu' facilmente il bersaglio. Il pianificatore invece, ha lo scopo principale di pianificare i movimenti del manipolatore in base ai diversi compiti attraverso un controllore, che guida ciascun giunto per tracciare il movimento desiderato. Le problematiche per il controllo del braccio robotico sono legate, principalmente, al sistema di attracco, al controllo dell'assetto e allo spazio di lavoro, data l'assenza di gravita'. Per questo motivo, il gruppo di ricerca di Meccanica Applicata alle Macchine ha deciso di progettare un test-rig da laboratorio per emulare il comportamento dinamico di un satellite in fase di Docking e durante missioni di OOS. Per questo scopo si e' deciso di impiegare un manipolatore parallelo a sei gradi di liberta', meglio nota come Piattaforma di Stewart, in grado di garantire elevata precisione e rigidezza per riprodurre in laboratorio

le condizioni di volo e di manovra per l'avvicinamento e l'aggancio tra velivoli in condizioni di microgravità. Attraverso procedure di modellazione CAD-MultiBody-FEM, è stata condotta una analisi cinematica e dinamica inversa per la definizione degli attuatori. Le analisi multibody sono state condotte nell'ambiente di simulazione multidominio Simscape che hanno permesso di testare il test-rig virtuale durante un rendezvous si suole indicare il complesso di manovre che occorre eseguire affinché due veicoli spaziali possano giungere a contatto.

Mimicking the Complex Human Circulatory System via a Custom Hydro-mechanical Pulse Duplicator

Eleonora Manzoni^{1,*}, Mirco Rampazzo^{1,†}, Luigi Di Micco², Paolo Peruzzo², Francesca M. Susin²

¹Department of Information Engineering, University of Padova, Via Gradenigo 6/B, 35131, Padova, Italy

²Institut für Theoretische Physik, Technische Univ. Berlin, Hardenbergstr. 36, 10623 Berlin, Germany

*eleonora.manzoni@phd.unipd.it

†mirco.rampazzo@unipd.it

Worldwide, cardiovascular diseases are the leading causes of morbidity and mortality, therefore there has been significant advancement in heart valve repair and replacement over the last 40 years. As a result, future basic, applied, and clinical research, as well as treatment advances, are in high demand [1]. Despite significant advancements in cardiovascular prosthetic device technology, these devices are still far from ideal, and continual adjustments are being made to improve their performance, efficacy, and life expectancy. One could say that biological and human systems, and surely even the in vitro workbenches that aim at their replication, are complex systems. Specifically, the term complex system was recently developed by the scientific community to represent events, structure, aggregation, species, or issues that have a similar theme. They are naturally sophisticated or elaborate; they are seldom totally deterministic; mathematical models of the system are frequently complex and feature non-linear, ill-posed, or chaotic behaviour; and the systems are prone to unpredictable results (so-called emergent behaviour) [2]. In other words, a complex system is one that has various interactions among its many diverse components, and biological systems, in particular, attain hierarchical complexity that has no parallel outside of biology. In the case of complex systems, however, it is incorrect to assume that the whole system's behavior can be reduced to the sum of its parts. This is also the case of the pulse duplicators, in which the components are strongly dependent on each other and interact in multiple ways. Cardiovascular hydrodynamic testing systems (e.g., pulse duplicators, PDs) simulate, indeed, the human systemic circulation, allowing in vitro testing of medical devices such as aortic valves and stents [3]. PD loops are hydraulic lumped models that simplify the complex dynamics of the cardiovascular system. For example, combining system effects like flow resistance (peripheral resistance), volume expansion under pressure (arterial compliance), and feed capacity (atrial supply) yields a useful simulation model. To evaluate cardiac and vascular devices a variety of approaches are used, including numerical models, laboratory experiments, and human trials, including animal tests. Cardiovascular engineering, in particular, makes good use of in vitro experiments to assess the performance and safety of medical devices. Specifically, in

contrast to commercial workbenches like the ViVitro PD (Vivitolabs, 2014), this paper presents the PD in use at the Healing Research Laboratory (HeR Lab) at the University of Padova, Italy. It is characterized by high customizability, modularity, and it simulates a wide range of physiological and pathologic conditions. According to the requirements, the custom PD enables for the architecture to be simplified or complicated (heaters, silicone physiological ventricular chambers replica instead of the representative chamber, etc.). In this fashion, the PD may simulate the complicated system of human systemic circulation to see how changes in hemodynamic parameters (such as heart flow rate and blood pressure) affect the prosthetic components' hemodynamic performance. HeR Lab's workbench, in particular, uses a lumped-parameter method to model physiological situations. It consists of stiff and flexible tubes, chambers, air tanks, taps, and silicone components. The mimic circulatory loop's flow passes through a series of devices, each representing a different aspect of the circulatory system. The PD is made up of the following major components. The Ventricle Chamber is fed by the linear electromagnetic Motor and Bellow, which is controlled by a mitral valve at the input and a flow meter at the exit. The valve housing, two pressure transducers (upstream and downstream of the aortic valve, respectively), and a deformable silicone aortic arch that is a physiological copy of the anatomic district are all situated downstream of the flow meter in the Aortic Chamber. Before the flow enters the Atrial Chamber, the system is completed by the Aortic Compliance, the Systemic Compliance Chamber, and the Peripheral Resistance Valve [4]. To conduct effective in-vitro experiments, the system must simulate the human systemic circulation under certain physiology conditions such as heart rate (the number of heart contractions per minute), cardiac output (the volume of blood pumped by the heart per unit time), and aortic pressure (the blood pressure at the root of the aorta). The PD control unit manipulates inputs (e.g. the stator variable voltage of the linear electromagnetic motor) that lead the system to deliver particular desired system outputs (e.g. heart rate and cardiac output set-points). The operator manually adjusts the Compliance Chamber volume, while the tap (Peripheral Resistance Valve) closing degree is automatically reached through automatic control algorithms that operating with dedicated hardware obtain other outputs characteristics (e.g. mean, maximum, minimum, spread related to the aortic pressure waveform shape).

References

- [1] P. A. Iaizzo, R. W. Bianco, A. J. Hill, and J. D. S. Louis, *Heart Valves*. Springer, 2013.
- [2] R. Frei and G. Di Marzo Serugendo, "Concepts in complexity engineering," *International Journal of Bio-Inspired Computation*, vol. 3, no. 2, pp. 123–139, 2011.
- [3] L. Di Micco, G. Comunale, S. Bonvini, P. Peruzzo, and F. M. Susin, "Distensibility of deformable aortic replicas assessed by an integrated in-vitro and in-silico approach," *Bioengineering*, vol. 9, no. 3, p. 94, 2022.
- [4] M. Rampazzo, E. Manzoni, M. Lionello, L. Di Micco, and F. M. Susin, "Automation

of the peripheral resistance valve in a hydro-mechanical cardiovascular pulse duplicator system," *Control Engineering Practice*, vol. 116, p. 104929, 2021.

Nonlinear oscillators with memory: solutions with the same period of perturbations

Paolo Maria Mariano^{1,*}, **Marco Spadini**^{2,†}

¹ DICeA, University of Florence, via Santa Marta 3, I-50139 Firenze, Italy

¹ DIMAI, University of Florence, via Santa Marta 3, I-50139 Firenze, Italy

* paolomaria.mariano@unifi.it

† marco.spadini@unifi.it

In \mathbb{R}^n , the functional equation

$$\ddot{x}(t) = g \left(x(t), \dot{x}(t), \int_{-\infty}^t \mathcal{K}(t-s)\varphi(x(s), \dot{x}(s))ds \right) \quad (0.1)$$

where $g : \mathbb{R}^n \times \mathbb{R}^n \times \mathbb{R}^k \rightarrow \mathbb{R}^n$ is a continuous map and $\varphi : \mathbb{R}^n \times \mathbb{R}^n \rightarrow \mathbb{R}^k$ is locally Lipschitz, is a model structure applying to the representation of a variegated class of local dynamics, above all those including lateral inhibition in the vision or local gene dynamics. We consider in equation (0.1) kernels \mathcal{K} with the structure of a gamma probability distribution, namely

$$\gamma_a^b(s) = \frac{a^b s^{b-1} e^{-as}}{(b-1)!} \text{ for } s \geq 0, \quad \gamma_a^b(s) = 0 \text{ for } s < 0,$$

with mean b/a and variance b/a^2 . With this, we aim at describing circumstances in which critical phenomena in the past influence more than others the memory. We also include a periodic living load with period T , so that the selected dynamical system becomes

$$\ddot{x}(t) = g \left(x(t), \dot{x}(t), \int_{-\infty}^t \gamma_a^b(t-s)\varphi(x(s), \dot{x}(s))ds \right) + \lambda f(t, x(t), \dot{x}(t)), \quad (0.2)$$

where $f : \mathbb{R} \times \mathbb{R}^n \times \mathbb{R}^n \rightarrow \mathbb{R}^n$ is periodic of period T in the first variable, and λ is a non-negative real parameter.

We determine conditions under which for given values of $\lambda \geq 0$ there are C^2 functions $x : \mathbb{R} \rightarrow \mathbb{R}^n$ of period T that satisfies identically equation (0.2). Our main result goes as follows:

Theorem 1. Let $U \subseteq \mathbb{R}^n$ be open and such that $\deg(\Phi, U)$ is well-defined and nonzero. Let also $\Omega \subseteq [0, \infty) \times C_T^1(\mathbb{R}^n)$ be open and such that $\tilde{\Omega} = U$. Then, in $X \cap \Omega$ there is a connected subset Γ of nontrivial T -forced pairs with relative closure to Ω non-compact; it intersects the set

$$(0.3) \quad \{(0, \bar{u}) \in \Omega : u \in (\alpha, \beta) \cap \Phi^{-1}(0)\},$$

where $\Phi : \mathbb{R}^n \rightarrow \mathbb{R}^n$ is defined by

$$(0.4) \quad \Phi(u) = g(u, \mathbf{0}_n, \varphi(u, \mathbf{0}_n)).$$

References

- [1] P. Poggi, M. Locatelli, E. Pugliese, D. Delle Donne, G. Lacanna, R. Meucci, M. Ripepe - Remote monitoring of building oscillation modes by means of real-time mid infrared digital holography. Scientific Reports 6(1) 1-8, 2016.
- [2] M. Locatelli, P. Poggi, E. Pugliese, G. Lacanna - Method and system for monitoring a building structure. EP 3250964A1, 4/8/2016, European Patent Office.

Dynamics of interneurons in the presence of a sodium channel mutation

Paolo Seghetti^{1,2}, Michael Pusch³, Angelo Di Garbo^{4,5}

¹ Scuola Superiore S. Anna, Pisa (Italia)

² CNR - Istituto di Fisiologia Clinica, Pisa (Italia)

³ CNR - Istituto di Biofisica, Genova (Italia)

⁴ CNR - Istituto di Biofisica, Pisa (Italia)

⁵ Dipartimento di Fisica, Università di Pisa, Pisa (Italia)

Background: Familial Hemiplegic Migraine is a genetic migraine which is caused by specific mutations mostly affecting interneurons' membrane ion transport. The mutations cause an increase in the persistent sodium current, which is thought to be the cause of neuronal hyperexcitability and, consequently, migraine. We investigate the electrophysiological effects of SCN1A mutations on the NAv1.1 ionic channel that are involved in Familial Hemiplegic Migraine of type 3 (FHM3). Moreover, we study the effect of a sodium channel blocker as a therapeutic solution.

Methods: We modified a previously published interneuron dynamical model and studied the effect of an increased persistent sodium current. Moreover, we investigated the effect of a sodium channel blocker. The effects of persistent current and channel blocker were represented by 2 parameters in the model. Concerning the model, we classified the bifurcation that causes the onset of the tonic firing when the input current is increased. Moreover, we calculated the states of phase lock for 2 coupled neurons as a function of the input current to the neuron, for both electrical and chemical synapses; when feasible a reduction to second order of accuracy with isostable coordinate reduction was used. Additionally, we calculated the metabolic efficiency and consumption of the neuron while in the firing regime. Every analysis reported above was performed for different values of persistent sodium current and blocker concentration.

Results: We observed that, opposing the current clinical hypothesis, the mutation causes a decrease in the firing frequency in the FHM3 neuron model. Moreover, the increase in persistent sodium current causes an increase in the metabolic cost of the firing regime and an increase in ionic currents overlap, which is a marker of inefficiency of the action potential. Moreover, the mutation causes an increase in synchrony for the synaptic coupling of 2 neurons. The channel blocker has an effect opposed to the one of the mutation in a dose dependant way and is able to partially restore the wild type properties of the neuron. **Conclusions:** Our results suggest that hyperexcitability may not be the only cause for the onset of migraine, but more than one mechanism, including metabolic stress, may be active in causing the migraine phenotype.

Mining Intraday Electricity Market Trades

Saeed Mohammadi and Mohammad Reza Hesamzadeh

School of Electrical Engineering and Computer Science KTH Royal Institute of Technology,
Stockholm, Sweden
{saeedmoh, mrhesa}@kth.se

Intraday electricity market offers an adjustment platform for electricity market participants. A liquid intraday market is an essential requirement for the future fossil-free electricity system with numerous uncertainties. The intraday market is a relatively new trading platform. The historical intraday trades often follow different statistical regimes partly due to frequently new introduced regulations. Its unique features such as being closer to the time of delivery, pay-as-bid option, and 24/7 operation, make it an enabler for integrating more renewable energy resources. The intraday electricity market operated by Nord Pool is a pay-as-bid market with continuous trades until one hour before real-time delivery. We analyze the historical intraday trades in the Nord Pool market. We analyze the relationship between the day-ahead and intraday electricity market prices and traded volumes. Mining the intraday market data leads to a better understanding of the behaviour of its market itself as well as the market participants.

Acknowledgements

This work was financially supported by the Swedish Energy Agency (Energimyndigheten) under Grant 3233. The required computation is performed by computing resources from the Swedish National Infrastructure for Computing (SNIC) at PDC center for high performance computing at KTH Royal Institute of Technology which was supported by the Swedish Research Council under Grant 2018-05973. (Corresponding author: Saeed Mohammadi.) Saeed Mohammadi and Mohammad Reza Hesamzadeh are with the School of Electrical Engineering and Computer Science at KTH Royal Institute of Technology, 10044 Stockholm, Sweden (e-mail: saeedmoh@kth.se; mrhesa@kth.se).

Bioinspired controller for a robotic knee orthosis

Petrarca M¹, Bottoni M¹, Favetta M¹, Bogaert K¹, Carniel S¹, Castelli E¹, Piscitelli D^{2,3}, Summa S¹

¹Movement Analysis and Robotics Laboratory (MAR Lab), Intensive Neurorehabilitation and Robotics Department, “Bambino Gesù” Children’s Hospital, IRCCS, Rome, 00050, Italy

² School of Medicine and Surgery, University of Milano Bicocca, 20126 Milano, Italy

³School of Physical and Occupational Therapy, McGill University, Montreal, QC H3G 1Y5, Canada

Introduction:

Robotic wearable orthosis faces many challenges. A list, but not exhaustive, can include biomechanical coupling, wearability, intention detecting, functional coupling, energy autonomy, trajectory, and torque anticipation. Notably, from a rehabilitative perspective emerges the necessity to define the more proficient rule of interaction to induce learning processes or support the function when the recovery limit is reached. In other words, it seems necessary to select the optimal controller among the technological solution currently available [1]. The learning attitude of an exoskeleton needs to be driven by a hypothesis on motor control. This last requirement answers two challenges: i) verify the scientific theory on motor control and ii) facilitate the interpretation of the results achieved during functional recovery.

Methods:

We decided to utilize the referent control of action and perception theory (RC theory), also known as the equilibrium-point hypothesis [2], applied to gait as a driven theory for developing a robotic knee controller. We developed a friendly-customized, wearable, and light prototype of robotic knee orthosis. We selected the knee as a relatively simple joint assimilable to a one- degree articulation. Then, we simplified the low- level control of actuators by choosing a commercial device including an embedded high-resolution encoder, a PID, and a current-based controller (Dynamixel MX-AT64, ROBOTIS Co, Korea). This simple solution allowed to concentrate the effort on the interaction control rule. The critical aspect of the RC theory is to detect the referent configuration for the initial and final position of the limb used by the central nervous systems for regulating the threshold of muscle activation (i.e., λ) that allows the transition from the initial joint position (actual joint position) to the desired one. The regulation of λ threshold of the agonist-antagonist muscles also allows the torque control linked to the length-force invariant characteristic of muscles [3].

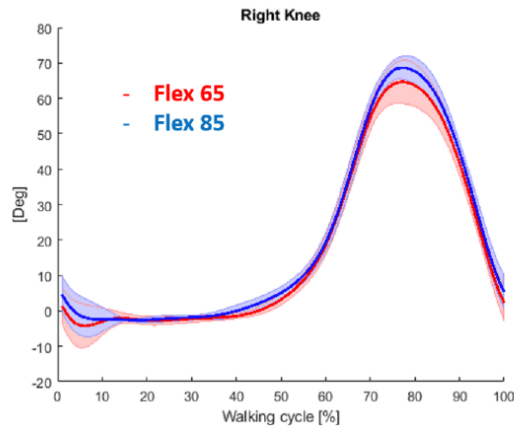


Figure 0.1: Knee angle patterns while walking. The red and blue lines represent the joint angle when a flexion of respectively 65 and 85 (deg) was set to the actuator.

Results:

To achieve the goal of a device able to simulate this control, we utilized an IMU positioned on the thigh portion of the orthosis; we collected during the gait of the subject the encoder of the actuators and the IMU data. We analyzed the data, and we utilized the pose of the IMU as a thigh frame of reference for differentiating the phases of knee flexion-extension during gait. We used the temporal encoder series to define the maximum flexion and extension degree as the desired joint position (Fig 1). Then, we used the thigh pose threshold as a trigger for changing the referent position of the actuator and the current-based control to interact with the gait, increasing or decreasing the support to the action. The device was positioned on the subjects' right side, and no discomfort was reported. This represents the first step for moving to an oscillation towards a gait pattern modification.

References

- [1] Wen-Zhou Li, Guang-Zhong Cao, Ai-Bin Zhu. Review on Control Strategies for Lower Limb Rehabilitation Exoskeletons. IEEE Access, 2021-09-06, DOI: 10.1109/access.2021.3110595
- [2] Anatol G. Feldman, Mindy F. Levin, Alessandro Garofolini, Daniele Piscitelli, Lei Zhang. Central pattern generator and human locomotion in the context of referent control of motor actions. Clinical Neurophysiology 132 (2021) 2870–2889.
- [3] Anatol G. Feldman. Once More on the Equilibrium-Point Hypothesis (λ Model) for Motor Control. Journal of Motor Behavior, 18, 1986 - Issue 1. doi: 10.1080/00222895.1986.10735369

Wednesday 20th

On the effect of the number of photons on the generation and transfer of entangled states between toroidal cavities via a chain of artificial atoms

Emilio H. S. Sousa, A. Vidiella-Barranco, and J. A. Roversi

Gleb Wataghin Institute of Physics, University of Campinas – UNICAMP, 13083-859
Campinas, SP, Brazil

We present an efficient scheme for the generation of entangled states of two spatially separated whispering-gallery-mode (WGM) micro-resonators which are coupled via two two-level atoms. The cavities support two counter propagating WGMs that may also interact with each other via a coupling constant j_i . Each cavity interacts with one atom (coupling constants, g_i) and the atoms are dipole coupled to each other with coupling constant Ω . Using the atoms chain as bridges we explore the possibility of generation, transfer as well distributing quantum entanglement between the two cavities. In a previous work, we found that it is possible to generate different entangled states of cavity fields depending on the (intra-cavity or extra-cavity) couplings if the cavities are coupled via a single two-level atom. For instance, a 4-partite entangled (W-type) state involving all four cavity modes can be generated from an initial product state. In contrast, the presence of a second atom will bring substantial changes to the entanglement's dynamics. We show that, for an initial preparation with the system having only one photon, the atoms can become periodically (and maximally) entangled while the intra-cavity modes in each cavity become periodically (partially) entangled. On the other hand, initial preparation with two photons in the system, the dynamics can be adjusted in such a way that the intra-cavity modes in each cavity become periodically (and maximally) entangled while the atoms remain unentangled all time. In both cases mentioned above, the entanglement evolves synchronously in each cavity, having its maxima and minima at the same times, showing signature of 4-partite entanglement.

High photosensitivity in band-to-band tunneling regime of carbon nanotube field-effect phototransistor: Numerical investigation

Khalil Tamersit ^{1,2,3,*},

¹ Department of Electronics and Telecommunications, Université 8 Mai 1945 Guelma, Guelma 24000, Algeria.

² Department of Electrical and Automatic Engineering, Université 8 Mai 1945 Guelma, Guelma 24000, Algeria.

³ Laboratory of Inverse Problems, Modeling, Information, and Systems (PIMIS), Guelma University, Guelma 24000, Algeria.

* tamersit_khalil@hotmail.fr, khalil.tamersit@univ-guelma.dz

In this work, we show how the band-to-band tunneling (BTBT) regime of ultra-scaled carbon nanotube field-effect transistor (CNTFET) [1] can be exploited to get ultra- high photosensitivity to low infrared (IR) optical power. The CNT-based phototransistor has been computationally assessed by solving self-consistently the Poisson solver including the photovoltage with the non-equilibrium Green's function formalism within the ballistic limit [2]. This quantum simulation approach is adopted to take into account the BTBT mechanisms on which the photosensing principle is based in the proposed device. It has been found that ultra- high photosensitivity can be recorded to low gate photovoltages induced by weak IR incident optical powers. The obtained results indicate that the proposed nanoscale CNT phototransistor operating in BTBT photosensing regime can serve the modern optoelectronics, which is in dire need for ultra-sensitive phototransistors with low detection limits.

References

[1] K. Tamersit, "New nanoscale band-to-band tunneling junctionless GNR-FETs: potential high-performance devices for the ultrascaled regime," *Journal of Computational Electronics*, vol. 20, no. 3, pp. 1147–1156, Apr. 23, 2021.

[2] K. Tamersit, "Energy-Efficient Carbon Nanotube Field-Effect Phototransistors: Quantum Simulation, Device Physics, and Photosensitivity Analysis," *IEEE Sensors Journal*, vol. 22, no. 1, pp. 288–296, Jan. 01, 2022.

Experimental evidence of a nonlinear dynamics in a two-level non-autonomous laser model

Michele Castelluzzo¹, Matteo Cescato¹ Alessio Perinelli¹ Riccardo Meucci² and Leonardo Ricci¹

¹Department of Physics, University of Trento, 38123 Trento, Italy.

²National Institute of Optics - CNR, 50125 Florence, Italy.

In 2021, the three-dimensional laser model proposed in the 1980s [1] to investigate the instabilities of a laser with feedback was revisited both from a theoretical and, by relying on electronic implementations, an experimental perspective [2, 3]. Very recently such minimal universal model was theoretically and numerically investigated in a situation in which feedback is replaced by a sinusoidal modulation of the cavity losses parameter [4, 5]. This last study showed the occurrence of generalized multistability and its dependence from different parameters, in particular the modulation bias. We describe here an electronic implementation of the modified minimal universal model in which the system's parameters can be set with a high degree of reproducibility by leveraging on state-of-the-art electronic circuitry and remotely-controlled, digital programmable devices. The experimental results show a remarkably good agreement with the numerical predictions, thus highlighting the validity of the theory model and the reliability and flexibility of its experimental implementation. Future developments that exploit the versatility of both the model and its implementation are briefly discussed.

References

- [1] F. T. Arecchi, W. Gadomski, and R. Meucci. Generation of chaotic dynamics by feedback on a laser. *Phys. Rev. A*, 34:1617–1620, 1986.
- [2] R. Meucci, S. Euzzor, F. T. Arecchi, and J.-M. Ginoux. Minimal Universal Model for Chaos in Laser with Feedback. *Int. J. Bifurcation and Chaos*, 31:2130013, 2021.
- [3] L. Ricci, A. Perinelli, M. Castelluzzo, S. Euzzor, and R. Meucci. Experimental Evidence of Chaos Generated by a Minimal Universal Oscillator Model. *Int. J. Bifurcation and Chaos*, 31:2150205, 2021.
- [4] F. T. Arecchi, R. Meucci, G. P. Puccioni, and J. R. Tredicce. Experimental evidence of subharmonic bifurcations, multistability, and turbulence in a q-switched gas laser. *Phys. Rev. Lett.*, 49:1217–1220, 1982.
- [5] R. Meucci, J.-M. Ginoux, M. Mehrabbeik, S. Jafari, and J. C. Sprott. Generalized Multistability and its Control in a Laser. accepted for publication in *Chaos*, 2022.

Modern solutions for Remote SHM

Alessandro Mitillo, Michele Pedroni, Giuliano Manfredini, Mauro Spampani

LUNITEK S.r.L. Via Variante Aurelia, 115bis 19038 Sarzana – Italy info.sarzana@lunitek.it

Structural health monitoring (SHM) is a process of in-service health assessment for a structure through an automated monitoring system, and it is a key element of cost-effective strategies for condition based maintenance. An SHM strategy consists of many important components including sensing network, data processing and analysis, damage assessment and decision making. SHM technology has great potential to offer significant economic and life-safety benefits.

However, the application of SHM technology to actual civil engineering structures cannot reach its full potential without taking advantage of the most advanced resources in terms of connectivity, remotizing protocols and remote or cloud computing.

Lunitek started its experience in Remote Structural Health Monitoring in the early 2000s as it was commissioned by DPC (Dipartimento di Protezione Civile) of Rome to install a large network of SHM systems in order to monitor relevant public buildings and structures, such as schools, town halls, hospitals and bridges all over the Italian territory (especially in the most seismically hazardous regions) and connect them to a central computing server which is in charge to collect strong motion event recordings, make automatic analysis and send damage detection alerts in case of major seismic events. Data communication between the SHM systems and the server was made through broadband connections, 2G/3G/4G connections, plus a satellite channel for redundancy. In more than 15 years of 24h/7 activity, this network helped Civil Protection technicians to take life safety decisions during emergency events like L'Aquila earthquake (2009) or Amatrice seismic sequence (2016-2017).

Since the first Remote SHM system was installed, Lunitek introduced many advances and innovations in its SHM instrumentation portfolio, including distributed WiFi based devices, integrated 3G/4G seismic stations, satellite communication devices, cloud computing systems and narrow band long range communication (LoRa) devices to cover a wide range of remote monitoring applications. The latest development of Lunitek R&D department comes from "Atlante", a research project in collaboration with INO and other private companies (partially financed by Tuscany region), and it consists in a non invasive, laser based, self computing, Industry 4.0 guideline compatible device, which can be considered a step forward in modern SHM techniques in terms of reliability, versatility and manageability.

Seismic monitoring in the Tuscany region

Nicola Signorini

Regione Toscana - Settore Sismica, via San Gallo 34A - 50129 Firenze
nicola.signorini@regione.toscana.it

For over twenty years, the Seismic Sector of the Tuscany Region has been monitoring the level of seismicity of the regional territory and the precursor parameters connected to it, as required by the Regional Law n ° 58/2009 "Rules for the prevention and reduction of seismic risk".

The activities are carried out through collaboration with the national structures in charge for seismic monitoring such as with the INGV for the National Seismic Network as regards seismometric monitoring, with the Department of Civil Protection for the National Accelerometric Network as regards accelerometric monitoring or through scientific collaboration agreements with Research Institutions, co-financed by the Tuscany Region, for the establishment of local networks.

The local networks are dedicated to the seismic monitoring of portions of the regional territory as for the northern Tuscany the Lunigiana and Garfagnana Seismic Network (RSLG) managed by the DISTAV of the University of Genova and the North Eastern Tuscany Seismic Network (RSTNO) managed by the Parsec Foundation through the Tuscan Geophysical Institute.

The geodetic and geochemical monitoring of the regional territory is carried out through multi-year collaboration agreements. With the DSFTA of the University of Siena, the movement connected with the geodynamic evolution of the regional territory, closely connected with the seismotectonic characteristics of the area, is monitored through a network of GPS stations. With the CNR-IGG of Siena, a monitoring is carried out aimed at the search for seismic precursors and the study of the relationships between water chemistry and seismic activity, through a network of multiparametric stations, located in the most seismic areas of the regional territory such as Garfagnana, Lunigiana, Mugello, Valtiberina and Amiata.

We also follow the Seismic Observatory of Structures (OSS) managed by the Civil Protection Department which monitors the oscillations caused by an earthquake to assess the expected damage. The OSS through a series of fixed accelerometers allows to detect the dynamic response parameters of strategic structures providing useful information for the management of the seismic emergency.

Infrastructure remote monitoring in Tuscany

E. Pugliese, M. Locatelli, D. Jafrancesco, P. Poggi, S. Euzzor, R. Meucci

CNR-INO, Largo E. Fermi 6, 50125 Firenze

We present an application of IR Digital Holography (IRDH) in the field of civil structure monitoring [1,2]. The holographic technique has been tested on various buildings located in Tuscany: former Primary School in Castell'Azzara (GR), Santa Caterina Church of Collegnago (MC), Palazzo Medici-Riccardi (FI), Rocca di Radicofani (SI). The first three structures are subjected to the continuous surveillance of the National Civil Protection Department by means conventional accelerometers, while the last one was monitored by the Earth Science Department of the Florence University, by means of seismometers. From the comparisons of the data obtained by IRDH and by the accelerometers and seismometers, it emerges that our remote sensing technique is particularly advantageous in terms of acquisition times and sensitivity. Indeed, the holographic technique is able to detect sub micrometric displacements (that is of the order of 1/100 of the used laser wavelength of 10.6 μ m) and to reveal the spectral content of the structure oscillations from a distance up to 30m. The obtained results confirm that IRDH is well suited for non-invasive monitoring in the field of structural engineering, seismic vulnerability and cultural heritage preservation. Furthermore, we believe that interesting tests could be sequentially performed on historical monuments and artistic heritage to determine their aging process. Future applications could be the checking of urban infrastructures in not accessible or hazardous area.

References

- [1] P. Poggi, M. Locatelli, E. Pugliese, D. Delle Donne, G. Lacanna, R. Meucci, M. Ripepe - Remote monitoring of building oscillation modes by means of real-time mid infrared digital holography. Scientific Reports 6(1) 1-8, 2016.
- [2] M. Locatelli, P. Poggi, E. Pugliese, G. Lacanna - Method and system for monitoring a building structure. EP 3250964A1, 4/8/2016, European Patent Office.

A Machine Learning Based Model for Monitoring of Composite Drilling Tools During Assembly Production Using Laser Profiler Data

Amin Amini¹, Tat-Hean Gan¹

¹Brunel Innovation Centre, TWI, Granta park, Great Abington, Cambridge, CB21 6AL, United Kingdom

The composite materials are becoming more popular due to their advantages over traditional materials, including being lightweight, high stiffness-to-density and high strength-to-weight ratios. As a result, composite materials have been widely used in manufacturing sector for various industries including aerospace, automotive, marine and energy. Nonetheless, as machining of composites is unavoidable for assembly purposes, defects can be induced at various stages of manufacturing process. Drilling of fibre-reinforced composites is a complex task due to their anisotropic, inhomogeneous, and highly abrasive characteristics. Defects form during drilling process in a way that delamination and fibre pull-out can significantly affect the strength and performance of composites. There have been a wide variety of non-destructive testing (NDT) methods playing a major role in testing of composite materials. However, the current NDT solutions for in-service inspection are largely manual, which leads to higher inspection costs. The proposed solution is to use artificial intelligence (AI) based application utilising laser profilers' data to monitor composite drilling tool during manufacturing and assembly. A machine learning (ML) model has been developed to process the data obtained from both laser profilers to automatically detect and report the defects in composite drilling tool. In order to achieve such a system, a ML model based on faster R-CNN neural network for drill holes' defects detection and linear regression for drill bits' defects analysis. This automated system will have the ability to reduce the manual inspection time of the operator and the costs of inspection process as the ML model will be used for decision making. The developed system proved to have a statistically significant efficiency in both performance and speed.

Detecting fake news using machine learning and reasoning in Description Logics

Adrian Groza¹

¹Department of Computer Science, Technical University of Cluj-Napoca, Baritiu 28, 400391, Cluj-Napoca, Romania

When designing technical solutions for fighting against disinformation, it is important to consider the viral factors of fake news: (1) spreader agents (bots, humans); (2) to what extent the medium is regulated; (3) how the messages mutate from medium to medium; (4) immunisations programs (pre-bunking, skill building); (5) blending of fake news with real news. The speed and scale at which disinformation spread put pressure on regulators to address this phenomenon, yet its multifaceted nature - legal, technological, societal, political or ethical makes it a challenging task. For instance, social media bots are influencing spread of diseases (i.e. infodemics [1], e.g. Ebola, Covid-19), stock markets [2] (e.g. Associated Press, Vinci french construction company), natural persons (e.g. the journalist Jessikka Aro). has investigated the impact of algorithms and bots on political discourse in Europe and COVID misinformation. Major platforms have also responded by adapting their community guidelines or terms of service. The black market for social media manipulations is flourishing as an increasing number of buyers and sellers meet to trade clicks, likes, comments subscribers [3]. One can buy tools and services for media manipulation with customer support for tasks like: (i) fake accounts: the price depends how the account will be registered (automatically, manually, or hacked accounts), the content quantity, or age of the account (from days to 7 years old grown account); (ii) manipulating social metrics using: fake accounts, special freelance platforms (with individuals working for less than \$1 per hour), likes exchanges, malicious software; (iii) DDoS2.0: the new distributed Denial-of-Service attacks specific pages inside social media platforms. The usual targets are activists, journalists, for a price for such DDoS service from \$5 to \$200 [3]. Fighting against computational propaganda requires integrated efforts from various domains like law or education, but there is also a need for computational tools [4], [5]. I investigate here how reasoning in Description Logics (DLs) can detect inconsistencies between trusted knowledge and not trusted sources. The proposed method is exemplified on fake news for the new coronavirus. Indeed, in the context of the Covid-19 pandemic, many were quick to spread deceptive information. Since, the not-trusted information comes in natural language (e.g. "Covid-19 affects only the elderly"), the natural language text is automatically converted into DLs with the FRED tool. Machine learning has two roles: (1) during this automatic translation from text to logic and (2) to generate DL axioms from positive (fake news) and negative examples using tools such as DL-Learner. The resulted knowledge graph formalised in DL is merged with the trusted ontologies on Covid-19. Reasoning in DL is then performed

with the Racer reasoner, which is responsible to detect inconsistencies within the ontology. When detecting inconsistencies, a “red flag” is raised to signal possible fake news. The reasoner can provide justifications for the detected inconsistency. This availability of justifications is the main advantage compared to approaches based on machine learning, since the system is able to explain its reasoning steps to a human agent. Hence, the approach is a step towards human-centric AI systems. Notarmuzi et al. have found that the complexity of information propagation in social media is correlated with its semantic content [6]. In case of infodemic, the agent is a text broadcast in a given medium [1] (e.g. “Vitamin and mineral supplements can cure COVID-19” or “Rinsing my nose with saline can stop COVID-19.”). These agents can mutate from medium to medium (e.g. a mutation of the previous myth would be “Vitamin C can cure the new coronavirus.”). By performing semantic analyses, the reasoner is able to infer the message represents the same propagation agent. This semantic identification of mutated messages is relevant to increase the quality of analysing fake news propagation. First Amendment theory [7] argues that counterspeech (e.g. more speech about real news) is the tenet against fake news [8]. By verbalising the conflict detected by reasoning in Description systems, our approach can automatically generate counterspeech for the identified fake news.

References

- [1] S. C. Briand, M. Cinelli, T. Nguyen, R. Lewis, D. Prybylski, C. M. Valensise, V. Colizza, A. E. Tozzi, N. Perra, A. Baronchelli et al., “Infodemics: A new challenge for public health,” *Cell*, vol. 184, no. 25, pp. 6010–6014, 2021.
- [2] Panel for the Future of Science and Technology European Science-Media Hub, “Automated tackling of disinformation,” European Parliamentary Research Service, Tech. Rep., 03 2019.
- [3] Singularex, “The Black Market for Social Media Manipulation,” Riga: NATO Strategic Communications Centre of Excellence, Tech. Rep., 2019.
- [4] P. L. Gentili, “Why is complexity science valuable for reaching the goals of the un 2030 agenda?” *Rendiconti Lincei. Scienze fisiche e naturali*, vol. 32, no. 1, pp. 117–134, 2021.
- [5] V. Mazzeo, A. Rapisarda, and G. Giuffrida, “Detection of fake news on covid-19 on web search engines,” *Frontiers in Physics*, vol. 9, 2021. [Online]. Available: <https://www.frontiersin.org/article/10.3389/fphy.2021.685730>
- [6] D. Notarmuzi, C. Castellano, A. Flammini, D. Mazzilli, and F. Radicchi, “Universality, criticality and complexity of information propagation in social media,” *Nature communications*, vol. 13, no. 1, pp. 1–8, 2022.
- [7] N. Syed, “Real talk about fake news: Towards a better theory for platform governance,” *Yale Law Journal*, vol. 127, pp. 337–357, 2017.
- [8] A. Gupta, H. Li, A. Farnoush, and W. Jiang, “Understanding patterns of covid infodemic: A systematic and pragmatic approach to curb fake news,” *Journal of business research*, vol. 140, pp. 670–683, 2022.

Predictive maintenance and Structural Health Monitoring via IoT system

Angelo Lo Russo

Dipartimento di Ingegneria Industriale, Università degli Studi di Salerno

Reinforced concrete buildings have proven the need to monitor the concrete and steel parts over time. The topic of structural monitoring of a building is becoming more topical with time, and many buildings from the 1960s and 1970s are under observation. The current challenge is to monitor structures effectively and continuously, applying the meaning of preventive maintenance, a concept well developed in engineering disciplines. New technologies allow us to assess the impact of time, wear, and tear, which in the long term can challenge the safety of buildings by monitoring the natural vibrations of a building. However, traditional monitoring systems in the civil infrastructure sector have always been expensive and undervalued. Therefore, borrowing innovations from computer science, a sensor system based on the new paradigms of the Internet of Things (IoT) was developed to provide a valuable alternative to proven vibration monitoring systems. The proposed system consists of a microprocessor (Raspberry Pi) and a low-cost accelerometer for microelectromechanical systems (MEMS), this type of lower costs sensor allows for investment in the safety of structures. The architecture of the monitoring system and the visualization of the vibrational model and its operation mechanism are presented. The performance of the monitoring system and the data collected are then integrated with Deep Learning techniques in order to obtain possible future scenarios and forecasts practical to perform tests that are as close as possible to the reality and thus be able to act with the necessary maintenance in order to prevent undesired structural effects.

Attention-based Dependability Prediction for Industrial Wireless Communication Systems

Danfeng Sun^{1,2}, Yang Yang³, Hongping Wu⁴

¹Institute of Industrial Internet Hangzhou Dianzi University, 310018, Hangzhou, China,

²Hangzhou Bi-foil Information Technology Co., Ltd., Hangzhou, China, yangyang@taocexin.com

³College of Information Engineering Hangzhou Vocational & Technical College Hangzhou, China, whp413@163.com

The wireless communication systems are everincreasing important for industrial applications, supported by organizations such as the German Electro and Digital Industry Association (ZVEI), 5G Alliance for Connected Industries and Automation (5G ACIA), and 3rd Generation Partnership Project (3GPP). Industrial wireless communication systems (IWCSs) have high requirements for dependability, where dependability prediction can support to assess and improve the IWCSs. With the fast development of machine learning techniques, several Long Short-term Memory models have been proposed and indicate effectiveness for the dependability prediction task. However, these models ignore the truth that wireless devices are always resource-constrained and relationships between the sequences can increase the prediction accuracy. Therefore, we propose the attention-based dependability prediction model which combined local and global attention mechanisms to reduce time complexity while improving the performance. We conducted experiments on three measured data sets and compared the execution time of our model with past LSTM-based models, which indicates that the proposed model has lower time complexity and also meets the requirement of industrial applications.

A Machine Learning Approach for Prosumer Management in Intraday Electricity Markets

Saeed Mohammadi^{1,*}, Mohammad Reza Hesamzadeh^{2,†}

¹School of Electrical Engineering and Computer Science KTH Royal Institute of Technology Stockholm, Sweden

* saeedmoh@kth.se

† mrhesa@kth.se

Prosumer operators are dealing with extensive challenges to participate in short-term electricity markets while taking uncertainties into account. Challenges such as variation in demand, solar energy, wind power, and electricity prices as well as faster response time in intraday electricity markets. Machine learning approaches could resolve these challenges due to their ability to continuous learning of complex relations and providing a real-time response. Such approaches are applicable with presence of the high performance computing and big data. To tackle these challenges, a Markov decision process is proposed and solved with a reinforcement learning algorithm with proper observations and actions employing tabular Q-learning. Trained agent converges to a policy which is similar to the global optimal solution. It increases the prosumer's profit by 13.39% compared to the well-known stochastic optimization approach.

Integrating modal analysis and seismic interferometry for structural dynamic identification and soil-structure interaction

G. Lacanna and M. Ripepe

University of Firenze, Via G. La Pira n°4, Firenze, Italy

The preservation of historical building requires monitoring their long-term behaviour as well as to quickly detect possible damage. In this respect, dynamic characteristics (frequency, shapes mode and seismic wave velocity) can be identified and tracked in real-time combining modal analysis with seismic interferometry, as it is shown in this paper for the Giotto's Bell-Tower in Firenze (Italy) by using a temporary seismic network. Natural frequencies and modal shapes of the structure are calculated by classic Enhanced Frequency Domain Decomposition (EFDD). Changes of the modal frequencies may reflect changes in the dynamic properties of the building and/or in the soil-structure interaction effects. The effects of soil- structure interaction are analysed with the seismic velocity and transfer function of the structure estimated using seismic interferometry technique. Seismic wave velocity inside the building depends only on the structural properties of the building and it is uncoupled from the soil- structure interaction system. The results of seismic interferometry (i.e fixed-base frequency, pseudo-flexible body frequency) combined with the first modal frequency allow to define the degree of the soil-structure interactions on the dynamic behaviour of the Giotto's bell tower. The full structural dynamic identification shows a weak contribution of the soil-structure interaction, that is supported by the high values of the horizontal and rocking stiffness, evaluated from the geotechnical properties of the soil. It is suggested that integrating the Operational Modal analysis and the seismic interferometry of the same ambient noise recording provides a unique and complete dynamic response of one of the worldwide important monument like the Giotto's Bell-Tower.

Web scraping technology for a dynamics analysis of tree crown streamlining, in relationships with wind and meteorological data

Giambastiani Y^{1,3,*}, Romanelli S², Giusti R¹, Cecchi S¹, Antonini A¹, Bottai L², Gozzini B^{1,2}, Ortolani A^{1,2}

¹ National Research Council, Institute of Bioeconomy, Italy

² LaMMA Consortium – Florence, Italy

³ Bluebiloba Startup Innovativa SRL, Florence, Italy

* giambastiani@lamma.toscana.it

The life quality in our cities is also determined by the presence of urban greenery, in particular by the arboreal heritage, which provides multiple ecosystem services. On the other hand, trees by their nature are subject to external stresses, from decay and therefore collapse phenomena. In order to monitor the trees stability, numerous analyzes are carried out concerning physiological and biomechanical aspects. Among these we find the controlled pulling test, an analysis that reproduces the wind action (in a static way) on the tree and studies the resistance to overturning, in particular with regard to root anchoring to the ground. The models applied within this analysis present an important gap: the behaviour of the canopy of trees subject to the force of the wind. This undergoes a reconfiguration of the branching in order to reduce the drag force, with direct repercussions on the impact area, the canopy porosity and the frequency of oscillation. The study of reconfiguration is a complex analysis, in the literature there are few works in relation to the wide variability given by the age, the species, the position of the trees. This preliminary study aims to introduce a new survey technique based on the use of opportunity data. By exploiting the presence of many meteorological webcams and applying web scraping procedures, it is possible to acquire a lot of data all over the world regarding the behaviour of the canopy during meteorological events, taking into account wind and precipitation. It is shown that by developing a web scraping procedure and through RGB image processing techniques, applied to a meteorological station in Tuscany, it is possible to acquire a database of data to be studied and deepened in order to understand the dynamic behaviour of the canopy. The results obtained are preliminary, as some improvements are still needed from a processing point of view, such as the automatic procedure that determines the crown area. We believe that sharing this technique with the scientific community can create new development opportunities and thus allow a more effective stability analysis.

A Methodology for The Design of Dynamic Absorbers for Structural Mitigation of Steel Buildings

Marco Claudio De Simone^{1*}, **Francesca Colucci**², **Domenico Guida**^{1,*}

¹Department of Industrial Engineering University of Salerno, Via Giovanni Paolo II, 132 Fisciano, 84084, Italy

*{mdesimone, guida}@unisa.it

Due to the increasing use of high-strength materials and advanced construction techniques, buildings have become more flexible and taller. The rising height of modern buildings has posed several challenges for structural engineers. When designing a lean and tall building, the structural system must meet three main requirements: strength, stiffness, and stability. As is well known, the strength requirement is the dominant factor in the design of low structures. However, as the height of the building increases, the stiffness and stability requirements become more critical and are often the dominant factors in structural design. Therefore, structural dynamic behaviour is one of the most critical design considerations. Through structural control, engineers aim to reduce the response of such buildings subjected to dynamic actions. Generally, structural control systems are classified into passive, active, and semi-active control systems. Researchers and engineers commonly state that passive control systems are the most straightforward and robust. Among the passive control systems, the most common is the Dynamic Vibration Absorbers (DVA), also called TMD (Tuned Mass Damper). Vibrations in structures are undesirable because they affect the functional efficiency of buildings and, sometimes, the safety of the structure itself. The causes of vibrations are environmental (earthquake and wind) and anthropogenic (pedestrian traffic on walkways, vehicular traffic on viaducts, operating machines, moving crowds). Passive vibration control is when the system is not retro-acted when dissipative elements are used. Instead, active control is used when the exciting cause is opposed by a controlled force that depends on the system's state. In the case of dynamic absorbers, the mitigation of vibrations is based on the modification of the system's structure, making sure that the incoming energy is channelled into a part of the system that does not affect the functionality of the building itself. Some of these components are called Tuned Mass Dampers (TMDs), devices for passive control of structures defined by mass, damping, and stiffness. TMDs reduce the amplitude of the responses that characterize the proper modes of the structure. In such devices, the mass values are around 1 and 5A limitation of these devices is their lack of robustness under conditions other than tuning. In fact, outside these restricted conditions, these systems' systems drastically lower their characteristics of dissipation devices (detuning). Therefore, a perfect operation of these devices occurs when they are perfectly calibrated in the design phase and remains if these characteristics are maintained throughout the duration of the useful life. Apart from these significant limitations, these types of devices

continue to be used because they are relatively inexpensive and work

well when they are well designed. In addition, the presence of an external actuator means an additional cost that these types of devices do not have. The most common types of passive TMD are translational TTMD and pendulum PTMD. In this work, following the current construction regulations (NTC2018, Eurocode 3), a multi-story steel building project is developed with the support of Midas Gen Software. After performing the verifications according to the current regulations (NTC - Eurocodes) and sizing the joints with Design Plus environment, the mass and stiffness of the dynamic absorber are calculated based on the modal parameters extracted from the model. The results obtained in the simulation phase showed a reduction in maximum displacements of 33% in the presence of TMD with the absence of damping. The methodology developed was effective and efficient; in fact, it was possible to size and verify through appropriate simulations the dynamic behaviour of the building in the presence of Tuned Mass Dampers. The ultimate goal of this study is the application of this methodology for the design of TMD for existing buildings through the use of structural monitoring techniques to estimate the structural parameters necessary for the optimal design of the passive device.

An adaptive modal filter for tracking frequency variation in the operating condition

Flavio Bocchi¹, Gianluca Acunzo², Noemi Fiorini³, Daniele Spina¹

¹Dipartimento della Protezione Civile, via Vitorchiano 4 00189 Roma

² Theta Group Via S. Pantaleo Campano 60/B, 00149 Roma

³Tecne Gruppo Autostrade per l'Italia, via A. Bergamini, 50 - 00159 Roma

In the last two decades, the combination of vibration-based modal analysis methods and new automated algorithms and techniques has seen an increasing development for the dynamic monitoring of infrastructures. The use of Operational Modal Analysis (OMA) techniques, with its large scientific literature [1, 2, 3], well-known methods [4, 5] and recognized algorithms [6] mostly implemented also in commercial software, are increasingly used to make modal parameters identification more and more automatic [7, 8, 9]. The faculty to track, manage and control the variation of modal parameters, being the correlation of such variation with damage of civil constructions well- demonstrated, provides strong motivations for the research effort on this topic. In this work a simplified methodology for periodically identifying, step by step, the modal parameters of a structure is presented. The fundamental idea of the proposed method is to perform the automatic tracking of the modal parameters of a structure in state $i + 1$, by exploiting the knowledge of its mode shapes in state i . In particular, given the ambient noise measurements $\mathbf{x}_{i+1}(t)$ at state $i + 1$ at N -DOFs (Degrees Of Freedom), if the $(N \times M)$, where M is the number of identified modes) eigenvector matrix \mathbf{U}_i at state i is known, it is possible to apply a modal filter to the original measures $\mathbf{x}_{i+1}(t)$ in order to express them in a new coordinate system, where the signals $\mathbf{x}_{i+1}(t)$ are almost decoupled in the single modal components $q_{i+1}(t)$ of the structure:

$$\bar{\mathbf{x}}_{i+1}(t) = \mathbf{U}_i^T \mathbf{x}_{i+1}(t) = \mathbf{U}_i^T \mathbf{U}_{i+1} q_{i+1}(t) = \mathbf{U}_i^T (\mathbf{U}_i + \Delta \mathbf{U}_{i+1}) q_{i+1}(t) = q_{i+1}(t) + \mathbf{U}_i^T \Delta \mathbf{U}_{i+1} q_{i+1}(t)$$

In the above equation it is assumed that the modal matrix \mathbf{U}_{i+1} at state $i + 1$ has varied of a quantity $\Delta \mathbf{U}_{i+1}$ with respect to previous state. If this variation is "small", the coupling term $\mathbf{U}_i^T \Delta \mathbf{U}_{i+1} q_{i+1}(t)$ is also "small" and the measurements in the new coordinates system are nearly decoupled in their modal component $q_{i+1}(t)$. Therefore, in the new coordinates system, it is possible to extract the modal matrix from the cross-spectra of the new signals $\bar{\mathbf{x}}_{i+1}(t)$, using simple Single DOF identification methods, such as the peak-picking technique [10]. Moreover, since is: $\mathbf{U}_{i+1} = \mathbf{U}_i \mathbf{T}_{i+1}$, the method also provides the modal matrix at state $i + 1$ which in turn can be used for the identification of modal parameter of state $i + 2$.

In order to demonstrate the validity and the effectiveness of the method, this approach has been applied both to a small theoretical-numerical model and to a real case. In the first example (a 2-DOFs Mathworks Simulink model with 2 masses and 3 springs connected in

series), the method is used to calculate modal parameters after simulating the dynamic response of the system to white noise and progressively reducing the stiffness of one spring to reproduce evolving states of damage. The real case refers to data continuously collected for six months (from 1 October 2021 to 1 April 2022) on a monitoring system installed on the historic bell tower of the Messina Cathedral. The application of the proposed technique to these experimental data allowed to show clearly the variation of the natural frequencies strictly due to daily and seasonal changing of the operating condition (i.e. temperature and humidity [11]).

References

- [1] R. Brincker, C. Ventura - Introduction to Operational Modal Analysis, Wiley, 2015
- [2] C. Ranieri, G. Fabbrocino - Operational Modal Analysis of Civil Engineering Structures: An Introduction and Guide for Applications, Springer, Berlin, 2014.
- [3] B. Peeters, G. De Roeck - Stochastic system identification for operational modal analysis: a Review. *J Dyn Syst Meas Contr* 2001; 123 (4):659-67
- [4] R. Brincker, L. Zhang, P. Andersen - Modal identification from ambient responses using frequency domain decomposition, Proceedings of the 18th International Modal Analysis Conference, San Antonio, USA, 2000.
- [5] C. Rainieri, G. Fabbrocino - Automated output-only dynamic identification of civil engineering structures, *Mechanical Systems and Signal Processing*, 2010, 24:678–695.
- [6] B. Peeters, H. Van der Auweraer – PolyMAX: a revolution in operational analysis, Proceedings of the 1st IOMAC, Copenhagen, 2005, pp. 25-26
- [7] M. Filipe; Á. Cunha, E. Caetano, Online automatic identification of the modal parameters of a long span arch bridge, *Mech. Syst. Signal Process*, 2009, 23, 316–329
- [8] J. Teng, D. Tang, X. Zhang, W. Hu, S. Said, R. Rohrmann - Automated Modal Analysis for Tracking Structural Change during Construction and Operation Phases, *Sensors*, 2019, 19(4), 927 h <https://doi.org/10.3390/s19040927>
- [9] A. Cabboi, F. Magalhães, C. Gentile, Á. Cunha, Automated modal identification and tracking: Application to an iron arch bridge. *Structural Control and Health Monitoring*, 2017, 24. ISSN 1545-2255
- [10] D. J. Ewins, *Modal Testing: theory, practice and application*. Second edition, 2000, Research Studies Press LTD
- [11] M. Regni, D. Arezzo, S. Carbonari, F. Gara, D. Zonta, Effect of environmental conditions on the modal response of a 10-story reinforced concrete tower. *Shock and Vibration*, 2018. 9476146. ISSN 1875-9203

A quality based OMA framework for data-driven SHM of heritage buildings

Giacomo Zini , Gianni Bartoli, Michele Betti*, Francesca Marafini

Department of Civil and Environmental Engineering, University of Florence via di S. Marta
3 – I-50139 Florence – Italy

*michele.betti@unifi.it

The Structural Health Monitoring (SHM) framework based on the Modal Tracking (MT) of the dynamic parameters (main frequencies, mode shapes and modal damping), allows today for the control of the operative conditions of both structures and infrastructures. Considering the needs of a continuous monitoring system, in the last decade many efforts have been done to set-up automated Operational Modal Analysis (OMA) procedures able to process the large datasets obtained from such systems. Among all the proposed automated procedures, this paper describes a new automated one to be used for extraction and tracking of the modal properties directly from the signals recorded by the dynamic sensor focusing on its application on heritage buildings. Such buildings are usually exposed to a low level of environmental excitation and, in addition, allow only a limited number of sensors in order to preserve their architectural feature. Considering these issues, this paper provides an operative automated workflow for MT of the damage sensitive features in a data-driven SHM approach.

List of Posters

Exploring the complexity of African populations variability with Machine Learning

T. Mori¹, A. Riga¹, J. Moggi-Cecchi¹, C. Canfailla^{2,3}, A. Barucci²

¹ Department of Biology, University of Florence, via del Proconsolo 12, 50122 Firenze, Italy.

²Institute of Applied Physics "Nello Carrara", Italian National Research Council, via Madonna del Piano 10, Sesto Fiorentino, 50019, Italy

³ Department of Information Engineering, University of Florence, Via di Santa Marta, 3 - 50139 Florence, Italy

Human skeletal remains are an immense source of data to describe human biodiversity with an intrinsic complexity due to the multifactorial origin of human variability. Evolution and ontogeny produced complex patterns of variation through contingent events and adaptations. Multivariate approaches have been widely adopted in physical anthropology; however, at present, Artificial Intelligence algorithms have scarcely been applied to such datasets. Data analysis techniques based on Artificial Intelligence algorithms have shown to be suitable in many different fields, from engineering and medicine up to cultural heritage and Egyptology. In this work we aim to show how Machine Learning algorithms can be applied in the field of anthropology, using the W.W. Howells dataset of cranial measurements, limited to the analysis of African populations. Principal Component Analysis (PCA), t-distributed stochastic neighbor embedding (t-SNE), Spectral Embedding and Uniform Manifold Approximation and Projection (UMAP) were used for dimensionality reduction, along with supervised and unsupervised methods to explore and quantify the differences due to ancestry and sex in the skulls of African populations. Algorithms such as Support Vector Machines and the unsupervised DBSCAN were applied to the data in order to quantify this similarity. This strategy allows a discrimination of sex and ancestry (about 85% of accuracy for both) in human remains, ultimately opening up new routes for anthropological research.

References

[1] Mori, Tommaso, and Katerina Harvati. "Basiscranial ontogeny comparison in Pan troglodytes and Homo sapiens and its use for developmental stage definition of KNM-ER 42700." *American Journal of Physical Anthropology* 170.4 (2019): 579-594.

[1] Barucci, Andrea, et al., "A Deep Learning Approach to Ancient Egyptian Hieroglyphs Classification," in *IEEE Access*, vol. 9, pp. 123438-123447, 2021, doi: 10.1109/ACCESS.2021.3110082.

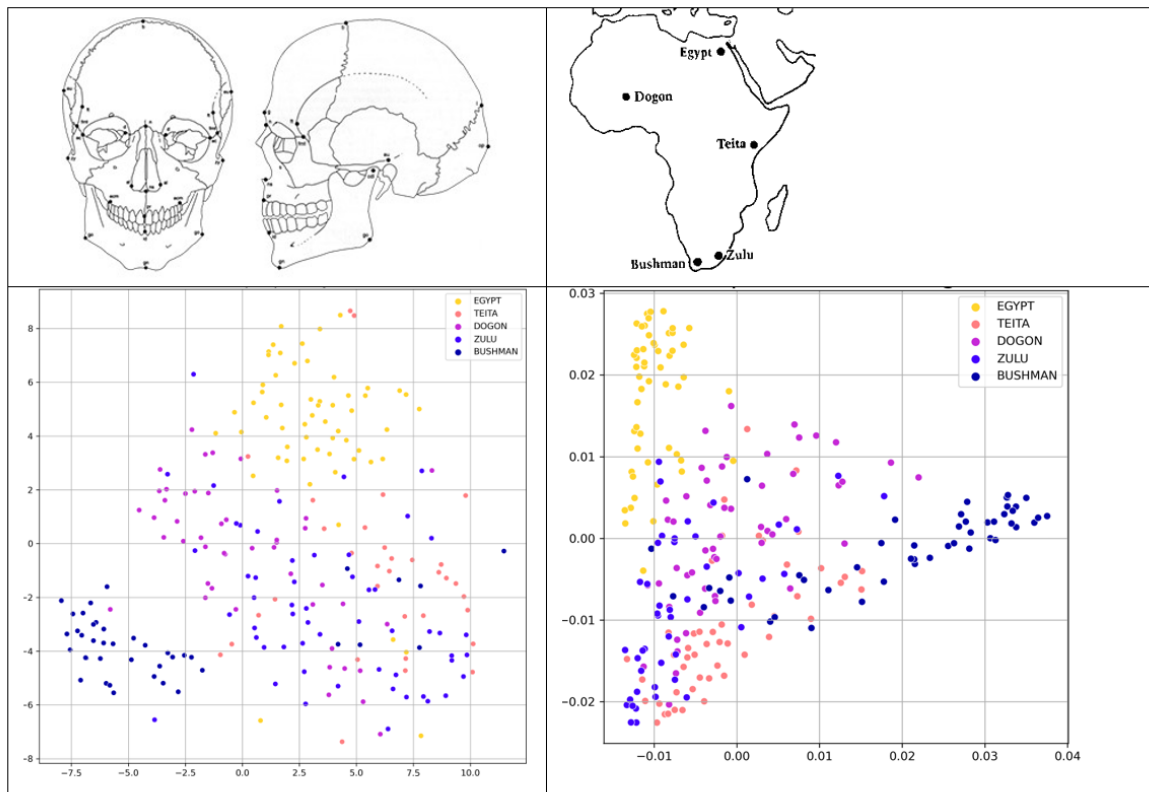


Figure 0.1: Top Left) scheme of the Howell measurements used in this study; Top right) African distribution of ancestry. Bottom Left: results of PCA and t-SNE combination for men ancestry; bottom right) Spectral embedding women ancestry results.

Exoskeleton in stepping on even and compliant surface

K. Bogaert¹, S. Summa², M. Petrarca², M. Bottoni², M. Favetta²

¹Department of Movement Sciences, KU Leuven, Belgium

²MARLAB, Ospedale Pediatrico Bambino Gesù, Roma, Italy

Introduction: It is known that orthotics can improve the gait within the population of children with walking problems. The Eurobench group (e.g., European robotic framework for bipedal locomotion benchmarking) includes several projects to develop or improve human-centered robots, such as orthosis or even more progressive, humanoids. This European group started the BEAT (e.g., Balance evaluation automated testbed) project in 2019. The protocol consists of different tasks on a moving platform including both standing and stepping. This platform can either be fixed in position or compliant around roll-pitch and the vertical axes. The goal of BEAT is to understand the regain of an

equilibrium in simulated daily life situations. Continuing this protocol a new project will test the functionality of a developing exoskeleton (e.g., robotic knee) to assist the regain balance on the Doris platform (e.g., 6-DOF). The main interest is to see how the functionality of the orthosis reacts in regain of stability to further adjust the development.

Methods: Healthy participants (20-55 yo) perform two stepping tasks in place for one minute (60 sec.) on the Doris platform. First the platform will be in non-compliant (e.g., fixed) and immediately thereafter in compliant mode for both pitch and roll. On the right leg the participant wears a knee orthosis (KOD) that can be controlled in impedance and admittance, this creates two conditions, KODoff and KODon. The two conditions are collected in two different sessions on the same day. The data is collected with Vicon Nexus for the movement collection of all segments with a full body plug-in gait markering. The analysis is performed in MATLAB (Mathworks Inc., Sherborn, MA).

Results: The parameter of interest in this first stage is the knee angle on the leg where the orthosis is worn (e.g., right leg). Data collection is ongoing, the preliminary data of one participant (female, 21 yo) showed overall similar results between the KODon and KODoff conditions. There was no difference significant different found between the averaged maximum knee angle of all steps. The knee angle at in the KODon condition was even slightly bigger as shown in the figure 1.

Conclusion: These first results are positive though wants the function ability of the orthosis. The knee is supported to create the maximum angle in each step. It will be necessary to further analyze the other participants and conducts more extended tasks on Doris. In the future when the mechanism shows to be working in these closed tasks on the platform, free walking trails can be performed to generalize the possible use for patients.

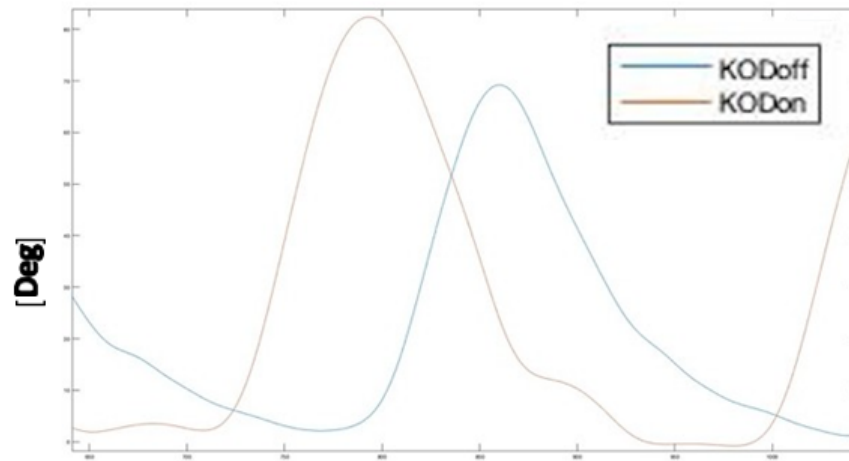


Figure 0.1: One single step on non-compliant platform.

Comparing Calibration Update Techniques for Concept Drift Mitigation: A Low-Cost NO₂ Sensors Air Quality Monitoring Application

G. D'Elia^{1,2}, M. Ferro², P. Sommella², S. Ferlito¹, S. De Vito¹, G. Di Francia¹

¹ ENEA CR-Portici, TERIN-FSD Division, P. le E. Fermi 1, 80055 Portici, Italy

² University of Salerno DIIN Department of Industrial Engineering, Via Giovanni Paolo II, 132, 84084 Fisciano, Italy

The calibration of low-cost sensors using machine learning techniques is getting an increasingly widespread practice in all industrial sectors [1]. Generally, such sensors undergo a first calibration or in laboratory or in field to then operate in dynamic and nonstationary environments, requiring reliable performance as well as compliance with Data Quality Objectives (DQO). One of the crucial phenomena behind the calibration model performance degradation, is the Concept Drift (it refers to differences in data distributions associated with input and target variables of an incremental or batch streaming data) [2]. Handling concept drift should have therefore high priority in machine learning pipeline, furthermore the lack of reference data in practical scenario is challenging for sensors re-calibration. In the present study we will address this issue in a Low-Cost NO₂ Sensors Air Quality Monitoring Application employing the data collected in an experimental campaign carried out in Portici (Naples, Italy) in 2020 two month long. The dataset is characterized by the presence of concept drift verified applying Two-Sample Kolmogorov-Smirnov Test. Since the calibration update process is triggered via a concept drift detector, the first question to address is to understand which data to be selected appropriately to get results within the upper limit represented by the metric values (MAE and MAPE) obtained in co-location and the lower limit obtained from a dummy re-training with the reference data.

In such approach three possible answers are investigated: the data preceding the concept drift alert (called "Last"), the data subsequent the concept drift alert ("Next") or part of both ("Mixed") [3]. After that, two approaches are compared for the calibration update: a weighted multivariate linear regression (that considers a vector of weights [4] computed as the density ratio of test to training target) and a generalized calibration model [5] (that takes into account the median of the training data from the total devices under test). The obtained results show the effectiveness of both techniques, even though the generalized calibration model exhibits a superior capability in mitigation of the concept drift effects, revealing outcomes that fall within the desired eligibility range.

- References** [1] R. Gemaque, A. Costa, R. Giusti and E. Dossantos, "An overview of unsupervised drift detection methods", *Wiley Interdisciplinary Reviews: Data Mining and Knowledge Discovery*, vol. 10, no. 6, pp. 1381, Nov. 2020 DOI: 10.1002/widm.1381
- [2] J. Lu, A. Liu, F. Dong, F. Gu, J. Gama and G. Zhang, "Learning under Concept Drift: A Review," *IEEE Transactions on Knowledge and Data Engineering*, vol. 31, no. 12, pp. 2346-2363, 1 Dec. 2019, DOI: 10.1109/TKDE.2018.2876857
- [3] L. Baier, J. Reimold and N. Kühl, "Handling concept drift for predictions in business process mining", *Proc. IEEE on Business Informatics (CBI)*, pp. 76-83, Jul. 2020
- [4] M. Sugiyama, M. Krauledat and K. R. Müller, "Covariate shift adaptation by importance weighted cross validation", *J. Mach. Learn. Res.*, vol. 8, pp. 985-1005, May 2007.
- [5] C. Malings et al., "Development of a general calibration model and long-term performance evaluation of low-cost sensors for air pollutant gas monitoring", *Atmos. Meas. Tech.*, vol. 12, no. 2, pp. 903-920, 2019 8)

Raman microspectroscopy and multivariate analysis in radiobiology: Study of the effects of X-ray irradiation on neuroblastoma cells

V. Ricciardi¹, L. Manti¹, M. Lepore², G. Perna³, M. Lasalvia³, V. Capozzi³, I. Delfino⁴

¹ Dipartimento di Scienze Fisiche Università di Napoli "Federico II", Napoli, Italy

² Dipartimento di Medicina Sperimentale Università della Campania "L. Vanvitelli", Napoli, Italy

³ Dipartimento di Medicina Clinica e Sperimentale Università di Foggia

⁴ Dipartimento di Scienze Ecologiche e Biologiche Università degli Studi della Tuscia Viterbo, Italy

Raman micro-spectroscopy is becoming very popular in the field of radiobiology and radiation oncology for its ability to assess the cellular damage at the molecular level. Raman spectroscopy technique has been used to monitor the minimum doses required to lethally damage tumor cells, as well as to reduce the risk of excess dose being delivered to healthy surrounding cells. These results can also be achieved thanks to development of specific data analysis methods enabling the extraction of information embedded in the Raman spectra of complex samples, such as human cells. Among different data analysis procedures, multivariate analysis has been proven to be particularly effective. The principal component analysis (PCA) method has been largely used for analyzing Raman spectra from cells and tissues. In some cases, the PCA can be performed on selected wavenumber ranges of Raman spectra in order to get information embedded in those specific ranges (interval-PCA) method, has gained popularity for biomedical applications of Raman spectroscopy. In the present work, the application of these methods to the analysis of Raman spectra from single SH-SY5Y neuroblastoma cells following the exposure to graded doses of X-rays are reported and specific information from nucleus and cytoplasm regions are obtained. In addition, the biochemical changes occurring in these cells are also discussed by using an alternative approach, namely the analysis of difference spectra, obtained by subtracting the cytoplasm-related spectrum from the corresponding one detected at the nucleus. It's worth to note that multivariate analysis has allowed us to unravel the subtle modifications, due to X-ray irradiation, of Raman features related to specific components. These results pave the way to develop proper data analysis methods allowing to manage, on one hand, the complexity of the Raman spectra of cells and tissues and, on the other hand, the high number of spectra needed to take into account the intrinsic variability of biological samples.

Assessing the Complexity of DC-System Simulations

J. Ihrens¹, T. Schneider¹, T. A. Kern¹

¹ Hamburg University of Technology, Institute for Mechatronics in Mechanics, Germany

Due to the deteriorating climate crisis, the work towards a sustainable energy supply intensifies. The increasing use of renewable energies enables the more widespread use of DC grids [1], as both loads and sources are inherent DC components and their integration into a DC grid can increase system efficiency by evading conversion losses. The penetration of DC grids is increasing in land and domestic grids as well as in marine grids [1]. However, since hardly any DC grids of a certain complexity are currently available for testing components, control strategies and developing grid structures and topologies, simulations are the only available tool in the development of DC grids, imposing risks due to missing validations and practical experiences. Considering the investments connected to complex DC-grid technology, the decision between risk-taking and system oversizing is critical for the successful introduction of this key technology. This makes it utterly important that simulations for this new domain validly represent reality, but at the same time place the lowest possible demands on development time and computing power. With this necessary level of modeling detail to be achieved for a certain system-stability-statement is often unclear and there is a lack of methodology for balancing complexity and accuracy. This paper focuses on the first step in tackling this problem, which is to analyze the complexity of different simulations. High-complexity simulations do not necessarily give the best results and can have significant drawbacks, such as a high development and computational cost [2], which can add up, especially when using different subsystems multiple times. To obtain optimal performance, the prediction must be sufficiently accurate for the application domain in question, but should not go beyond this in order to keep the cost of the simulation reasonable [3].

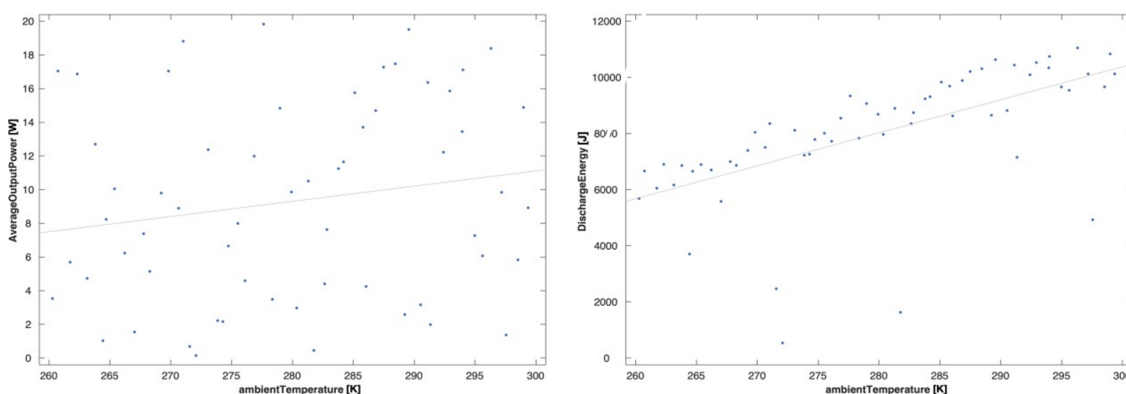


Figure 0.1: Monte Carlo sensitivity analysis for a discharge cycle of a Li-Ion cell model.

This paper aims to show ways to objectively measure and quantify the complexity of a DC-grid simulation. Various metrics can be used to evaluate the complexity [4], including the computing time, the number of different branches, components and variables as well as the boundary conditions. A statistical analysis of the computing time provides initial information about the complexity. Existing branches, components and their count can be used for a more precise analysis and can open up possibilities for simplification. Boundary conditions such as spatial and temporal resolution additionally influence the complexity of the simulation. As shown in Figure 1, a sensitivity analysis can be used to identify insignificant parameters. In an outlook, this paper demonstrates how to use the evaluation and objectification of the complexity of a simulation in future systematic optimizations of simulations.

References

- [1] Ertugrul, N.; Abbott, D. DC is the Future [Point of View]. Proc. IEEE 2020, 108, 615–624.
- [2] F. Netter, F. Gauterin und C. Xu, „Complexity adaptation of simulation models in a function-based modular framework“ in ICMSAO, Hammamet, 2013.
- [3] D. B. Webster, M. L. Padgett, G. S. Hines und D. L. Sirois, "Determining the level of detail in a simulation model - a case study", Computing & Industry, Vol. 8, 3/4, S. 215–225, 1984.
- [4] O. Masmali und O. Badreddin, „Comprehensive Model-Driven Complexity Metrics for Software Systems“ in IEEE 20th QRS-C, Macau, China, 2020.

Distance between movies using Multilayer Network Laplacian Spectra Descriptor

M. Lafhel¹, L. Abrouk², H. Cherifi², M. El Hassouni¹

¹ Mohammed V University,

²University of Burgundy

A movie recommendation system suggests to users a set of movies based on filtration of their data or recent online activities. In recent years, social networks have become increasingly used to analyze movie storylines. To the best of our knowledge, there is currently no method for measuring the similarity between movies based on graph distance. Given a couple of networks, a graph distance measure consists of extracting network features and computing the distance between them. In network science, determining the distance between networks is a difficult task. That is because a measure can perform well on one sort of graph but not on another, depending on the network structure and topology. Our main goal is to investigate graph distance measures for estimating movie similarities and incorporating them into recommendation systems. In this work, we compare the similarity between the 3-cycle movies of Scream Saga using The Network Laplacian Spectra Descriptor (NetLSD) [1]. We used a recent multilayer network model [2] to represent each episode in three layers: character, keyword, and location. So, we can compare the similarity between movie stories in terms of the three aspects.

Our methodology (Fig. 1) is composed of three main steps: (i) extraction of the multilayer network for each movie script; (ii) extraction of the network features; and (iii) computation of the distance between layers.

- (i) The first step consists of extracting for each movie script three layers (characters, keywords, and locations), intra-relationships, and inter-relationships. We ignore inter-relationships to compare layers of the same entity.
- (ii) The second step consists of extracting network features. To do this, we first assign a property to nodes or edges. Then, for each network, we extract a feature vector including properties. The properties play the principal role in analyzing networks as it captures local/global structural information.
- (iii) The third step is determining the distance between layers of the same entity. The distance between two layers is the difference between their structural information. In other words, the distance between their extracted feature vectors.

Experiments are performed using the movie scripts of the three first episodes of the Scream saga. We present the distance between character, keyword, and location layers

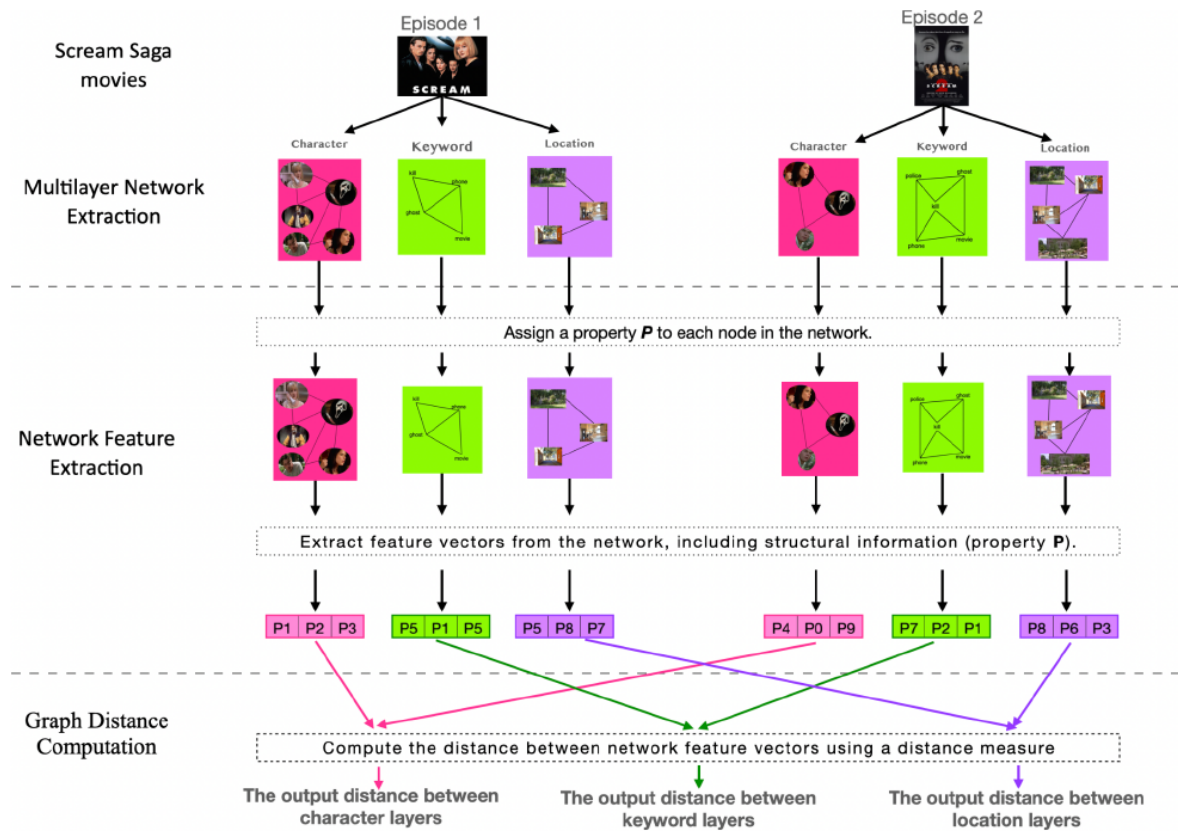


Figure 0.1: The pipeline of computing the distance between movie layers.

using NetLSD in Table 1.

The relationship between the characters in Episode I is closer to Episode II than in Episode III. The relationship between the characters in Episode III is closer to Episode II than in Episode I. On the other hand, Episode II displays the same level of similarity as Episodes I and III. That reveals how the similarity between characters degrades as the series progresses. In other words, the relationship between the characters changes from Episode I to Episode III. That may be due to the disappearance of many characters and the appearance of new ones. Indeed, the movie tells a series of murders where Sandy's friends are killed one after the other by a ghost-faced killer; and in each episode, Sandy

Layers	Characters	Keywords	Locations
Episode I vs Episode II	2.27	1.2	3.57
Episode I vs Episode III	4.60	6.79	8.59
Episode II vs Episode III	2.34	7.99	2.34

Table 0.1: NetLSD of the characters in the 3-cycle movies of the Scream saga.

forms new friendships. Keyword layers suggest a high similarity between keywords in episodes I and II. Indeed, the movie is about murders, killers, and victims. Similar to character layers, the relationship between keywords in Episode II is closer to Episode I than in Episode III. In opposition, the relationship between keywords in Episode III is far from Episode II than in Episode I. That may be because, in Episode III, characters tell the stories of previous victims killed in previous movies. The structure of Episode III is different from episodes I and II. Comparing location layers, episodes I and II are more similar than episodes II and III, and episodes II and III are nearer than episodes I and III. So, Episode II is closer to Episode I than Episode III. That tells us a transition of locations from Episode I to Episode III. Most of the murders in Episode I happened in a home or a garden. Besides, the characters spend most of their time at home or school. In Episode II, besides home, killers started following and attacking their victims in different places, such as a cinema or a car. While in Episode III, there was a high transition of locations. For instance, Sidney has gone to live on a mountain. In future work, we will investigate other distance measures for assessing the similarity between movies in different movie genres.

References

- [1] Tsitsulin, A., Mottin, D., Karras, P., Bronstein, A., & Müller, E. (2018, July). NetIsd: hearing the shape of a graph. In Proceedings of the 24th ACM SIGKDD International Conference on Knowledge Discovery & Data Mining (pp. 2347-2356).
- [2] Mouchid, Y., Renoust, B., Cherifi, H., & El Hassouni, M. (2018, December). Multilayer network model of movie script. In International Conference on Complex Networks and their Applications (pp. 782-796). Springer, Cham.

Investigation of Impact-Detection Methodology for Smart Shipping Containers via Time-Series Acceleration Signal Processing Techniques

**Sergej Jakovlev¹, Tomas Eglynas², Miroslav Voznak¹, Pavol Partila¹, Jaromir Tovarek¹,
Valdas Jankunas², Mindaugas Jusis²**

¹ Department of Telecommunications, VSB - Technical University of Ostrava, Studentská 6231/1B, 708 33 Ostrava-Poruba, Czech Republic

² Klaipeda University, Marine Research Institute, Universiteto ave. 17, LT-92294, Klaipėda, Lithuania

Shipping container transportation is a complex and highly demanding operation that requires high levels of security during the full work cycles in container terminals. During handling operations, performed by quay and yard cranes, containers tend to physically impact the surrounding concrete and metal infrastructures, resulting in heavy damages to the cargo, to the ships, to other containers and heavy machineries on-sites. In this paper we continue to investigate the engineering possibilities to detect these impacts during container handling inside the container ships, detecting impacts to the vertical cell guides, by means of acceleration signals processing using the highly adaptable impact-detection methodology (IDM) proposed earlier. We investigate the methodology by including new evaluation parameters, namely, all three movement axes – X, Y and Z, and improve the decision criteria's, whereas these impacts were detected more efficiently. The methodology was using the real operational data from equipment mounted on the quay crane in Klaipeda city "Smelte" container terminal. Initial results show that it is possible to detect true critical impacts using the three axes evaluation, in comparison with a single X-axis technique proposed earlier. In addition, the results indicate that the presented modified IDM, the MIDM, can be used to recognize repeated impacts in the same space of each bay of the ship, and can be used as a decision support tool for predictive maintenance systems.

Acknowledgement

This work was supported by the ESF in "Science without borders 2.0" project, reg. nr. CZ.02.2.69/0.0/0.0/18_053/0016985 *within the Operational Programme Research, Development*

Analyzing the Statistical Backbone Filtering Techniques on the Air Transportation Network

A. Yassin¹, H. Cherifi¹, H. Seba², O. Togni¹.

¹ Laboratoire d'Informatique de Bourgogne - Univ. Bourgogne - Franche-Comté, Dijon, France,

² Univ Lyon, UCBL, CNRS, INSA Lyon, LIRIS, UMR5205, F-69622 Villeurbanne, France

Networks provide an informative description of complex systems, yet the size and the density of many real-world networks form a barrier to visualization and processing. Therefore, many Backbone extraction techniques have been developed, reducing their size while preserving essential information. Among these techniques, structural-based filtering techniques focus on removing edges and nodes while preserving a topological property. In contrast, using a statistical test, model-based techniques remove insignificant edges and nodes. They compare an edge's observed weight to the distribution of its weights under a predefined null model. This study investigates five influential model-based edge filtering techniques briefly described in the table of Figure. 1. We study the evolution of the Backbone's main topological properties in the Worldwide Air Transportation Network. It consists of 2734 nodes and 16665 edges. Nodes represent cities, and edges are air routes between the cities. The weight of an edge is the total number of flights flying the route. Figure 1 presents the evolution of the properties versus the fraction of edges remaining in the Backbone (fraction of nodes, density, average edge weight, and average edge betweenness). Figure 1(a) illustrates the effectiveness of the Noise Corrected Filter at preserving the nodes while filtering a high fraction of edges. Figure 1 (b) shows that the Noise Corrected Filter and the Polya Urn Filter extract a backbone with a lower density than the original network. The backbone density fluctuates around the density of the original network for the other techniques. Figure 1(c) reports the evolution of the average edge weight as a function of the fraction of edges. One can observe that the Polya Filter preserves the average edge weight of the original network. The Disparity Filter and the Marginal Likelihood Filter preserve high-weight edges. In contrast, the Noise Corrected Filter retains many low-weight edges, decreasing the average edge weight. Figure 1(d) reports the evolution of the average edge betweenness. One can see that all backbones exhibit similar behavior. As the fraction of retained edges grows, the average edge betweenness increases to a maximum due to the emergence of a large connected component in the Backbone. Then it decreases until it reaches the value observed in the original network. However, one can observe that overall, the Noise Corrected Filter retains the highest average edge betweenness. Indeed, it preserves shortest-path edges that connect the network's parts. Even though model-based filtering techniques do not aim to preserve specific topological properties, the extracted Backbone exhibits typical behavior. The last column of the table in Fig. 1 shows these properties. These preliminary

results pave the way for future research investigating complementary global and local topological properties and their distributions. Indeed, a better understanding of their main characteristics is critical in practical situations to use model-based filtering techniques wisely.

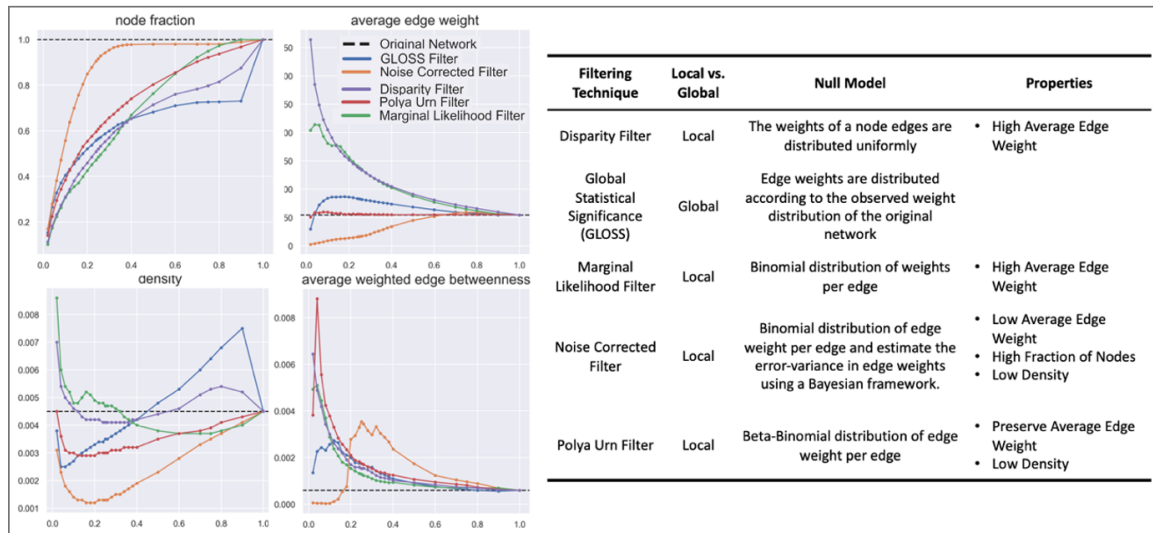


Figure 0.1: (a) The fraction of nodes, (b) density, (c) average edge weight, (d) and average edge betweenness of seven backbones as a function of the preserved edge fraction in the worldwide air transportation network. The table defines the Model-based edge filtering techniques.

Useful Information

Talks will be held at the **GGI – Galileo Galilei Institute for Theoretical Physics**, Largo Enrico Fermi, 2, 50125 Firenze FI, Italia. Website: www.ggi.infn.it

The **conference dinner** will be held at Antico Ristoro di Cambi, Via Sant’Onofrio, 1R, 50124 Firenze FI

